TECHNISCHE UNIVERSITÄT DRESDEN

12th German Ferrofluid Workshop

Benediktbeuern
September 26th – 28th
2012

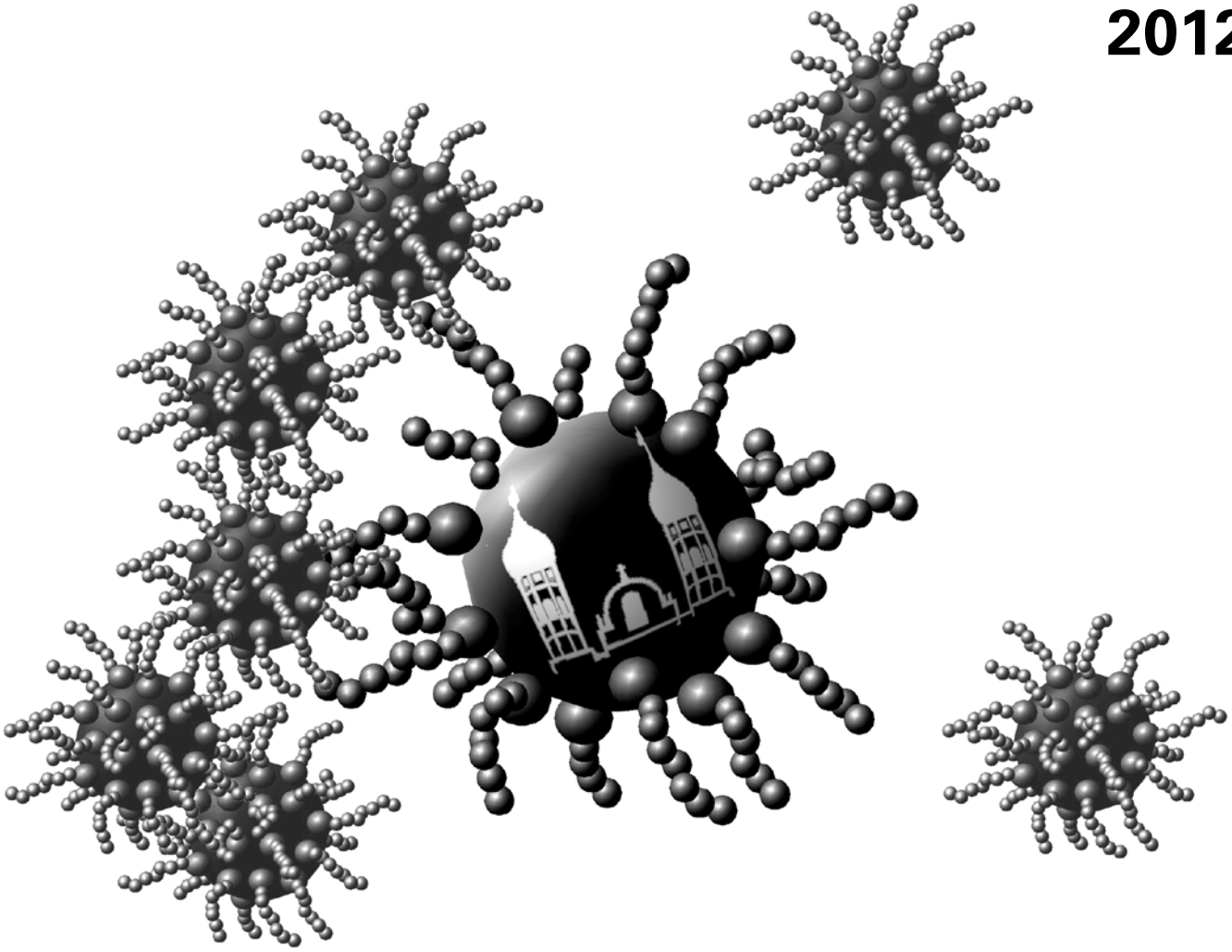

Book of Abstracts

Program of the

12th German Ferrofluid Workshop

Benediktbeuern, 26.9.-28.9.2012

Wednesday, September 26th

13:00 – 13:30	***Opening***		
13:30 - 13:55	J. Jakobi, S. Barcikowski	*Surfactant-free alloy ferrofluids by laser ablation of solid magnets in organic liquids and subsequent matrix embedding*	14
13:55 - 14:20	F. Wittbracht, B. Eickenberg, M. Schäfers, J. Meyer, A. Hütten	*Magnetic nanoparticles as reconfigurable matter*	40
14:20 - 14:45	R. Meckenstock, A. Terwey, C. Schoeppner, A. Trunova, N. Reckers, M. Farle	*Relaxation and Anisotropy in magnetic nanocubes*	42
14:45 - 15:10	J. Popp, K. Zimmermann, V.A. Naletova, D. Pelevina, V. Böhm, I. Zeidis	*Analysis of the Enhanced Deformation of a Magnetic Fluid Contour*	46
15:10 - 15:35	S. Schrittwieser, F. Ludwig, J. Dieckhoff, A.Tschoepe, A. Guenther, A. Huetten, H. Brueckl, J. Schotter	*Optical detection of the rotational dynamics of anisotropic magnetic Nickel nanorods*	44
15:35 - 16:00	T. Gundermann, S. Günther, D. Borin, S. Odenbach	*A comparison between micro- and macro-structure of magnetoactive composites*	50
16:00 - 16:40	***Coffee break***	***Postersession 1***	
16:40 - 17:05	L. Roeder, M. Reckenthäler, L. Belkoura, A. M. Schmidt	*Magneto-mechanical Coupling in Ferrohydrogels*	52
17:05 - 17:30	A. Weikl, M. Krekhova, H. Schmalz, R. Richter	*Birefringence as a Tool to Characaterize the Matrix of Thermoreversibel Ferrogels*	54
17:30 - 17:55	R. Weeber, S. Kantorovich, C. Holm	*Computer simulations on the deformation of ferrogels*	56
17:55 - 18:20	D. Yu. Borin, Th. Richter, G.V. Stepanov, A.V. Bakhtiiarov, S. Odenbach	*Permanent soft elastic magnets with controllable mechanical properties*	58
18:20 - 20:30	***Postersession 2***		

Thursday, September 27th

8:30	***Departure for excursion***		
		Mountain Talks	
	S. Behrens	*Synthesis of Metal Nanoparticles in Room Temperature Ionic Liquids:Co-Nanoparticles and Co-based Magnetic Fluids*	6
	S. H. L. Klapp	*Network formation of unconventional dipolar particles*	22
	R. Müller	*Investigations on quantification of magnetic nanoparticles after perfusion of a placenta*	81
16:15	***Return from excursion***		
17:00 - 17:25	L. Sprenger, A. Lange, S. Odenbach	*The influence of thermodiffusion in ferrofluids on thermomagnetic convection*	26
17:25 - 17:50	G. K. Auernhammer, M. Roth, J. Wenzl, R. Seto, C. Schilde, A. Kwade, H.-J. Butt	*Following mechanical deformation in colloidal systems on a single particle level*	28
17:50 - 18:15	S. Kantorovich, L. Rovigatti, A. Ivanov, F. Sciortino	*Structural transitions in the system of magnetic dipolar particles at low temperature*	30
18:30	***General Assembly of the Ferrofluidverein Deutschland e.V.***		
		Postersession 3	
19:30 - ???	***Conference Dinner***		

Friday, September 28th

9:00 - 9:25	E. Roeben, S. Teusch, M. Dörfer, M. Effertz, A. M. Schmidt	*Nanorheology of polymer solutions using magnetically blocked $CoFe_2O_4$ nanoparticles*	60
9:25 - 9:50	J. Linke, S. Odenbach	*The anisotropy of the magnetoviscous effect in ferrofluids*	62
9:50 - 10:15	A. Sreekumari, P. Ilg	*Fast relaxation in structure forming ferrofluids*	64
10:15 - 10:40	A. Dobroserdova, E. Minina, T. Prokopyeva, E. Novak, E. Pyanzina, S. Kantorovich	*How to study theoretically the influence of magnetic particle shape anisotropy on the macroproperties of magnetic fluids*	66
10:40 - 11:10	***Coffee break***	***Postersession 4***	

11:10 - 11:35	R. Tietze, S. Lyer, S. Dürr, J. Mann, E. Schreiber, R. Turcu, A. Schmidt, C. Alexiou	*Magnetite microgels and fatty acid coated nanoparticles for Drug Delivery*	59
11:35 - 12:00	O. Lunov, T. Syrovets, Th. Simmet	*Towards Therapeutic Applications of Superparamagnetic Nanoparticles*	90
12:00 - 12:25	D. Vlaskou, O. Mykhaylyk, C. Plank	*Concept of magnetic microbubbles for magnetic field and ultrasound triggered drug and gene delivery*	92
12:25 - 12:50	F. Schlenk; F. Bähring; C. Bergemann; J.H. Clement; D. Fischer	*Charge dependent influence of polymeric coated superparamagnetic iron oxide nanoparticles on blood and blood brain barrier*	94

12:50 – 13:15 ***Closing***

Overview of all contributions

Abstracts

for the

12th German Ferrofluid Workshop

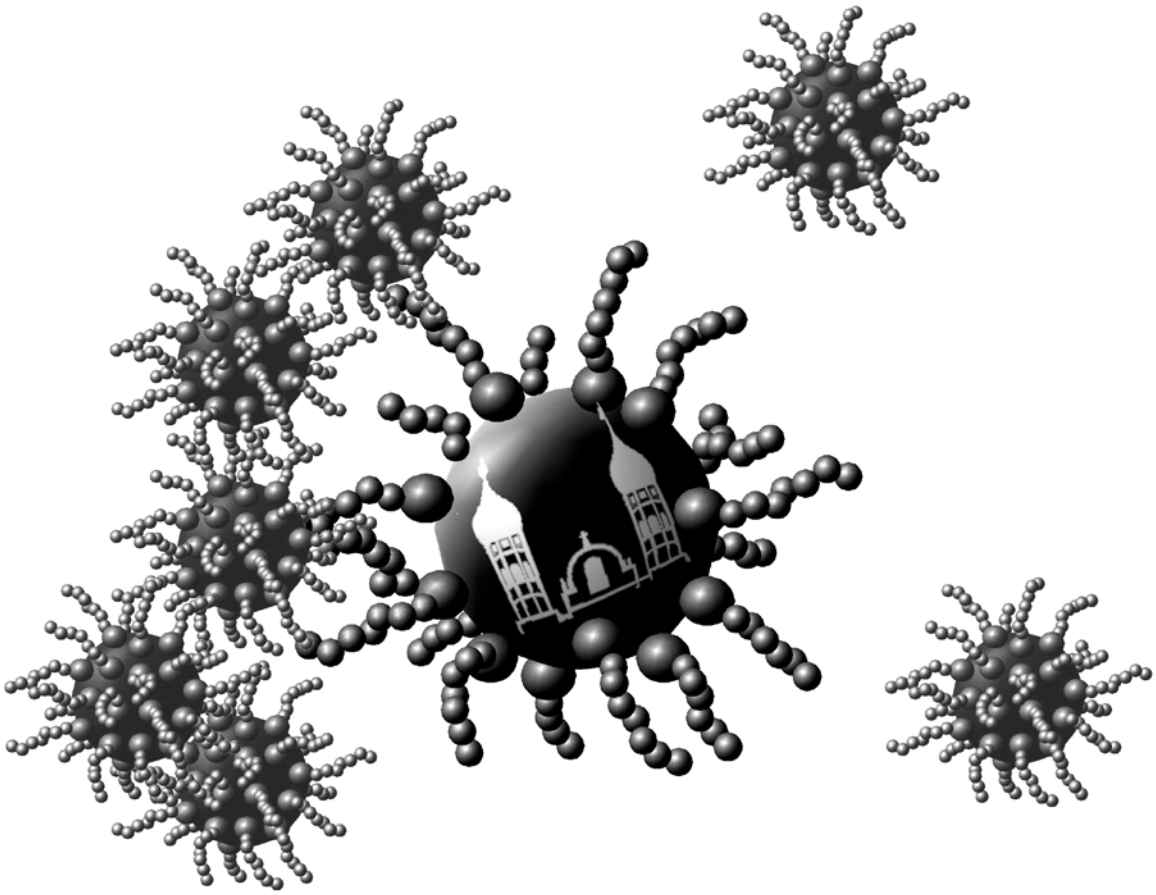

Benediktbeuern, 26.-28.9.2012

Room temperature ferromagnetism in poly(3-alkylthiophene)s with tailored regioregularity

S. Pelz[1], A. M. Schmidt[1*]

[1] *Department Chemie, Institut für Physikalische Chemie, Universität zu Köln, Luxemburger Str. 116, D-50939 Köln*
[*] *E-Mail:annette.schmidt@uni-koeln.de*

The magnetism in metal-free organic materials arises solely from unpaired s-and p-electrons and is a novel and fascinating area of research in materials chemistry.[1] Many different conceptual and synthetic strategies for this purpose are developed with more or less benefit.[2] Possible applications of such materials are on the horizont for magneto-optical switching, organic memories and spintronics.[3]
In this respect, it has recently been discovered that poly(3-alkylthiophene)s offer the possibility to combine optical and electronic characteristics with magnetic properties, as poly(3-alkylthiophene)s show room temperature ferromagnetic behavior after introduction of permanent doping charge.[4] The effect is based on the inter- and intramolecular interaction of polarons and is likely to be affected by the molecular structure (see figure 1). Furthermore, superparamagnetism is also observed for neutral poly(3-alkylthiophene)s at room temperature, whose origin to date is rather poorly understood.[5]

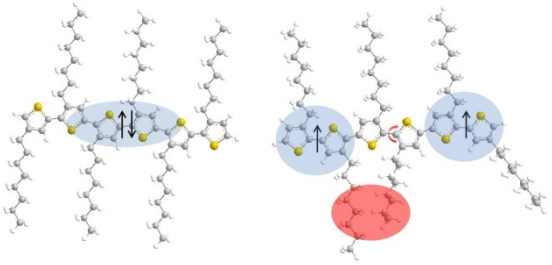

Fig.1: Schematic Illustration of polarons and bipolarons in poly(alkylthiophene)s of different regioregularity.

Our aim is to understand basic principles of these unusual room temperature molecular magnets. More information on the physical properties (e.g. optical, thermal, electrochemical and electronic) of poly(alkylthiophene)s is gained through structure-activity relationships with respect to their magnetic behavior. For this purpose, a synthetic strategy is developed that allows to tailor the sequence length of regioregular coupled monomers, i. e. to imply statistical irregularities within the electron conjugation along the chain. The regioregularity of the resulting metal-free, room temperature polymeric magnets is determined by ^{1}H NMR spectra,[6] indicating a direct correspondence with optical, thermal and electronic properties of the materials, and also with the magnetic properties. Interestingly, some samples even show magnetic hysteresis at room temperature (see figure 2).

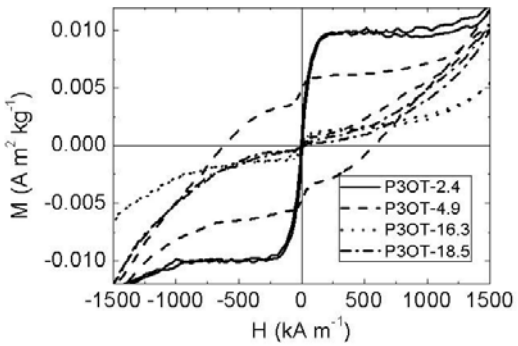

Fig.2: Experimental room temperature magnetization curves of metall-free and undoped poly(3-alkylthiophene) powder samples employing different sequence length of regioregular (HT) coupled monomers.

The magnetic properties of the metal-free polymers are investigated by vibrating sample magnetometry (VSM) and electron paramagnetic resonance (EPR). Additional, SQUID measurements at different temperatures reveal information on the T-dependent magnetic behavior of the polymers.

---

[1] S. J. Blundell, F. L. Pratt, *J. Phys.: Condens. Matter.* **2004**, 16, R771.

[2] J. A. Crayston, J. N. Devine, J. C. Walton, *Tetrahedron***2000**, 56, 7829.

[3]a)M. Fonk, B. Bräuer, J. Kortus, O. G. Schmidt, D. R. T. Zahn, G. Salvan, *Phys. Rev.* **2009**, 79, 235305. b) J. M. D. Coey, S. A. Chambers, *MRS Bulletin* **2008**, 33, 1053.

[4]O. R. Nascimento, A. J. A. de Oliveira, E. C. Pereira, A. A. Correa, L. Walmsley, *J. Phys.: Condens. Matter*.**2008**, 20, 035214.

[5]S. Vandeleene, M. Jivanescu, A. Stesmans, J. Cuppens, M. J. Van Bael, T. Verbiest, G. Koeckelberghs, *Macromolecules***2011**, 44, 4911.

[6]T.- A. Chen, X. Wu, R. D. Rieke, *J. Am. Chem. Soc.***1995**, 7, 631.

Magnetic Catalysts: Synthesis and Application

A. Gorschinski[1], R. Posselt, W. Habicht[1], S. Behrens[1]

[1] *Institut für Katalyseforschung und –technologie; Karlsruher Institut für Technologie (KIT), Postfach 3640, 76021 Karlsruhe*

Magnetic nanoparticles are interesting components of multifunctional structures and nanocomposite materials, combining superparamagnetic behaviour with fluorescent, Plasmon resonant and catalytic properties. In catalysis research, the use of magnetic nanoparticles has attracted a lot of interest for the recovery and reuse of supported homogeneous and heterogeneous catalysts after reaction by use of an external magnetic field, a new perspective for a sustainable process management.

We have developed a multi-step protocol for novel multifunctional nanocomposite particles of core/shell-type combining superparamagnetic and catalytic properties. In an initial step, functional Co nanoparticles were synthesized by thermolysis of $Co_2(CO)_8$ in the presence of various amino-functional organo siloxanes [1]. The morphology of the particles can be tuned from colloidal nanoparticles to mesoscale nanocrystal clusters, depending on the alkyl chain length of the organo siloxane. Each aggregate is composed of primary nanocrystals, which retain their superparamagnetic properties with a much higher magnetic moment.

Multifunctional mesoscaled nanocomposite particles with superparamagnetic and photocatalytic properties were prepared by consecutive coating of the aggregates with SiO_2 and TiO_2 (Figure 1). TiO_2 is a semiconductor and photocatalyst for the treatment of biological or organic pollutants in waste water.

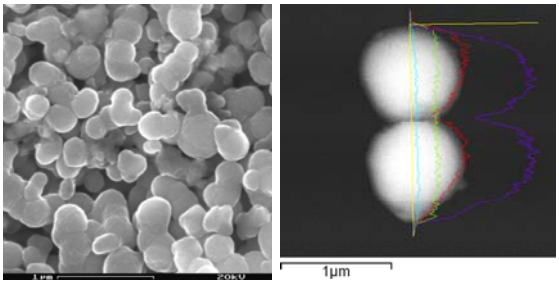

Figure 1: Magnetic $Co@SiO_2@TiO_2$ particles: SE image (left) and BSE image (right) with EDX line scan (Co violet, O red, Si green, Ti turquois).

In order to increase the photocatalytic performance, the Co core was partially etched, resulting in hollow superparamagnetic nanocomposite structures (Figure 2).

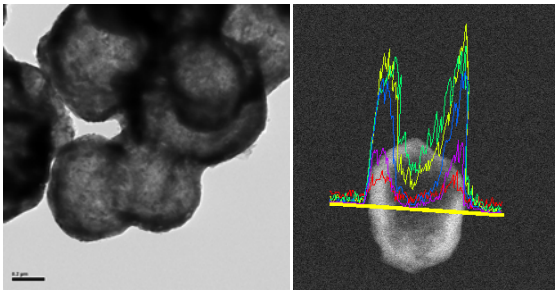

Figure 2: Hollow magnetic spheres: TEM image (left) and REM (BSE) image (right) with EDX line scan (O yellow, C red, Si green, Ti blue, Co violet).

Alternatively, Co nanoparticle were deposited in situ during nanoparticle synthesis on SiO_2 spheres (Figure 3) and eventually coated with a photocatalytically active TiO_2 layer.

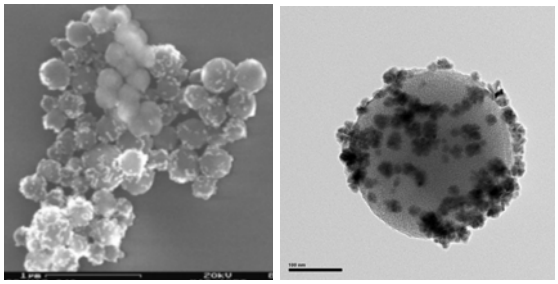

Figure 3: REM (left) and TEM (right) image of Co nanoparticles on SiO_2 spheres.

Size, crystal structure, and magnetic properties of the particles were characterized by TEM, REM/EDX, XRD, AES-ICP, and magnetic measurements (AGM). The photocatalytic properties of the materials were investigated using methylene blue as a model compound. As compared to the original $Co@SiO_2@TiO_2$ particles, these novel materials exhibit an enhanced photocatalytic activity.

References

[1] A. Gorschinski, G. Khelashvili, D. Schild, W. Habicht, R. Brand, M. Ghafari, H. Bönnemann, E. Dinjus, S. Behrens, J. Mater. Chem. 2009, 19, 8829.

Perfluoropolyether-Based Magnetic Fluids

E. Sahin, S. Behrens

Institut für Katalyseforschung und –technologie; Karlsruher Institut für Technologie (KIT), Postfach 3640, 76021 Karlsruhe

Ferrofluids reveal interesting properties for a range of technical applications including seals, coolants for loud-speakers, and inks for printers. Hence, the preparation of appropriate magnetic fluids with high saturation magnetisation, long-term stability and low viscosity is of current academic and industrial interest. MFs based on magnetic metal nanoparticles, e.g. Co nanoparticles, were shown to exhibit better magnetic properties as compared to the conventionally iron oxide-based fluids [1]. Besides the nature and content of dispersed magnetic particles, the physico-chemical properties of the carrier medium and the surfactant, e.g., vapour pressure, thermal and chemical stability, solvent miscibility and rheological properties are an important issue and impact MF performance during application. They further affect the long-term stability of the MF and a change in rheological properties (gumming) may be observed over time.

Here, we address the synthesis and properties of ferrofluids in perfluoropolyether-based carrier media with long-term stability.

Figure 1. Perfluoropolyether-based Co-MF (a) in hydrocarbon, (b) in water and (c) in silicone oil.

Initially, 8 nm-sized, superparamagnetic Co nanoparticles were obtained by thermal decomposition of $Co_2(CO)_8$ as previously described by Bönnemann et al. [1, 2].The particles were successively stabilized in perfluoropolyether-based carrier media by using appropriate surfactants.

The physico-chemical properties of the MFs were characterized by using an alternating gradient magnetometer, scanning electron microscopy, atomic-emission spectroscopy with inductively coupled plasma, dynamic light scattering, thermogravimetric analysis and a rheometer. The as-prepared Co-MFs in perfluoropolyether-based carrier oils display not only good magnetic properties but also a good thermal, chemical and long-term stability.

Acknowledgements

Financial support by the Bmbf (grant number 03X0092B) is gratefully acknowledged.

References

[1] S. Behrens, H. Bönnemann, N. Matoussevitch, E. Dinjus, H. Modrow, N. Palina, M. Frerichs, V. Kempter, W. Maus-Friedrichs, A. Heinemann, M. Kammel, A. Wiedenmann, L. Pop, S. Odenbach, E. Uhlmann, N. Bayat, J. Hesselbach, J. M. Guldbacke, Z. Phys. Chem. (2006) 220, 3 – 40.

[1] H. Bönnemann,W. Brijoux,R. Brinkmann, N. Matoussevitch, N. Waldöfner, N. Palina, H. Modrow. Inorganica Chimica Acta 350 (2003) 617 – 624.

Synthesis of Metal Nanoparticles in Room Temperature Ionic Liquids: Co Nanoparticles and Co-based Magnetic Fluids

S. Behrens[1], S. Essig[1]

[1] *Institut für Katalyseforschung und –technologie; Karlsruher Institut für Technologie (KIT), Postfach 3640, 76021 Karlsruhe*

Recently, room-temperature ionic liquids (ILs) with low melting points (<100°C) have attracted great interest, e.g. as reaction medium, reactant or template for the synthesis of inorganic Nanomaterials [1]. ILs are well known for their interesting physico-chemical properties, e.g. the low vapor pressure, good thermal stability, and high polarity. Overall, these unusual physico-chemical properties are very promising for synthetic approaches, which clearly differ from classic material synthesis, as well as for replacing conventional organic carrier media in magnetic fluids.

Usually, small, unprotected metal nanoparticles tend to instantly form aggregates and thus eventually loose their beneficial properties. Hence, surfactants or ligands are employed during nanoparticle synthesis which control both particle nucleation and growth and stabilize the particles. They coordinatively saturate the surface and ultimately determine the surface properties of the particles. Due to their high density of ionic charges and their supramolecular structure, ILs have been shown to directly control particle nucleation and growth and to further contribute to the stabilization of the nanoparticles. In this case, the absence of strongly coordinating ligands affords the controlled modification of the surface properties and accordingly functionalities of the nanoparticles after synthesis.

Herein, we address the use of Ils as a fine-tuning tool for the synthesis of metal nanoparticles [2]. We show that ILs provide a favorable environment for the synthesis of various metal nanoparticles, e.g. magnetic Co nanoparticles, without adding any further stabilizing ligands. The nature of the applied IL influences nanoparticle nucleation and growth. Thus, the impact of cation and anion on nanoparticle size and shape has been investigated systematically (Figure 1).

The surface of the nanoparticles was modified post-synthesis by adding a surfactant and the as modified particles could be extracted into conventional organic carrier media forming magnetic fluids in various oils, viz. aromatic and aliphatic hydrocarbons. The IL was recycled after synthesis and could be applied for several consecutive steps of Co nanoparticle synthesis and magnetic fluid preparation.

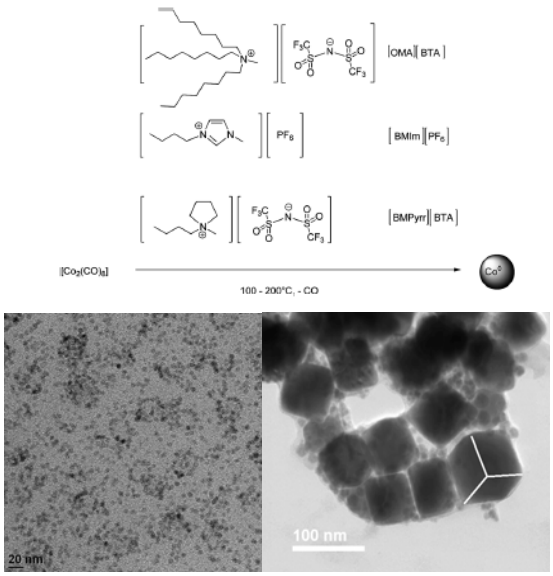

Figure 1: Spherical and cubic Co nanoparticles synthesized in [OMA][BTA] and [EMIm][BTA], respectively.

References

[1] T. Torimoto, T. Tsuda, K. Okazaki and S. Kuwabata, Adv. Mater., 2010, 22, 1196; P. Wasserscheid and T. Welton (Eds.); Ionic Liquids in Synthesis, 2007, VCH-Wiley; J. Dupont and J. Scholten, Chem. Soc. Rev., 2010, 39, 1780.

[2] S. Behrens, S. Essig, J. Mater. Chem., 2012, 22, 3811.

Formation of protein corona around magnetic nanoparticles as a temperature-controlled process

Silvio Dutz [1] and Joachim H. Clement [2]

[1] *Institut für Photonische Technologien, Albert-Einstein-Straße 9, Jena, 07745, Deutschland*
Email: Silvio.Dutz@ipht-jena.de
[2] *Klinik für Innere Medizin II, Abteilung Hämatologie und Internistische Onkologie, Universitätsklinikum Jena, Erlanger Allee 101, Jena, 07745, Deutschland*
Email: joachim.clement@med.uni-jena.de

Introduction

Nanomaterials are fascinating tools for biomedical applications. A common route to transfer pharmaceutical substances to their destination is the administration of nanoparticles (serving as drug carriers) loaded with suitable drugs to the peripheral blood. When exposing these nanomaterials, e.g. superparamagnetic iron oxide nanoparticles (SPION), to the peripheral blood a protein corona consisting of various components is formed immediately. The composition of corona as well as their amount bound to the particle surface is dependent on different factors, e.g. particle size and surface charge [1]. Composition of formed protein corona might be of major importance for cellular uptake of magnetic nanoparticles [2,3]. A less investigated factor is the influence of temperature on the protein corona formation.

Aims

The aim of these initial experiments is to analyse the importance of temperature on the formation as well as the composition of the protein corona during *in vitro* serum incubation. Vision of these investigations is the preparation of highly biocompatible corona coated magnetic nanoparticles by means of a defined pre-treatment, e.g. incubation with serum.

Methods

SPION were prepared following the alkaline precipitation route and coated with different shells (amino-dextran, dextran, and carboxymethyl-dextran). The obtained core/shell nanoparticles were incubated in fetal calf serum (FCS) at 50°C, 37°C, and 15°C. 50°C and 37°C were realized by magnetic heating (hyperthermia) of the SPION within the serum in an alternating magnetic field (f = 400 kHz and H = 24 kA/m). 37°C and 15°C were achieved by adding the SPION to FCS with the desired temperature. The SPION were incubated for 15 minutes and then cooled down to room temperature. Before incubation and after washing the incubated nanoparticles by magnetic separation and resuspension in phosphate-buffered saline the zeta potential and the magnetic concentration of the incubated particles were determined. A part of the nanoparticle solution was applied to a TBS polyacrylamide gradient gel (4-12%) under denaturing conditions and protein bands were visualized by Coomassie blue staining.

Results

Applied SPION have a magnetic core size of around 9 nm (XRD, VSM) and the core/shell particles show a hydrodynamic diameter of about 100 nm (PCS, z-average). At field parameters f = 400 kHz and H = 24 kA/m the specific heating power of the uncoated particles is 105 W/g. Table 1 shows the zeta potential as function of incubation temperature for selected samples (CM-Dextran coated). It is clearly demonstrated that incubation temperature has an explicit influence on the composition of the corona. The electrophoretic analysis of the components of the protein

corona shows a more or less similar behaviour at first glance (Figure 1).

Table 1: Zeta potential of carboxymethyl-dextran coated SPION before and after FCS incubation.

sample	heating	zeta (mV)
no incubation	-	-19.5
15 °C	bath	+0.1
37 °C	bath	-35.4
37 °C	magnetic	-34.9
50 °C	magnetic	-12.7

The predominant protein is serum albumin with its derivatives. The SPION which were treated with hyperthermia contain more protein than nanoparticles exposed to external heating. The general overview showed no differences with regard to the charge/type of the nanoparticle shells. This observation needs more detailed analysis of the distinct proteins which are involved in corona formation.

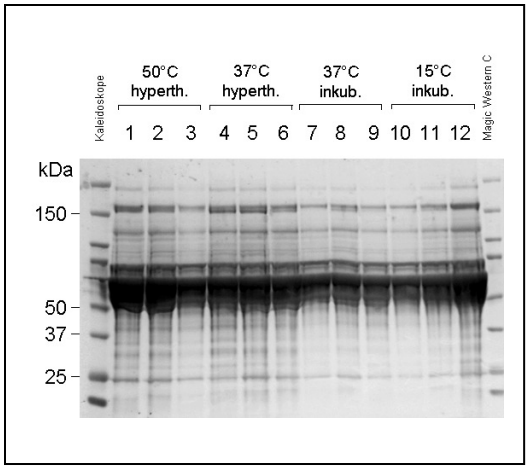

Figure 1: Electrophoretic separation of protein corona components from nanoparticles after treatment with FCS under various temperature conditions (1, 4, 7, 10: carboxymethyl-dextran SPION; 2, 5, 8, 11: amino-dextran SPION; 3, 6, 9, 12: dextran SPION)

Conclusion

The formation of the protein corona is dependent on the incubation conditions. We show that the incubation temperature affects the corona formation and might be an interesting parameter to modulate the composition and nature of the protein corona. Beside the absolute temperature, the heating regiment of the SPIONs within the serum is an additional important influencing factor.

In this proof-of-principle investigation we found first very promising results regarding the influence of temperature as well as the type of heating on corona formation. Due to the possibility of heating by magnetic losses (additionally to the external heating) magnetic nanoparticles are very interesting model particles for ongoing investigations.

Acknowledgements

This work was supported in part by Interdisziplinäres Zentrum für Klinische Forschung (IZKF) Jena.

References

[1] S. Tenzer et al., Nanoparticle Size Is a Critical Physicochemical Determinant of the Human Blood Plasma Corona: A Comprehensive Quantitative Proteomic Analysis, ACS Nano 5(9): 7155-67, 2011.

[2] X. Jiang et al., Quantitative Analysis of the Protein Corona on FePt Nanoparticles formed by Transferring Binding, J R Soc Interface 7(Suppl1): S5-S11, 2010

[3] A. Lesniak et al., Serum Heat Inactivation affects Protein Corona Composition and Nanoparticle uptake, Biomaterials 31(36) : 9511-8, 2010

A new route for biomedical coating of magnetic nanoparticles using layer-by-layer technique

E.-M. Prinz[1], R. Szamocki[2], V. Nica[1,3], R. Hempelmann[1]

[1] *Physical Chemistry, Saarland University, Saarbrücken, Germany*
[2] *Atotech Deutschland GmbH, Berlin*
[3] *Faculty of Physics, Alexandru Ioan Cuz, University, Iasi, Romania*

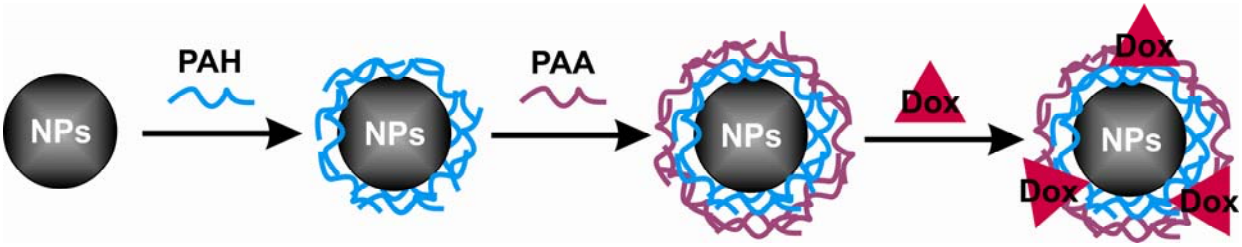

Schematic illustration of LbL assembly for building up a drug delivery system, with nanoparticles as magnetic core and doxorubicin as chemotherapeutic drug.

Bio-functionalized magnetic nanoparticles have been investigated intensively in the recent years due to their multifunctional applications in hyperthermia, drug delivery, protein and cell separation or magnetic resonance imaging. The method of preparation plays a major role to the structural, magnetic and biocompatibility properties of nanostructures [1]. Spinel magnetic nanoparticles, synthesized by co-precipitation, have been coated alternately with poly(allylamine hydrocloride) and polyacrylic acid using the layer-by-layer technique [2].

Transmission electron microscopy (TEM), Fourier-Transform Infrared spectroscopy (FTIR), Zeta-potential and Dynamic Light Scattering (DLS) were used to substantiate the coating and the colloidal stability of the nanoparticles. Because of its auto-fluorescence doxorubicin was used as model drug. The successful covalent bonding of the drug to the coated particles was verified by using FT-IR, UV/VIS, fluorescence spectroscopy, Zeta-potential measurements and DLS. The system combines magnetic properties with the therapeutic efficiency, an attractive feature for future drug delivery applications.

References

[1] Q. Song and Z. J. Zhang, J. Am. Chem. Soc. **134**, 10182 (2012).
[2] G. Decher, Science **277**, 1232 (1997)

Effect of iron-oleate decomposition rate and temperature on size distribution and magnetic performance of iron oxide nanoparticles

A. Lak, F. Ludwig, J. M. Scholtyssek, J. Dieckhoff, and M. Schilling

Institut für Elektrische Messtechnik und Grundlagen der Elektrotechnik, TU Braunschweig, Hans-Sommer-Str. 66, 38106 Braunschweig

Introduction

Magnetic nanoparticles (MNPs) have gained significant attention in the last two decades due to their exceptional properties. Since the MNPs technological and scientific importance has been realized, there has been an substantial effort to synthesize MNPs in a dimensionally and magnetically controlled fashion. Thermal decomposition of iron-oleate precursor has been proposed as an environmentally friendly procedure for the fabrication of iron oxide nanoparticles with different shapes and sizes in a reproducible manner [1]. However, the influence of the thermal decomposition behavior of iron-oleate on particle size distribution and magnetic performance has not been completely understood.

This study aims to explore the effect of iron-oleate's decomposition pathways, determined by reaction temperature and heating rate, on size distribution and magnetic performance of iron oxide MNPs.

Synthesis procedure

The iron-oleate precursor was synthesized according to our recipe described in [2].

In this study, iron oxide MNPs with different size distributions and magnetic properties were fabricated using a slightly modified recipe described in [2]. By changing the reaction temperature from 317°C to 351°C and the heating rate from 1°C/min to 2°C/min, single core iron oxide MNPs with various size distributions were synthesized which are readily dispersible in nonpolar solvents.

Characterization

The particle core size distribution and morphology were characterized by Transmission Electron Microscopy (TEM). The sample net magnetic moment m_{sample} was explored by measuring the flux density B using a fluxgate-based measurement setup [3]. In a typical measurement, a DC magnetic field $\mu_0 H$ is swept from zero to 10 mT in two seconds and B at the given distance from the sample is measured.

Results and discussions

Typical TEM images of the sythesized iron oxide nanoparticles with their corresponding size histograms are depicted in Fig. 1. The particles synthesized at 317°C via slow decomposition of iron-oleate (i.e. 1°C/min) (Fig. 1(a)) show a broad size distribution with a mean core diameter of 14 nm. According to our previous study on the decomposition of iron-oleate [2], both nucleation and growth processes occur in an abrupt and quick step launching at $\approx$ 317°C and terminating at $\approx$ 347°C. Therefore, by aging the synthesis mixture at 317°C, a gradual and time dependent decomposition of iron-oleate happens. This results in low monomer supply, multi-step nucleation, and slow growth. Conversely, the particles nucleated and grown at 337°C with the same heating rate (Fig. 1(b)) reveal a much narrower size distribution and shape uniformity with the average core diameter of 22 nm. It appeares that these particles went through completely different nucleation and growth mechanisms characterized

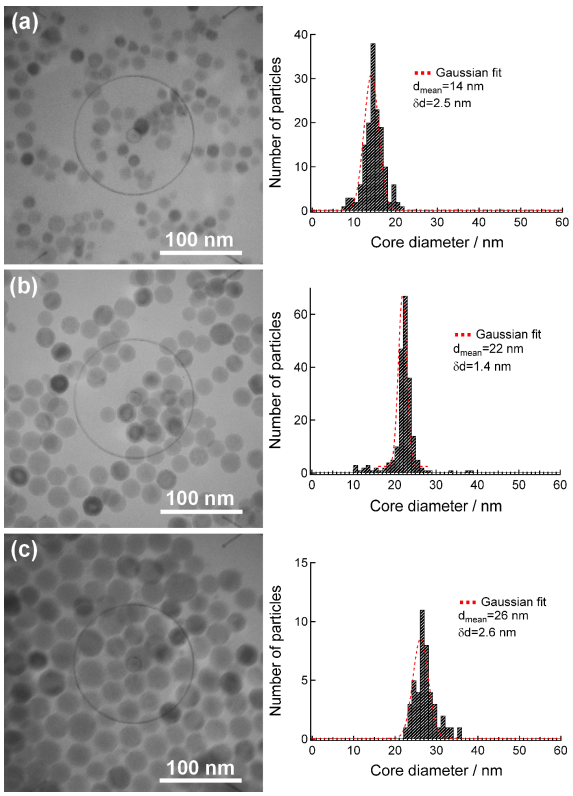

Fig. 1: Typical TEM micrographs of the synthesized MNPs and their corresponding size histograms.

by sudden nucleation and fast growth. However, the presence of a very small portion of particles with core diameters < 15 nm is discernible which may have been caused by an additional nucleation step. By decomposition of the precursor at 351°C with the heating rate of 2°C/min, particles with a mean core diameter of 26 nm were obtained (Fig. 1(c)). However, the size distribution is slightly broader compared to the ones synthesized at 337°C at the heating rate of 1°C/min.

The flux densities measured on particle suspensions are demonstrated in Fig. 2. The flux density B is proportional to the particle's saturation magnetization via [2]

$$\frac{B}{V_{mean}} \propto M_s^2, \qquad (1)$$

in which V_{mean} is the mean core volume. By looking at the $\frac{B}{V_{mean}}$ values at the linear magnetization regime (listed in Fig. 2), one can qualitatively compare the magnetic properties of the particles. Unexpectedly, the particles with bigger core sizes reveal an inferior

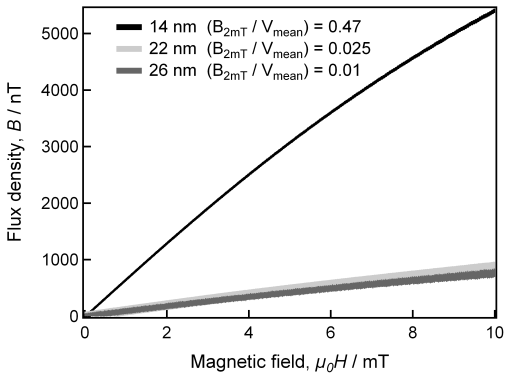

Fig. 2: Flux density B of 150 μL particle's suspensions with 70 mM Fe concentration.

magnetic performance compared to the ones with smaller core sizes. This phenomenon could be linked to the formation of bigger antiferri(o)magnetic wüstite cores with further particle growth.

Conclusion

The iron oxide MNPs with tunable size distributions and magnetic properties have been synthesized by chosing different iron-oleate decomposition pathways.

Acknowledgments

This work was financially supported by the DFG via SFB 578. Financial support by the International Graduate School of Metrology at Braunschweig (igsm) for PhD thesis (A.L.) is appreciated.

References

[1] M. V. Kovalenko, M. I. Bodnarchuk, R. T. Lechner, G. Hesser, F. Schäffler, and W. Heiss. *J. Am. Chem. Soc.*, 129:6352, 2007.

[2] A. Lak, F. Ludwig, J. M. Scholtyssek, J. Dieckhoff, K. Fiege, and M. Schilling. IEEE Trans. Magn. (submitted).

[3] J. Dieckhoff, M. Schilling, and F. Ludwig. *Appl. Phys. lett.*, 99:112501, 2011.

Synthesis of iron oxide particles for magnetic fluids by ultrasonic aerosol assisted pyrolysis

M. Besser[1], J. Schipp[1], J. Linke[1], S. Odenbach[1]

[1] *Institute of Fluid Mechanics, Chari of Magnetofluiddynamics, 01062 Dresden, Germany*

Introduction and Background

The research in nanoscience has developed vastly in the past years. Magnetic nanoparticles are found in numerous applications, like ferrofluids, catalysts or medical drug carriers. With the growing interest in nanoscience the question arises: how nanoparticles with specific tailor-made properties can be synthesized for a systematic and targeted research. This project investigates the feasibility of an ultrasonic aerosol assisted pyrolysis (UAAP) process [1] as a new synthesis method for size-controlled Fe_3O_4 particles.

Synthesis method

An aqueous precursor solution of dilute iron(III) chloride, $FeCl_3$ and ethanol is atomized by an ultrasonic aerosol generator. The precursor aerosol is carried into a heated reaction zone where the droplets react to solid iron oxide particles at appr. 750 °C. At the end of the reaction zone the particles are collected from the inert gas in an acetic solution. They can be transferred, coated and concentrated further with oleic acid and kerosene.

Preliminary results

The particle size depends on the concentration of the precursor salt and the droplet size of the aerosol which can be controlled by the ultrasonic frequency. Figure 1 shows a SEM-image of the particles from the first experiments at an atomization frequency of 1.7 MHz. The magnetisation curve given in figure 2 confirms magnetite or maghemite in the particles due to the positive susceptibility and saturation. The mean particle size calculates to 67 nm.

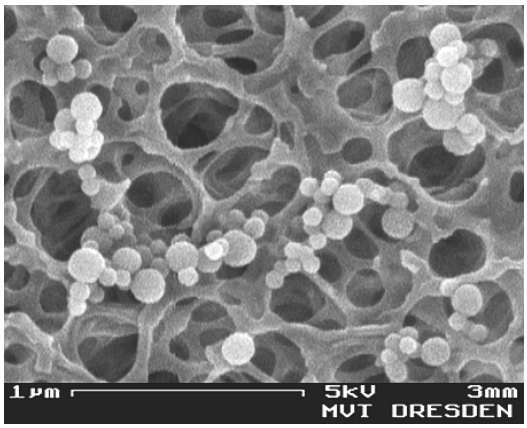

Fig. 1: SEM-image of iron oxide particles synthesized from a 0.3 mmolar iron chloride solution with 5m% ethanol, atomized at 1.7 MHz.

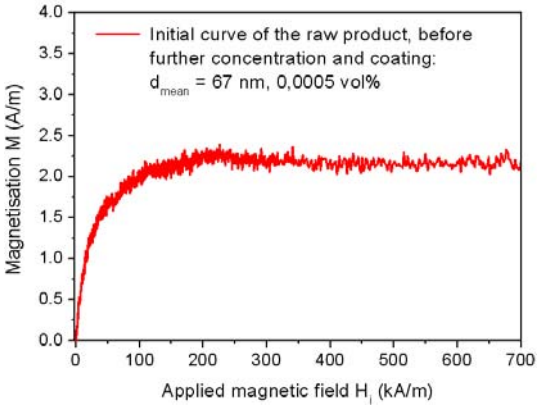

Fig. 2: Initial magnetisation curve of the particles, prior further treatment.

Outlook

The subsequent work will focus on the improvement of the efficiency of the method and the particle size distribution at higher ultrasonic frequencies (2.4 MHz).

References

[1] J. H. Bang, K.S. Suslick (2010), Adv. Mater. 22, 1039–1059.

Surfactant-free alloy ferrofluids by laser ablation of solid magnets in organic liquids and subsequent matrix embedding

J. Jakobi[1], S. Barcikowski[1]

[1] *University of Duisburg-Essen and Center for Nanointegration Duisburg-Essen (CENIDE), Faculty of Chemistry, Technical Chemistry I, Universitaetsstr. 7, 45141, Essen, Germany*

In the recent years a huge demand on functionalized ferrofluids with specific properties has arisen. In this context we present a one-step synthesis of ligand-free magnetic alloy nanoparticles in organic liquids, including the possibility of subsequent or in situ conjugation to polymer matrices. Specially designed colloids have attracted a lot of attention because of their use for biomedical, energy storage, or transformation applications. The combination of optical, electronic, catalytic, and biologically compatible properties/characteristics in a single nanoparticle may play an important role in tailoring nanoparticles for future applications.[1] Additionally, a combination of magnetic behavior with these properties provides a powerful tool for the manipulation and control of colloids during a wide range of applications.[1, 2]

The most common techniques to produce such colloids in the presence of surfactant and reducing agents is based on the chemical reduction of a precursor mixture.[3] Unfortunately, contamination of the product with organic remnants/residues from this synthesis is very difficult to avoid and it is nearly impossible to completely clean the nanoparticle surface.[4] This leads to a decrease of the active surface area of the nanoparticles and especially in the case of catalysis and biomolecule-binding this has a negative impact on the product quality.[5] Besides, the wet chemical synthesis procedure is not always suitable for creating specially designed materials because of e.g. complicated reaction mechanisms, incompatibility of the environmental conditions

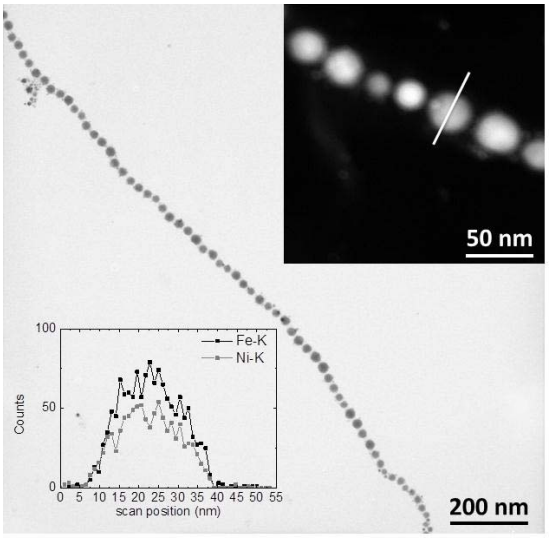

Fig. 1: TEM micrograph of laser-generated ligand-free Ni-Fe-nanoparticles. Insert: STEM-HAADF image with a line scan of element distribution in the alloy nanoparticle.

required for each precursor, or the unavailability of appropriate precursors.

Here we present an alternative method for the generation of specially tailored magnetic colloids by laser ablation of solid targets in liquids.[6, 7] This technique is already well known since the early Nineties and provides access to different kinds of nanoparticles consisting of e. g. metals, ceramics or organic polymers. This physical method enables the generation of nanoparticles in almost every liquid and gives access to diverse colloids.[7] Since target materials and solvents are available in high purity, the synthesized nanoparticles have very clean and reactive surfaces.[5] Because of this, laser-generated nanoparticles can be functionalized with dedicated quantities of appropriate ligands

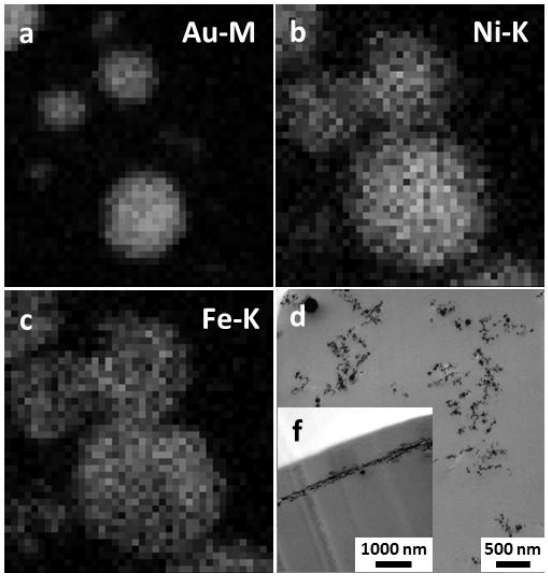

Fig. 2: Element maping of laser-generated Au@NiFe core-shell nanoparticles with a) Au b) Ni and c) Fe element distribution. Magnetic nanoparticles embedded in polymer d) without and f) with external magnetic field.

or stabilizing agents and as a result have a huge potential for the use in the bio- medical field or in catalysis.[8]

The versatile potential of this method also offers the opportunity to generate magnetic metal or metal oxide nanoparticles.[9] Additionally, laser ablation of an alloy target can also lead to alloy nanoparticles as it is illustrated in figure 1. It is shown that even magnetic alloy Ni-Fe nanoparticles with a permanent magnetic moment (coercivity of 59 Oe at 300 K), a size of 30 nm and homogenously distributed elements can be produced in this one-step synthesis.[10]

Furthermore, fabrication of nanoparticles with more complicated ultra-structures, such as core-shell, can be carried out by selecting appropriate target materials and ablation conditions. An exemplary element mapping of a Au@NiFe core-shell nanoparticle is shown in figure 2 (a-c). This element mapping clearly shows that during the laser ablation process nanoparticles with a gold core and a nickel-iron shell are formed. Via changing the ablation conditions, the ablation process can also induce the formation of core-shell structure with the element distributions inverted. In this case the oxidation of the magnetic core could be prevented by the gold shell.

As further possibility is ablating nanoparticles in suitable solvent/polymer combination or directly in monomers, after which the generated nanoparticle could be transferred into polymer matrix as is shown in figure 2 (d-f) by polymerization reaction.

These findings clearly indicate that laser ablation in liquids is a suitable tool for synthesizing diverse magnetic nanoparticles with different properties and can be viewed as an alternative method for generating of magnetic colloids.

References

[1] M. B. Cortie and A. M. McDonagh, *Chem. Rev.* **2011**, 111, 3713

[2] R. Ferrando, J. Jellinek, and R. L. Johnston, *Chem. Rev.* **2008**, 108, 845

[3] N. Pazos-Pérez, B. Rodríguez-González, M. Hilgendorff, M. Giersig, and L. M. Liz-Marzán, *J. Mater. Chem.* **2010**, 20, 61

[4] J. A. Lopez-Sanches, N. Dimitratos, C. Hammond, G. L. Brett, L. Kesavan, S. White, P. Miedziak, R. Tiruvalam, R. L. Jenkins, A. F. Carley, D. Knight, C. J. Kiely, and G. J. Hutchings, *Nature Chem.* **2011**, 3, 551

[5] P. Wagener, A. Schwenke, and S. Barcikowski, *Langmuir* **2012**, 28, 6132

[6] S. Barcikowski, F. Mafune, *J. Phys. Chem. C* **2011**, 115, Nr. 12, 4985

[7] H. Zeng, X.-W. Du, S. C. Singh, S. A. Kulinich, S. Yang, J. He, and W. Cai, *Adv. Funct. Mater.* **2012**, 22, 7, 1333

[8] S. Petersen, S. Barcikowski, *Adv. Funct. Mater.* **2009**, 19

[9] V. Amendola, P. Riello, and M. Meneghetti, *J. Phys. Chem. C* **2011**, 115, 5140

[10] J. Jakobi, S. Petersen, A. Menéndez-Manjón, P. Wagener, and S. Barcikowski, *Langmuir* **2010**, 26 (10), 6892

Magnetic properties of magnetic particles diluted in water and in liquid crystals

Fabiana R. Arantes[1], Carlos A. Ramos[2], Daniel R. Cornejo[1]

[1] *Institute of Physics, University of Sao Paulo, Brazil*
[2] *Centro Atomico Bariloche, San Carlos de Bariloche, Argentina*

Lyotropic liquid crystals are constituted by aggregates of amphiphilic molecules that show long-range orientational order. In the nematic phase, for example, there are anisotropic micelles that on average are ordered along some privileged direction. Modifications in this ordering can be induced by application of intense magnetic fields ($\sim 10kOe$), however it is known that the doping of the lyotropic liquid crystals with magnetic nanoparticles, with concentrations as diluted as one particle per 10^6 micelles, reduces this field by a factor of 10^3 [1]. Recently, our work also showed that in those systems magnetic measurements can give information about the phase transition of liquid crystals [2]. In this work we used magnetization versus temperature curves, ferromagnetic resonance, hysteresis loops and Δm on systems composed by magnetite nanoparticles diluted at the same concentration in water (ferrofluid) and in liquid crystal to explore the magnetic behavior of those nanoparticles in those different media. We used the commercial water based ferrofluid EMG605 from Ferrotec and lyotropic liquid crystals made with laurate potassium soap.

In figure 1 we can see that in the magnetization curves it was possible to distinguish the nematic from the isotropic phase since the magnetization of the nanoparticles mimics the bell-shape displayed by the nematic orientational order parameter in the pure liquid crystal.

In the resonance measurements, we observed that the ferrofluid sample showed a wider spectra than that corresponding to the liquid crystal. This can be seen as an evidence of the effect of the liquid crystal, that constrains the spatial configuration of the nanoparticles, thus increasing their overall ordering and consequently decreasing the distribution of resonant fields. This could also be related to a more pronounced dipolar interaction in ferrofluid sample, that was observed in the Δm curves, where the ferrofluid sample showed a more negative curve than that of the liquid crystal, as we can see in figure 2.

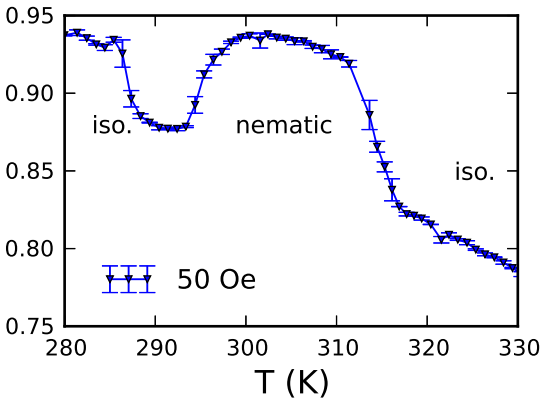

Figure 1: Magnetization versus temperature curves for the liquid crystal and ferrofluid samples.

Acknowledgments

The authors thank professor Antonio Martins Figueiredo Neto and FAPESP for supporting this work.

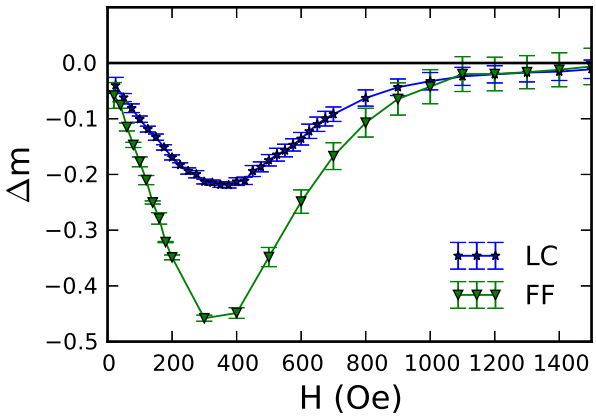

Figure 2: Δm curves for the liquid crystal and ferrofluid samples.

References

[1] F. Brochard, P. G. de Gennes, J. Physique **31**, 691 (1970).

[2] F. R. Arantes, A. M. Figueiredo Neto and D. R. Cornejo, Journal of Applied Physics **109**, 07E315 (2011).

Characterisation of multicore magnetic nanoparticles

D. Eberbeck[1], R. Müller[2], C. Schmidt[2], H. Kratz[3] and L. Trahms[1]

[1] *Physikalisch-Technische Bundesanstalt, Braunschweig und Berlin, Germany*
[2] *Institut für Photonische Technologien, Jena, Germany*
[3] *Charité, Berlin , Germany*

Introduction

Beside single core magnetic nanoparticles (MNP) also multicore MNP gained attention because of a large variety in structure. This opens the possibility to produce MNP well tuned for a given application. Here, we will investigate two multicore systems the cluster structure of which differs strongly. In particular, we will relate the the magnetic moment (in terms of magnetic diameter), to the physical structure comprising the sizes of the cluster and the cluster forming single cores as well as its packing density within the clusters.

Materials and methods

In the present work we investigated two ferrofluids composed of multicore MNP namely Resovist® (Bayer Health Care) and fluidMAG-HAES (chemicell) and one fluid, MNP1, composed of citrate coated single core MNP referred to as control system. From the molecular structure of the coatings we roughly estimated the thicknesses of the coating layers, δ_l, to be about 0.5 nm in case of citrate (MNP1) and 4.5 nm in case of carboxymethyldextran (for Resovist®) and starch (for fluidMAG-HAES).

For all size distributions, we assumed spherical particles with diameters d obeying a lognormal function, $f(d)$, here characterized by the diameter of the mean volume, d_V, and the dispersion parameter σ.

The distributions of the core diameters d were estimated from TEM-data analysing only well defined single cores. Alternatively, we obtained the core size *distribution* in terms of crystallite sizes, as well, analysing the Debye-Scherrer-line profiles measured with a X-ray diffractometer X'Pert Pro MPD.

The distribution $f(d_m)$ of the effective magnetic diameters d_m referring to the diameter of a fictive single domain sphere with the saturation magnetisation M_S was estimated analysing M(H) and Magnetorelaxometry (MRX) data [1].

Results and discussion

The core and crystallite size distributions estimated by TEM and by XRD agree roughly in case of MNP1 and fluidMAG-HAES where the relation between the mean volume crystallite diameters $\bar{d}_{V,cr}$ and core diameters $\bar{d}_V$ amounts to $\bar{d}_{V,cr}/\bar{d}_V \approx 0.84(5)$ and $\sigma_{cr}/\sigma \approx 1.5(2)$ (Fig. 2a,b). For DDM128, the precurser of Resovist®, on the other hand, f_{cr} is found to be (at least) bimodal (Fig. 2c), also visually indicated by the significant deviation of the shape of the Debye-Scherrer-lines from that of single core system MNP1 (Fig. 1).

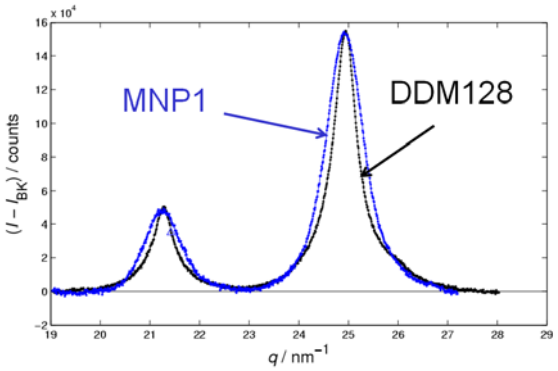

Figure 1: XRD-intensity pattern after subtraction of background intensity I_{BK} for MNP1 and DDM128 being the particle base of Resovist®.

From hydrodynamic diameters d_{hyd} we estimated the diameters $d_c = d_{hyd} - 2\delta_l - 2\delta_s$ (model in Fig. 2c), where δ_s is the thickness of the solvation layer of about 2 nm. The relations of the means $\bar{d}_{V,c}$ and $\bar{d}_V$ (Tab. 1) clearly indicate that the MNP of fluidMAG-HAES and Resovist appears to

be multicore- or cluster-MNP rendering d_c to a cluster diameter. The MNP of the system MNP1 appears to be mainly single core MNP.

Table 1: Mean volume diameters of cores, $\bar{d}_V$, clusters, $\bar{d}_{V,c}$, and magnetic equivalent particles, $\bar{d}_{V,m}$.

Sample	$\bar{d}_V$	$\bar{d}_{V,c}$	$\bar{d}_{V,m(2)}$
	nm	nm	nm
MNP1	6.4(2)	10(2)	7.1(1)
fluidMAG-HAES	8.7(3)	63(7)	15(1)
Resovist	4.6(2)	39(3)	22(1)

The magnetic size distributions of these systems, derived from *M*(*H*)-data, are bimodal for Resovist and fluidMAG-HAES where the second mode, representing the larger MNP, is quantitatively supported by MRX-data (Fig. 2b,c). Note that present MRX-setup is insensitive for MNP smaller than about 18 nm (magnetite). While the equivalent magnetic diameter of MNP1 matches the core size the mean of the second mode, $\bar{d}_{V,m2}$, of fluidMAG-HAES and Resovist range between $\bar{d}_V$ and $\bar{d}_{V,c}$ (Tab. 1, Fig. 2b,c).

Applying a model of *n* randomly oriented identical moments of the single cores, μ, the total moment of the cluster reads $\mu_c = \sqrt{n}\mu$. Combining $\bar{d}_V$, $\bar{d}_{V,c}$, $\bar{d}_{V,m2}$ we calculated the volume fraction of single cores within mean clusters to

$$\phi_c = \bar{d}_{V,m2}^6 / \left(\bar{d}_V^3 \, \bar{d}_{V,c}^3\right) \qquad (1)$$

The low value of 0.07 for fluidMAG-HAES indicates a loose MNP packing. For Resovist we found ϕ_c=20! Only applying $\bar{d}_V = 14\,\text{nm}$ which is close to observed larger mode of crystal size, $\bar{d}_{V,cr2} = 11(2)\,\text{nm}$, the model (Fig. 2c) may describe the observations for Resovist, assuming a rather compact cluster structure with a reasonable packing fraction of ϕ_c=0.7.

In conclusion, the combination of core size, cluster size and effective magnetic size allows the estimation of the inner structure of cluster MNP.

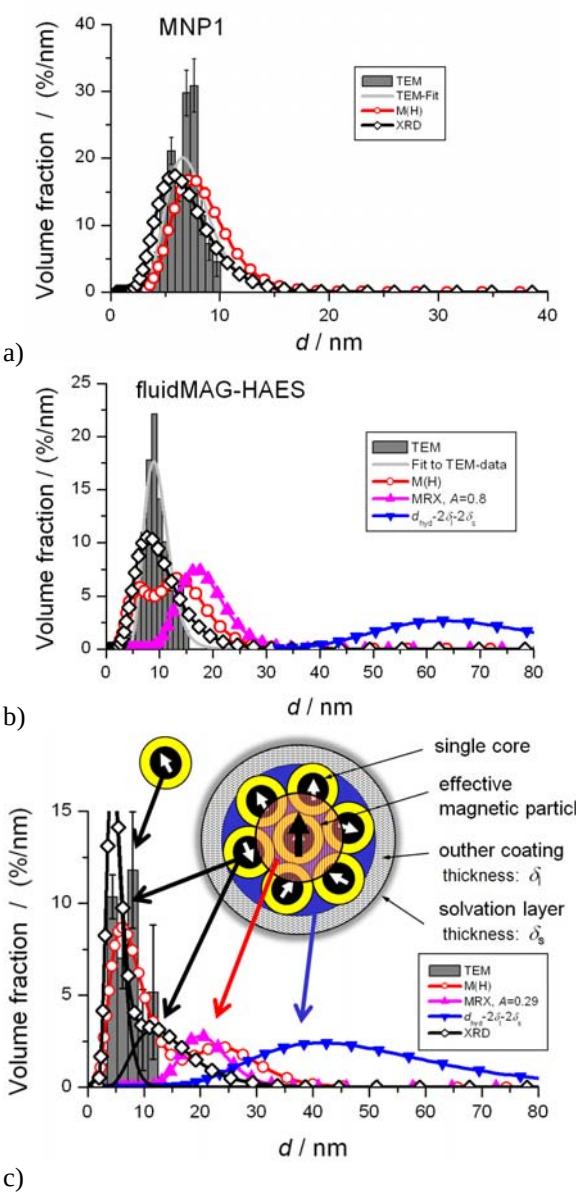

Figure 2: Distribution of core and crystallite sizes, obtained by TEM and XRD, effective magnetic diameters, obtained by M(H) and MRX, as well as physical diameters of cluster-MNPs estimated from DLS-data for MNP1 (a), fluidMAG-HAES (b) and Resovist (c). The drawing in (c) illustrates a model for the sample consisting of single core MNP and cluster-MNP where the arrows relate the structure components to observed size distributions.

Acknowledgements

The research was supported by the German Ministry for Education and Research (FKZ 13N11092), and by the German Research Foundation (KFO 213).

References

[1] D. Eberbeck, F. Wiekhorst, U. Steinhoff, L. Trahms, J. Phys.: Condens. matter 18 (2006), S2829-S2846.

Micromagnetic simulations as a reliable tool for predicting static and dynamic properties of mesoscopic ferromagnetic particles

D.V. Berkov[1]

[1] *Innovent Technology Development, Prüssingstr. 27B, D-07749, Jena, Germany*

1. Basic micromagnetic concept and main energy contributions

Theoretical micromagnetics [1] is a phenomenology for the evaluation of the magnetic free energy E_{tot} of a ferromagnet (FM) if its geometry, material parameters and magnetization state $\mathbf{M}(\mathbf{r})$ are known. In its 'standard' version, micromagnetics takes into account four energy contributions – energy E_{ext} in the external field $\mathbf{H}_{\text{ext}}$, magnetocrystalline anisotropy energy E_{an}, the exchange stiffness energy E_{exch} and the energy of the magnetodipolar interaction between magnetic moments of the ferromagnet:

$$E_{\text{tot}} = E_{\text{ext}} + E_{\text{an}} + E_{\text{exch}} + E_{\text{dip}} \qquad (1)$$

Other terms (e.g., the surface anisotropy) – can also be included.

Analytical expressions for the energy terms (1) may be derived on a very general basis using only a few assumptions about the energy behaviour with respect to the time inversion, the crystal symmetry, and the invariance properties of the exchange interaction with respect to the space transformations:

$$E_{\text{ext}} = -\int_V \mathbf{H}_{\text{ext}}(\mathbf{r}) \cdot \mathbf{M}(\mathbf{r}) dV \qquad (2)$$

$$E_{\text{an}}^{\text{un}} = -\int_V K_{\text{an}}(\mathbf{r}) \cdot [\mathbf{m}(\mathbf{r}) \cdot \mathbf{n}(\mathbf{r})]^2 \cdot dV \qquad (3)$$

$$E_{\text{exch}} = A \int_V \left[(\nabla m_x)^2 + (\nabla m_y)^2 + (\nabla m_z)^2 \right] dV \qquad (4)$$

$$E_{\text{dip}} = -\frac{1}{2} \int_V \mathbf{M}(\mathbf{r}) \cdot \mathbf{H}_{\text{dip}}(\mathbf{r}) \cdot dV \qquad (5)$$

Here K_{an} is the magnetocrystalline anisotropy constant (in (3) the uniaxial anisotropy is assumed), $\mathbf{m} = \mathbf{M}(\mathbf{r})/M_S$ (M_S is the material saturation magnetization), $\mathbf{n}_{\text{an}}$ – the unit vector of the anisotropy axis and A - the exchange stiffness constant. Magnetodipolar interaction field $\mathbf{H}_{\text{dip}}$ is calculated by integration of contributions from all parts of a ferromagnet. A very important role plays also a concept of the total effective field $\mathbf{H}_{\text{eff}} = \mathbf{H}_{\text{ext}} + \mathbf{H}_{\text{an}} + \mathbf{H}_{\text{exch}} + \mathbf{H}_{\text{dip}}$. Here each field term can be evaluated as the functional derivative of the corresponding energy term (2)-(5) over the magnetization as $\mathbf{H} = -\partial E / \partial \mathbf{M}$. This field is not only absolutely necessary in dynamical simulations, but is also very helpful when solving static problems (see below), because from the mathematical point of view $\mathbf{H}_{\text{eff}}$ is the energy gradient.

2. Evaluation of the equilibrium magnetization configurations

Solution of the main static problem - find the equilibrium magnetization state $\{\mathbf{M}(\mathrm{r})\}$ of a FM under given external condition - requires 'only' the minimization of the energy (1) with respect to $\{\mathbf{M}(\mathrm{r})\}$. Due to the non-locality of the functional (1) the corresponding task can be solved analytically only for a very few simplest cases [1], so that any practically relevant problem requires *numerical* solution.

There exist two main alternatives for handling of this problem: (i) the so called finite difference method (FDM), which uses a translationally invariant rectangular grid and (ii) the finite element method (FEM), employing the arbitrary tetrahedron mesh. The main advantage of FDM is its simplicity (e.g., the long-range magnetodipolar interaction can be computed using the fast Fourier transformation (FFT) technique), its main drawbacks - a poor approximation of complicated sample shapes by a rectangular mesh. In contrast, FEM allows an accurate approximation of any shape, but the price to pay is highly sophisticated and

much slower methods for the evaluation of exchange and magnetodipolar energies. For this reason FDM is normally used for simple sample geometries and large sample sizes, FEM – for small systems with complicated shapes.

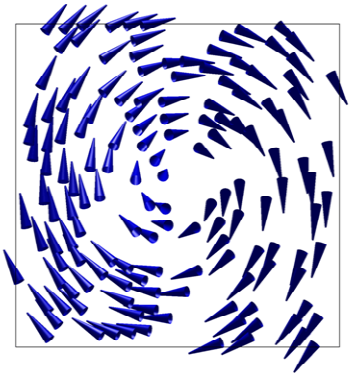

Abb. 1. Vortex magnetization configuration of a cubical particle (top view)

At present quasistatic micromagnetic simulations are a reliable tool for the evaluation of equilibrium configuration of ferromagnetic samples with mesoscopic sizes (thin films and particles with typical sizes from 100 nm to 10 μm) [2]. In our talk we present several such examples, showing that any significant quantitative disagreement between simulations and experimental data on well characterized samples should be considered as a serious problem, signaling that some important physical issues are not understood.

3. Simulations of the magnetization dynamics

In most application areas of micromagnetic simulations – optimization of hard disk drives, magnetic random access memory cells, domain wall motion in nanowires, energy dissipation in fine particle systems etc. – the magnetization *dynamics* is of primary interest. This means, that we have to simulate the time evolution of the magnetization when external conditions (usually the external field) rapidly change. The most common equation of motion for this purpose is the Landau-Lifshitz-Gilbert equation, where the first term describes the magnetization precession around the effective field $\mathbf{H}_{\text{eff}}$ with the frequency defined by this field and the gyromagnetic ration γ, and the second term is responsible for the magnetization precession [3]:

$$\frac{d\mathbf{M}}{dt} = -\gamma \cdot [\mathbf{M} \times (\mathbf{H}^{\text{det}} + \mathbf{H}^{\text{fl}})] - \\ -\lambda \cdot \frac{\gamma}{M_{\text{S}}} \cdot [\mathbf{M} \times [\mathbf{M} \times (\mathbf{H}^{\text{det}} + \mathbf{H}^{\text{fl}})]] \qquad (7)$$

Thermal fluctuations, included into this equation via the 'fluctuation field' $\mathbf{H}_i^{\text{fl}}$, are especially important for small particles (~ 10 - 100 nm), where kT has the same order of magnitude as energy barriers separating metastable magnetization states [4]. Components of $\mathbf{H}_i^{\text{fl}}$ are usually assumed to be δ-correlated in space and time and their amplitude is proportional to the system temperature T and the damping coefficient λ.

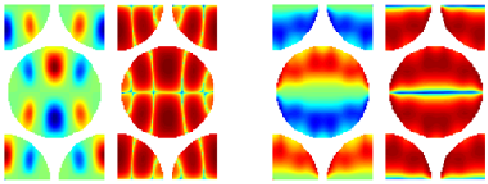

Abb. 2. Examples of the spatial power distribution in thin nanodisks (D = 370 nm) forming a hexagonal lattice

In our talk we demonstrate, that dynamical micromagnetic simulations both with and without thermal fluctuations also demonstrate a remarkable agreement with experimental findings.

References

[1] W.F.Brown, *Micromagnetics*, N.Y., Wiley, 1963

[2] A. Hubert, R.Schäfer, *Magnetic domains: the analysis of magnetic microstructures*, Springer-Verlag, 1998

[3] J Miltat, G. Albuquerque, A. Thiaville, An Introduction to Micromagnetics in the Dynamical Regime, in: *Spin Dynamics in Confined Magnetic Structures I*, Topics in Applied Physics, Vol. 83, Springer-Verlag Berlin, 2001

[4] D.V. Berkov, Magnetization dynamics including thermal fluctuations, in: *Handbook of Magnetism and Advanced Magnetic Materials*, H. Kronmüller, S. Parkin (eds), 2007, JohnWiley & Sons, UK

Network formation of unconventional dipolar particles

Heiko Schmidle[1], Sebastian Jäger[1], Carlos Alvarez[1], Carol K. Hall[2], Orlin D. Velev[2], and Sabine H. L. Klapp[1]

[1]*Institut für Theoretische Physik, Sekr. EW 7-1, Technische Universität Berlin, Hardenbergstrasse 39, 10623 Berlin*
[2] *Department of Chemical and Biomolecular Engineering, North Carolina State University, Raleigh, North Carolina, USA*

We present recent computer simulation results for the aggregation behavior of two types of systems with "unusual" dipole-like interactions.
The first model is inspired by recent optical-microscopy experiments involving polystyrene particles with (and without) gold patches in external fields [1]. We investigate the system on the basis of a colloidal mixture consisting of particles with either one or two, oppositely oriented, induced dipole moments. For a broad range of parameters, we find the model systems to self-assemble via a two-step scenario involving first percolation along the field, followed by a percolation transition in the *transversal* direction [2]. The resulting two-dimensional networks are characterized by strongly hindered translational dynamics.
The second system consists of magnetic nanorods composed of fused spheres with permanent magnetic dipole moments [3]. The resulting system behaves significantly different from a system of hard (non-magnetic) rods or magnetic rods with a single longitudinal dipole. In particular, we observe for the magnetic nanorods a significant decrease of the percolation threshold (as compared to non-magnetic rods) at low densities, and a stabilization of the high-density nematic phase. Moreover, the percolation threshold is tunable by an external magnetic field [4].

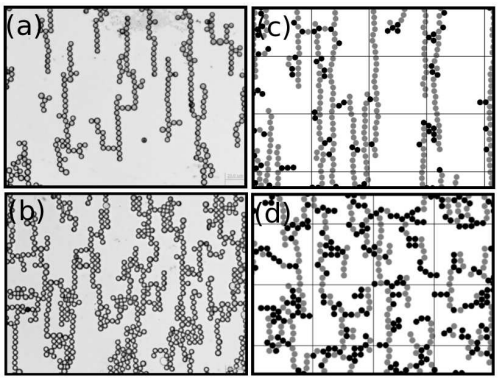

Figure 1: (a) and (b) Optical microscopy images of the experimental system of $5\mu m$ particles similar to the one studied in [1] at a supercritical frequency ($f = 400kHz$) and two sets of field strength and packing fractions. Right: MC simulation "snapshots" of model mixtures at $T^* = 0.15$ and (c) $c_{\mathrm{DID}} = 0.25$, $\rho^* = 0.25$, (d) $c_{\mathrm{DID}} = 0.5$, $\rho^* = 0.4$.

Acknowledgments
We thank the DFG for funding via the IGRTG 1524 "Self-Assembled soft matter nanostructures at interfaces" and the research grant KL1215/7.

References

[1] S. Gangwal, A. Pawar, I. Kretzschmar, and O. D. Velev, Soft Matter **6**, 1413 (2010).

[2] H. Schmidle, S. Jäger, C.K. Hall, O.D. Velev, and S. H. L. Klapp, submitted.

[3] R. Birringer, H. Wolf, C. Lang, A. Tschöpe and A. Michels, Z. Phys. Chem **222**, 229 (2008).

[4] C. Alvarez and S. H. L. Klapp, Soft Matter **8**, 3480 (2012).

New results on thermomagnetic convection in magnetic fluids caused by spatially modulated magnetic fields

A. Lange and S. Odenbach

TU Dresden, Institute of Fluid Mechanics, Chair of Magnetofluiddynamics, 01062 Dresden, Germany

Introduction

Systems which are driven out of equilibrium by the temperature dependence of the density of a fluid belong to established pattern forming systems [1,2]. If the fluid is a magnetic fluid (MF), additional paths open up to initiate patterns. The magnetization of the MF generates a magnetic force in interaction with an applied magnetic field which can also drive the system out of equilibrium. Thus, in a horizontal layer of MF subjected to a vertical gradient of temperature and a vertical magnetic field convection can be generate in two different ways.
The recent focus of interest for this type of setup has been the study of thermomagnetic convection with spatially modulated fields [3, 4]. Results for the case of a short-wave modulation are presented. Such a type of modulation is experimentally more relevant than a long-wave modulation [3] and leads to a new kind of flow field which is characterized by a double vortex of rolls of circular cross section, see Fig. 1.

System

The system studied consists of a laterally infinite horizontal layer of magnetic fluid in the x-y plane with thickness d which is bounded by two rigid impermeable boundaries in the planes $z = \pm d/2$. The setup is heated from below with a temperature of T_b for the bottom plate and cooled from the top with a temperature of T_t with $T_\mathrm{t} < T_\mathrm{b}$. The layer is sandwiched between two sinus-like shaped iron bars which cause the spatial and symmetrical modulation of a constant external magnetic field $\mathbf{H}_\mathrm{ext} = (0, 0, H_\mathrm{ext})$ the whole system is subjected to.

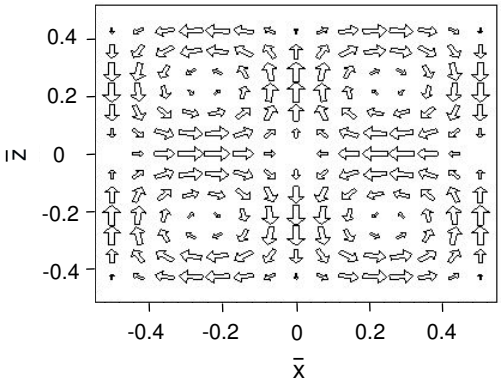

Figure 1: Plot of the flow field for a short-wave modulation of the external magnetic field. The dimensionless lengths are scaled with d. From [4].

Results

To determine the stationary base state it is used that the Prandtl number of real magnetic fluids is large compared to 1 [5]. For short-wave modulations a general ansatz with nine unknown functions is inserted into the governing equations which are the equation of continuity, the Navier-Stokes equation using the Boussinesq approximation, and the equation of heat conduction. By determining all these unknown functions, the non-trivial stationary base is then known analytically and appears as a double vortex structure of convection rolls (Fig. 1). The new character of the flow field is given by the cir-

cular cross section of the rolls.
In order to know the stability of the base state, a linear stability analysis is presented. A stream function Ψ is introduced since the components of the flow field of the base state can be expressed with the help of Ψ. Finally two coupled linear equations for small disturbances of the stream function and the temperature, respectively, appear which are solved by a separation ansatz of the Floquet-type. Solving the resulting eigenvalue problem, a stability chart results in dependence of two dimensionless parameters. The Rayleigh number Ra and its magnetic counterpart $\mathrm{Ra_m}$ relate the destabilizing effect of magnetic force and buoyancy, respectively, to the stabilizing effects of viscous friction and heat conduction. As function of the magnetic Rayleigh number $\mathrm{Ra_m}$ the results for the critical Rayleigh number $\mathrm{Ra_c}$ and the corresponding critical wave number q_c are presented and discussed.

References

[1] M. C. Cross and P. C. Hohenberg, Rev. Mod. Phys. **65**, 851 (1993)

[2] S. Chandrasekhar, *Hydrodynamics and hydrodynamic stability*, (1981)

[3] A. Lange and S. Odenbach, Phys. Rev. E **83**, 066305 (2011)

[4] A. Lange and S. Odenbach, Magnetohydrodynamics **47**, 175 (2011)

[5] S. A. Suslov, Phys. Fluids **20**, 084101 (2008)

The Influence of Thermodiffusion in Ferrofluids on Thermomagnetic Convection

L. Sprenger, A. Lange and S. Odenbach

TU Dresden, Institute of Fluid Mechanics, Chair of Magnetofluiddynamics, 01062 Dresden, Germany

Introduction

Thermomagnetic convection denotes a transport phenomenon in ferrofluids due to a temperature gradient and a magnetic field applied [1]. Convection sets in at a certain critical Rayleigh number. Recent experimental results [2] show an enhancement of the onset of convection when applying a magnetic field using the magnetic fluid APG513A, using the EMG905 fluid in the same setup, convection is fully suppressed. Since the magnetic field dependence of the fluid parameters can be excluded as reason for the suppression, it is searched for a different temperature driven transport process, such as thermodiffusion, already known as relevant in the convection process in zero magnetic field [3, 4]. Thermodiffusion describes the movement of the fluid's particles in a layer of fluid due to an applied temperature gradient. The intensity of the effect is characterised by the Soret coefficient [5] which can be changed by a magnetic field. This motivates an investigation on the correlation of thermomagnetic convection and thermodiffusion for the magnetic case.

Theoretical Investigations on Thermomagnetic Convection

The system of equations describing thermomagnetic convection includes as well the balance equations of mass, heat, momentum, and concentration as the Maxwell equations for the magnetic field and flux. A linear stability analysis is applied to this system to determine the critical Rayleigh number for the onset of convection. Therefore the equations are formulated linearly in the perturbations of the hydro- and magnetodynamic variables, namely velocity, temperature, concentration and magnetic potential.

The ansatz for the perturbations in direction of the height of the layer of fluid fulfills the boundary conditions at the layer's upper and lower boundary, for the other two spatial directions and time a general exponential ansatz is chosen. Solving this equation system for stationary deviations leads to $Ra = \frac{(k^2+\pi^2)^3}{k^2(1+\psi+M_1(1+M_c)(1-\pi^2/(M_3k^2+\pi^2)))}$ with k being the wave number, and M_1 and M_3 being factors including fluid and magnetic field parameters. The separation ratio ψ and the derivative of the magnetisation by the concentration M_c are direct proportional to the Soret coefficient. Figure 1 shows the dependence of the critical Rayleigh number on the Soret coefficient. Small negative values lead to a hindrance of the onset of convection in comparison to zero magnetic field,

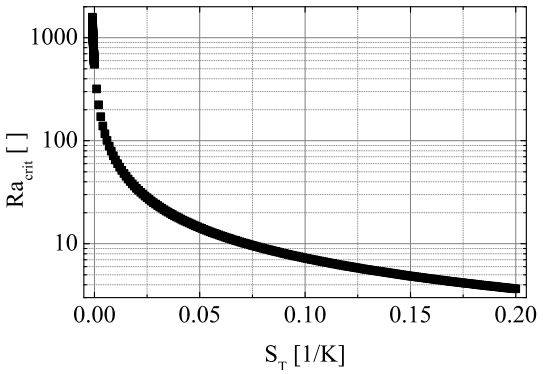

Figure 1: run of the critical Rayleigh number depending on the Soret coefficient

positive values to an enhancement. Larger negative values lead to exclusively negative Rayleigh numbers which means suppression of convection. Proofing the dependence of the convection on the Soret coefficient rises the necessity to experimentally determine the magnitude of the coefficient.

Experiments on Thermodiffusion

A horizontal thermodiffusion cell, based on the design of [5], has been used. A temperature gradient of 1 K/mm was applied to the fluid container filled with a magnetic fluid of the EMG900 series of Ferrotec. The fluid is kerosene-based and the magnetite particles' volume concentration can be determined as 8.7 vol.%. The magnetic field is either applied parallel or perpendicular to the temperature gradient.

The change in the particles' concentration

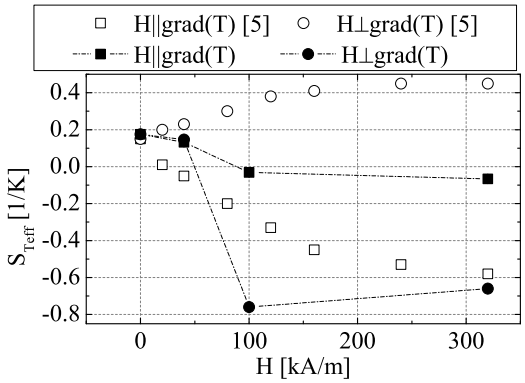

Figure 2: Soret coefficient depending on the magnetic field strength and direction of application

is detected by the inductance of two sensor coils wrapped around the upper and lower fluid container. The so-called separation curve represents the difference of the concentration in the lower and the upper container normalised by the initial homogeneous concentration of the fluid. The inclination of this curve is direct proportional to the Soret coefficient. Figure 2 shows the magnetic-field-dependent Soret coefficient for the current measurements compared to those of [5]. Independent of the direction of the magnetic field, and thereby contradicting former measurements of a different fluid, the Soret coefficient is measured as negative value for rising field strengths beginning at 100 kA/m. Hence the magnetic field dependence of the coefficient is highly dependent on the fluid.

Conclusion and Outlook

The linear stability analysis for magnetic fluids considering thermodiffusive processes stresses the strong influence of temperature driven diffusion on the onset of convection. Depending on the magnitude and sign of the Soret coefficient convection can be enhanced ($S_T>0$), hindered ($0>S_T>-0.001$) or even suppressed ($-0.001>S_T$). Experimental data determines the Soret coefficient depending on the magnetic field strength. A change in the coefficient's sign from positive to negative can be detected in the range of 50 kA/m to 100 kA/m. A more detailed analysis on the stability of the layer of fluid with rigid boundaries and more experimental data to overcome the mismatch between former and current experiments are planned.

Acknowledgments

Financial support by the DFG Grant No. LA 1182/3 is gratefully acknowledged.

References

[1] B. A. Finlayson, J. Fluid Mech. **40**, 753-767 (1970)

[2] H. Engler, Diss., Parametrische Modulation thermomagnetischer Konvektion in Ferrofluiden (2010)

[3] S. Odenbach, T. Völker, JMMM **289**, 122-125 (2005)

[4] A. Ryskin, et al., Phys. Rev. E **67**, 46302 (2003)

[5] T. Völker, S. Odenbach, Phys. Fluids **17**, 037104 (2005)

Following mechanical deformation in colloidal systems on a single particle level

Günter K. Auernhammer[1], Marcel Roth[1], Jennifer Wenzl[1], Ryohei Seto[1], Carsten Schilde[2], Arno Kwade[2], Hans-Jürgen Butt[1]

[1]*Experimental Physics of Interfaces, Max Planck Institute for Polymer Research, Mainz, Germany*
[2]*Institute for Particle Technology, TU Braunschweig, Braunschweig, Germany*

The mechanical properties of aggregated colloids depend on the mutual interplay of inter-particle potentials, contact forces, aggregate structure and material properties of particles and the embedding matrix. In this contribution I will discuss the possibilities and limitations of confocal microscopy for the analysis of colloidal systems under mechanical and magnetic fields.
We investigated the mechanical properties of aggregates made from monodisperse poly-methyl-meth-acrylate (PMMA) particles (diameter: 1.6 μm) via nano indentation in combination with confocal microscopy. In doing so the bare mechanical data were complemented by three-dimensional coordinates of all particles in the aggregate. Additionally, we measured the individual trajectories of all particles during the indentation. This information was used to identify reorganization processes and calculate the average displacement field and strain tensor [1,2], see Fig. 1.

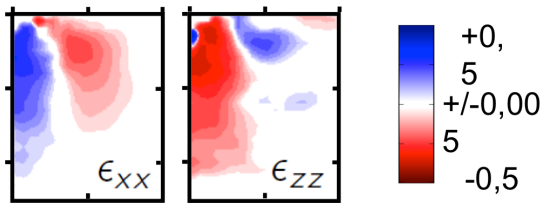

Figure 1: Two components of the stress tensor as measured through single particle tracking.

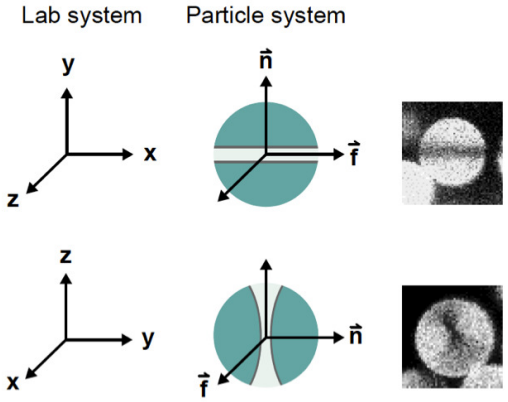

Figure 2: Geometry of the bleaching process in the lab and particle system (left) and real images of particles after bleaching (right)

The full information about colloidal motion consists of the positional and the rotational motion of the colloids. Whereas the positional tracking of particle motion is described in literature and used in our analysis (see above), the rotational motion of spherical particles is not directly accessible. I will demonstrate a way how selective bleaching of fluorescent particles (Fig. 2) can be used to determine the full rational motion of colloids [3,4].
Almost all magnetic materials are absorbing light. This makes the usage of confocal microscopy challenging for structural analysis of magnetic or magneto-rheological gels. First experiments with magnetic particles dispersed in a carrier liquid show however that the usage of high numerical

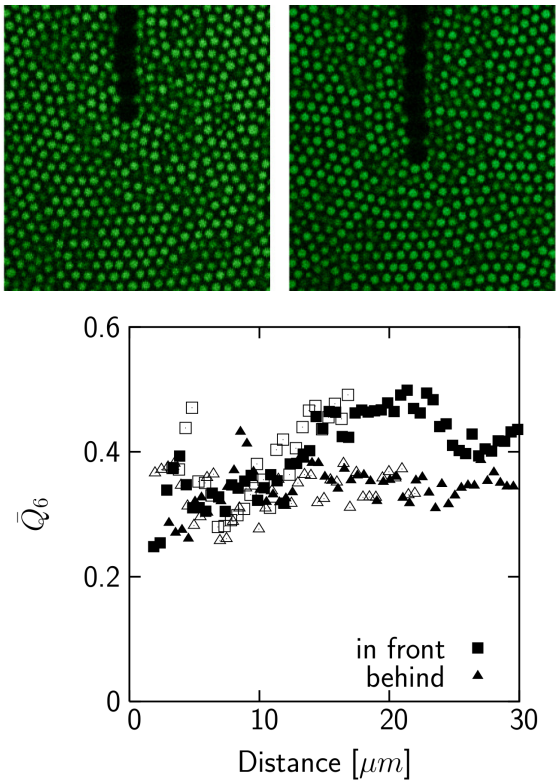

Figure 3: Top: Magnetic particles (black) moving through a colloidal crystal of fluorescently labeled colloids. Bottom: Degree of crystalline order in front (squares) and behind (triangles) the moving chain of magnetic particles.

aperture objective opens a way to (partially) circumvent this problem. I will discuss the results of this test and possibilities how the combined usage of fluorescent tracers and non fluorescent magnetic particles allows the detection of the motion of both species. This allowed us to study the response of the composite material on magnetic stimuli.

Acknowledgments
Financial support by the DFG through the SPP 1273, SPP 1486 and the SFB TR6 is gratefully acknowledged by GKA, RS, and JW, respectively. MR is a recipient of a fellowship through funding of the Excellence Initiative (DFG/GSC 266).

References

[1] M. Roth, C. Schilde, P. Lellig, A. Kwade, G. K. Auernhammer; *Simultaneous nanoindentation and 3D imaging on semi-crystalline colloidal films*. Chem. Lett. (2012), accepted for publication.

[2] M. Roth, C. Schilde, P. Lellig, A. Kwade, and G. K. Auernhammer, *Colloidal aggregates tested via nanoindentation and simultaneous 3D imaging*, arXiv:1102.4233v3 [condmat.soft] (2011).

[3] J. Wenzl, R. Seto, M. Roth, H.-J. Butt, G. K. Auernhammer; *Measurement of rotation of cohesive spherical granulates*. submitted.

[4] M. Roth, M. Franzmann, M. D'Acunzi, M. Kreiter, and G. K. Auernhammer; *Experimental analysis of single particle deformations and rotations in colloidal and granular systems*. arXiv: 1106.3623v2 [cond-mat. soft] (2011).

Structural transitions in the system of magnetic dipolar particles at low temperature

S. Kantorovich[1,2], L. Rovigatti[2], A. Ivanov[1], F. Sciortino[2]

[1] *Ural Federal University, Lenin av. 51, 620000, Ekaterinburg, Russia.*
[2] *Sapienza, University of Rome, Piazza A. Moro 5, 00185, Rome, Italy.*

One of the mostly often-used methods to model magnetic fluids is to mimic nanoparticles by dipolar hard spheres. This convenient and fundamentally interesting model has been actively studied since years [1-3]. Lately, one of the most revisited questions in this field is whether the system of monodisperse hard dipolar spheres could undergo a vapor-liquid type phase transition [4]. Despite various attempts, there is still no definite answer if any certain type of a phase transition could be or could not be driven by the presence of the anisotropic dipole-dipole interparticle interaction and hard-sphere repulsion only. Recent investigations [5,6] showed that at low temperature and at a very low density the competition between chains and rings took place. Importantly, the ratio "fraction of rings - fraction of chains" first grows with density and then starts decreasing again. On the other hand, rigorous analysis in [7,8] of the ground state structures in dipolar hard spheres showed that if a system of dipolar hard spheres contained more than four particles, the ring structure would be the ground state. We also found the initial susceptibility of a ring to be significantly lower than the one of a chain.

In the present contribution we perform computer simulations and develop a theoretical approach to describe the temperature dependence of the initial susceptibility for the systems of dipolar hard spheres.

The susceptibility of these systems first increases fast with inverse temperature (read, growing strength of magnetic dipole-dipole interaction) due to the chain formation. Then, at a certain value of the inverse temperature, the rings start forming. As a result, with decreasing temperature, initial susceptibility stops growing and even may start decreasing.

The presence of maximum in temperature of the initial susceptibility might usher in the new structural crossover. The existence of this crossover in its turn would explain why there is now vapor-liquid phase transition in the range of parameters studied here.

Acknowledgments

The work is supported by ERC Grant "Patchy Colloids".

References

[1] 1. J.-M. Caillol, J. Chem. Phys., 1993, 98, 9835
[2] J.J. Weis and D. Levesque, Phys. Rev. Lett. 1993, 71, 2729
[3] P.J. Camp et al, Phys. Rev. Lett., 2000, 84, 115.
[4] G. Ganzenmüller, P. J. Camp, J. Chem. Phys., 2007,126, 191104 and references therein.
[5] J. Russo et al., Phys. Rev. Lett., 2011, 106, 085703.
[6] L. Rovigatti et al., Soft Matter, 2012, 8, 6310.
[7] T. Prokopyeva et al, Phys. Rev. E., 2009, 80, 031404.
[8] T. Prokopyeva et al, manuscript in preparation.

„Localized flats on the surface of magnetic liquids“

M. C. Szech[1], I. Rehberg[1], R. Richter[1]

[1] *Experimentalphysik V, Universität Bayreuth, 95440 Bayreuth, Germany*

Introduction

By applying a normal field that exceeds a certain critical value, a plain layer of magnetic fluid (MF) is becoming unstable and a hexagonal pattern of spikes emerges, as first reported by Cowley & Rosensweig [1]. This phenomenon is known as the Rosensweig instability and was extensively studied theoretically as well as experimentally [2-5].

The hexagonal pattern can be described in a weakly nonlinear description as a resonant interaction of three degenerate wave modes. A strongly nonlinear approach to describe this kind of pattern regards the whole lattice as a crystal where an individual Rosensweig spike stands for an atom. This point of view was corroborated by the generation of localized spikes in an otherwise flat surface of the MF in the bi-stable regime [6,7], as discussed in Ref. [8].

Within the “atomistic” picture, the creation of voids or “flats” within the hexagonal pattern seems natural. Because the position of these flats, opposed to the spikes, should be well defined within the matrix of the regular pattern, they have been suggested for data storage [9].

In our contribution we demonstrate the possibility of creating a flat in an otherwise hexagonal pattern of the MF, as shown in Fig. 1. Moreover, we investigate the critical magnetic probe induction $B_{p,c}$ to switch off a local spike – or to give birth to a flat - for different values of the homogeneous magnetic induction B_h.

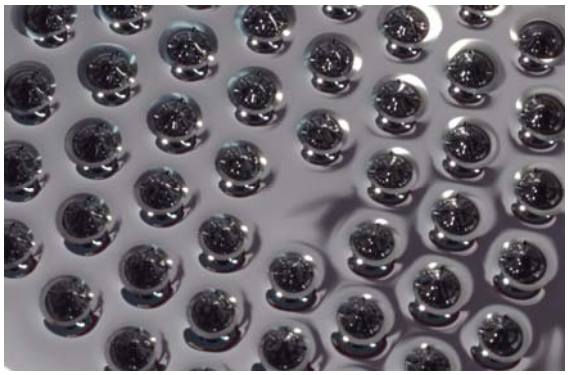

Figure 1: *A localized flat in a Rosensweig pattern.*

Experimental Setup

The MF (EMG 901 from Ferrotec Co.) is placed within a cylindrical vessel with an inner diameter of 120 mm, as shown in Fig. 2. The vessel is positioned in the center of a Helmholtz pair of coils with the same diameter. These are generating the homogenous induction B_h normal to the fluid surface. To reduce field inhomogeneities at the edge of the vessel we utilize a magnetic ramp, as described in [7].

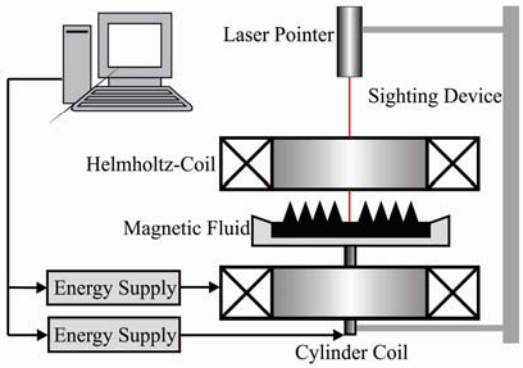

Figure 2: *Sketch of the experimental Setup.*

Beneath the MF a cylindrical air coil is situated to create the local perturbation of the homogenous induction that is needed to produce the flats. To switch off a single spike in the hexagonal pattern, the probe coil has to be centered exactly beneath one. To achieve this, a sighting device, as seen in Fig. 2, is used. It consists of a laser that points at the surface of the MF and can thus be aimed at a spike with high precision. The probe coil is connected to the sighting device in such a way that when the laser beam is at the center of the spike, so is the coil.

Experimental Results

By reducing the induction locally, a flat can be created within the hexagonal pattern, as seen in Fig. 1. After switching off B_p, the flat remains stable if B_h is roughly in the bistable regime of the hexagonal lattice, i. e. $B_h < \approx B_{h,c}$. For our current configuration and MF the surrounding spikes are drifting slowly into the void after the probe induction is turned off, yet the number of spikes does not change during the drifting process.
For $B_h > \approx B_{h,c}$ the flat is unstable, and a spike pops up again, as soon as B_p is switched off.
We have measured the critical magnetic induction $B_{p,c}$ in dependence of B_h. The outcome is presented in Fig. 3. The graph intersects the x-axis at a field $B_{h,s}$, which is close to the saddle node B^* of the branch describing the Rosensweig instability of a hexagonal lattice in a homogeneous field.

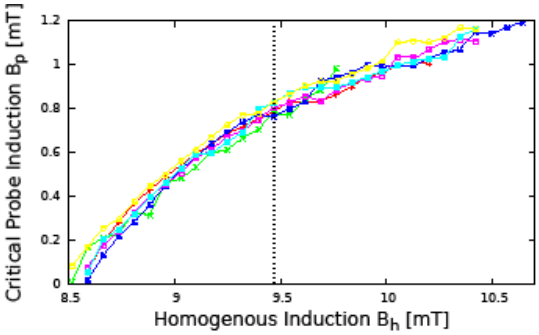

Figure 3: *Critical magnetic probe induction $B_{p,c}$ for different values of the homogeneous induction B_h. The vertical line denotes the critical homog. induction $B_{h,c}$.*

At that point the slope is approximately 1. For increasing B_h the slope of the curve diminishes.
We discuss our results in the context of an imperfect amplitude equation. For further insights numeric simulations, which are capable to take into account the inhomogeneous field configuration, seem the most promising attack.

References

[1] M. D. Cowley and R. E. Rosensweig, J. Fluid Mech. **30**, 671 (1967).

[2] R. E. Rosensweig, *Ferrohydrodynamics* (Cambridge University Press, Cambridge, New York , Melbourne, 1985).

[3] A. Gailitis, J. Fluid Mech. **82**, 401 (1977).

[4] R. Friedrichs and A. Engel, Phys. Rev. E **64**, 021406 (2001).

[5] R. Richter, A. Lange, in Vol. 763 of *Lect. Notes Phys.*, Springer, Berlin, pp. 157-247 (2009).

[6] R. Richter and I. V. Barashenkov, Phys. Rev. Lett. **94**, 184503 (2005).

[7] H. Knieling, I. Rehberg, R. Richter, Physics Procedia **9,** 199 (2010); H. Knieling, *PhD Thesis*, Universität Bayreuth (2009).

[8] E. Knobloch, Nonlinearity **21,** T45 (2008).

[9] P. Coullet , C. Riera and C. Tresser, Chaos **14,** 193 (2001).

Magnetic nanoparticle binding experiments in a rotating magnetic field

J. Dieckhoff, M. Schilling and F. Ludwig

Institut für Elektrische Messtechnik und Grundlagen der Elektrotechnik, TU Braunschweig, Hans-Sommer-Str. 66, 38106 Braunschweig

1. Introduction

Magnetic nanoparticles (MNPs) are used in a wide range of biomedical applications due to their potential of being magnetically controlled and specifically labeled. A recent example is the development of a homogenous biosensor concept for a high-sensitive biomolecule detection which is based on the magnetic manipulation of rod-shaped magnetic nanoparticles in a rotating magnetic field [1]. In contrast to prior methods where the MNPs response in an alternating magnetic field is analyzed by measuring the complex magnetic susceptibility [2],[3], here the phase lag φ between the rotating magnetic field H and the MNPs magnetization M is the value of interest. The phase lag φ is significantly affected by the ratio of the particle's magnetic moment m to hydrodynamic volume V_h. In this context the phase lag measurement in a rotating magnetic field offers the possibility to realize more sensitive and robust homogenous bioassays. This work aims on clarifying these findings by comparing the alternating and the rotating magnetic field method for the MNP manipulation and presenting simulation as well as measurement results of first binding experiments.

2. Theory

The dynamics of the MNPs magnetization in a magnetic field including thermal agitation is basically described by the Fokker-Planck equation [4], which is the basis for the analysis of the MNPs dynamics in alternating and rotating magnetic fields [5],[6]. In order to describe the nanoparticles magnetic flux density B_s with simulation results gained by numerically solving the Fokker-Planck equation, following equations for the real part B_s' and the imaginary part B_s'' can be used [6]:

$$\frac{B_\mathrm{s}'(H,\omega_H)}{B_\mathrm{s}'(H_0,0)} = (1-k)\frac{3k_\mathrm{B}T}{H_0 m_\mathrm{B}^2}\int_{d_\mathrm{h}} f_\mathrm{h}(d_\mathrm{h}) \quad (1)$$
$$\times\int_{d_\mathrm{c}} f_\mathrm{c}(d_\mathrm{c}) m_\mathrm{B}(d_\mathrm{c})\frac{M'(H,\omega_H)}{M_\mathrm{S}} dd_\mathrm{c} dd_h + k\frac{H}{H_0}$$

$$\frac{B_\mathrm{s}''(H,\omega_H)}{B_\mathrm{s}(H_0,0)} = (1-k)\frac{3k_\mathrm{B}T}{H_0 m_\mathrm{B}^2}\int_{d_\mathrm{h}} f_\mathrm{h}(d_\mathrm{h}) \quad (2)$$
$$\times\int_{d_\mathrm{c}} f_\mathrm{c}(d_\mathrm{c}) m_\mathrm{B}(d_\mathrm{c})\frac{M''(H,\omega_H)}{M_\mathrm{S}} dd_\mathrm{c} dd_h$$

The multidispersity of the MNPs is taken into account by introducing a lognormal size distribution $f_c(d_c)$ for the core and $f_h(d_h)$ for the hydrodynamic volume. Due to the presence of superparamagnetic particles in the investigated samples the MNPs magnetization does not only rotate via the Brownian motion of the whole particle but also via the internal Néel process. Therefore, the value k is defined as

$$k = n_\mathrm{N}\overline{m_\mathrm{N}^2} / \left(n_\mathrm{B}\overline{m_\mathrm{B}^2} + n_\mathrm{N}\overline{m_\mathrm{N}^2}\right) \quad (3)$$

where n_B and n_N represent the number of the particles dominated by the Brownian motion and the Néel process, respectively.

3. Field mode comparison

The dynamics of magnetic nanoparticles in a rotating (RMF) and an alternating magnetic field (ACF) exhibits distinct differ-

ences with a rising field amplitude H, which can be observed by analyzing the phase lag φ or the real and imaginary part of the magnetic flux density B_s. The measured phase lag φ of an aqueous suspension of Fe_3O_4 nanoparticles (Figure 1) shows that the particles possess a higher phase lag and a weaker dependency on the field amplitude in an alternating field, which is illustrated by a smaller spreading of the ACF phase curves.

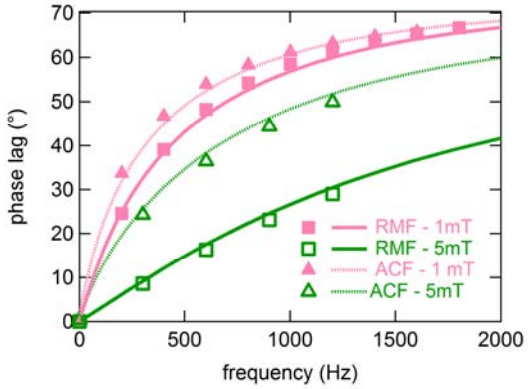

Figure 1. Measurement results of phase lag for aqueous Fe_3O_4 particle suspension in ACF and RMF with 1 mT and 5 mT field amplitude (markers) in comparison with simulation results for μ_h = 120 nm, σ_h = 0.26, μ_c = 48 nm, σ_c = 0.01, k = 0.016, M_s = 270 kA/m and η = 1 mPa·s (lines).

4. Binding experiments

The binding experiments rely on the effect that biomolecules binding to the functionalized shell of the nanoparticles cause a change in the nanoparticles dynamics which can be quantified by the difference of the measured phase lag before and after the binding, the phase lag change $\Delta\varphi$. In contrast to the measurement and analysis of the flux density's real and imaginary part B_s' and B_s'' the phase lag does not depend on the particle concentration that samples commonly possess in a bioassay. Measurement results also confirm the simulated findings [7] that predict a higher phase lag change $\Delta\varphi$ in the rotating magnetic field which corresponds to a higher sensitivity. Figure 2 depicts the measured $\Delta\varphi$ as a result of IgG antibodies binding to a 30 nm Fe_3O_4 particle with a protein G functionalized shell. Whereas $\Delta\varphi$ shows for 1 mT only a slight difference between both field modes, for 2.5 mT the rotating magnetic field results in a more than 20 % higher $\Delta\varphi$.

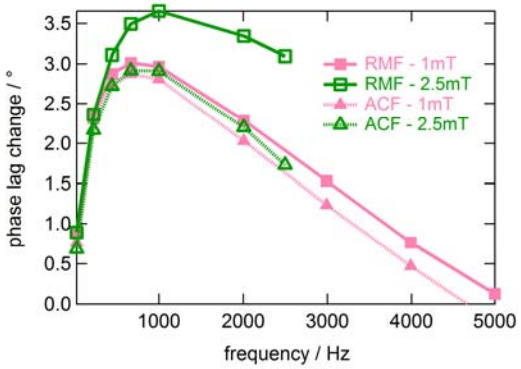

Figure 2. Measured phase lag change $\Delta\varphi$ caused by binding of IgG antibodies to protein G functionalized Fe_3O_4 30 nm particles in an aqueous suspension in ACF and RMF for 1 mT and 2.5 mT.

Acknowledgments

This work was supported by the European Commission Framework Programme 7 under the NAMDIATREAM project (NMP-2010-246479)

References

[1] S. Schrittwieser, F. Ludwig, J. Dieckhoff, et al., *ACS Nano*, vol. 6, pp. 791-801, January 2012.

[2] S. H. Chung, A. Hoffmann, S. D. Bader, et al., *Appl. Phys. Lett.*, vol. 85, pp. 2971-2973, October 2004.

[3] C.-Y. Hong, C. C. Wu, Y. C. Chiu, et al., *Appl. Phys. Lett.*, vol. 88, pp. 212512, May 2006.

[4] W. T. Coffey, P. J. Cregg, and Y. P. Kalmykov, *Advances in Chemical Physics*, vol. 83, I. Prigogine and S. A. Rice, Eds. New York: Wiley, 1993, pp. 263-464.

[5] T. Yoshida and K. Enpuku, *Japan. J. Appl. Phys.*, vol. 48, pp. 127002, December 2009.

[6] T. Yoshida, K. Enpuku, J. Dieckhoff, et al., *J. Appl. Phys.*, vol. 111, pp. 053901, March 2012.

[7] J. Dieckhoff, T. Yoshida, K. Enpuku, et al., *IEEE Trans. Magn.*, vol 48, no. 11, November 2012.

Rotational dynamics of Ni nanorod colloids characterized by optical transmission and neutron scattering

P. Bender[1], A. Wiedenmann[2], A. Tschöpe[1], R. Birringer[1]

[1]*Experimentalphysik, Universität des Saarlandes, 66041 Saarbrücken, Germany*
[2]*Institut Laue Langevin, 38042 Grenoble, France*

1. Introduction

With diameters < 42 nm, Ni nanorods are uniaxial ferromagnetic single-domain particles [1]. When dispersed in a liquid matrix, alignment of their magnetic moments along an external magnetic field is achieved by a rotation of the entire particle. In time-modulated magnetic fields the switching dynamics depends on the hydrodynamic interaction of the nanorods with the viscous matrix. Due to the anisotropic electrical polarizability optical transmission measurements can be used to detect the response of a colloidal dispersion of Ni nanorods to a rotating magnetic field [2]. In particular, the rotational diffusion coefficient D_r can be extracted from the phase shift Φ between the periodic variation of the rotating magnetic field and the resulting oscillation in the optical transmission. In the present study a similar approach is presented where Small Angle Neutron Scattering (SANS) is used in addition to the transmission of polarized light to experimentally determine the hydrodynamic interactions of Ni nanorods with the liquid matrix in a rotating magnetic field.

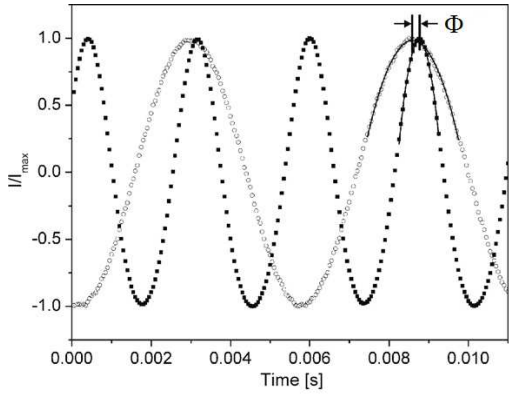

Figure 1: The normalized transmitted light intensity $I(t)/I_{max}$ (square) and the component of the magnetic field parallel to the light beam (circle).

2. Experimental results

2.1. Optical transmission

As shown in Figure 1 the phase shift Φ between the Ni nanorods and the rotating magnetic field can be determined from the shift of the maximum in the transmitted light intensity relative to the maximum in the magnetic field component, which is parallel to the light beam. In Figure 2 it can be seen that Φ is dependent both on the angular frequency ω and the field amplitude $\mu_0 H_0$.

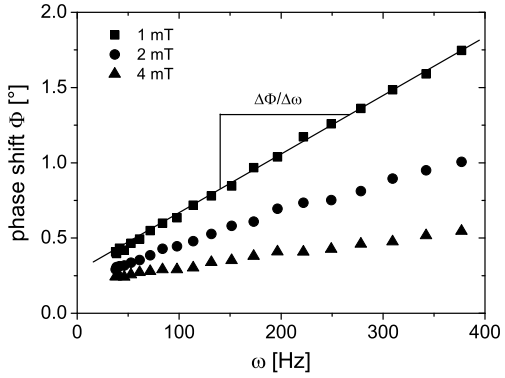

Figure 2: The frequency dependent phase shift Φ is shown for three different field amplitudes $\mu_0 H_0$.

Using the following approximation [2]

$$\Phi \approx \frac{k_B T}{D_r \mu} \frac{1}{\mu_0 H_0} \omega \qquad (1)$$

the product $D_r\mu = 1.943 \cdot 10^{-14}\ \mathrm{Am^2/s}$ can be extracted from the field dependence of the slope $\Delta\Phi/\Delta\omega$, where μ is the mean magnetic moment of the nanorods. For the Ni nanorods characterized in this study $\mu = 3.5 \cdot 10^{-17}\ \mathrm{Am^2}$ and therefore $D_r = 555$ 1/s.

2.2. SANS measurements

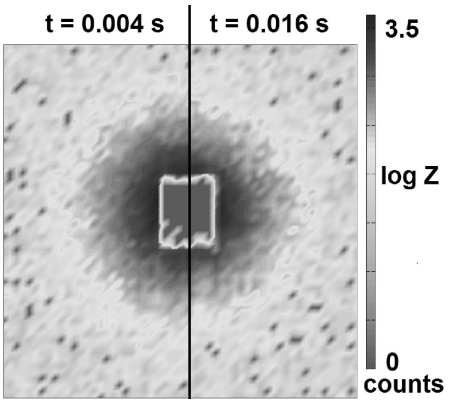

Figure 3: Two SANS scattering patterns of the magnetic fluid after $t = 0.004$ s (left) and 0.016 s (right).

For SANS experiments the magnetic fluid was also located in a rotating magnetic field and separate time dependent SANS scattering 2D patterns were detected via the TOF-mode (Time Of Flight) (Fig. 3). This means that each pattern correlates with a certain field orientation and therefore orientation distribution of the Ni nanorods. When the scattering patterns are averaged and the resulting SANS intensity I is plotted as a function of time an oscillation is observed (Fig. 4). Comparision of I with the component of the magnetic field parallel to the neutron beam $H_{||}$ allows the determination of the phase shift Φ. First results indicate that the field and frequency dependency of Φ obtained with SANS measurements is in fairly good agreement with the corresponding results from optical transmission. The advantage of SANS compared to optical transmission is that polarized small angle neutron scattering (SANSPOL [3]) allows the detection of the field and time dependent orientation of the nanorods and their magnetic moments separately. For future measurements this aspect seems to be interesting particularly with regards to highly viscous or even elastic matrices where a rotation of the magnetic moments out of the long rod axis can be expected.

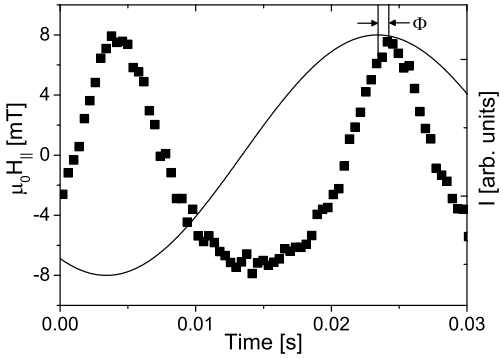

Figure 4: SANS intensity and the component of the magnetic field parallel to the neutron beam as a function of time. The field amplitude was $\mu_0 H_0 = 8$ mT and the frequency of the rotating field $f = 25$ Hz.

Acknowledgments
The authors would like to thank the ILL for the provision of neutron beamtime at D22 and the BMBF for financial support.

References

[1] C.A. Ross et al., Phys. Rev. B 65, 144417 (2002).

[2] A. Günther, P. Bender, A. Tschöpe, R. Birringer, J. of Phys.: Cond. Matt., 325103 (2011).

[3] A. Wiedenmann, U. Keiderling, R.P. May, C. Dewhurst, Physica B: Cond. Matt., 453 (206).

The influence of particle motion on thermal conductivity in ferrofluids

M. Krichler, S. Odenbach

TU Dresden, Institute of Fluid Mechanics, Chair of Magnetofluiddynamics, 01062 Dresden, Germany

Introduction

Heat conduction is a diffusive transport process. Hence the particle motion of colloidal suspensions most probably has an important impact on the heat transfer through conduction. The question arises how the heat transfer in ferrofluids is affected by an external magnetic field since a magnetic field can have an influence on particle motion. For this experimental investigation we carried out thermal conductivity measurements in magnetic fluids. Applying external homogeneous magnetic fields, varying in the magnitude and in the direction towards the heat flux direction, we considered the impact on heat transfer.

Experimental setup

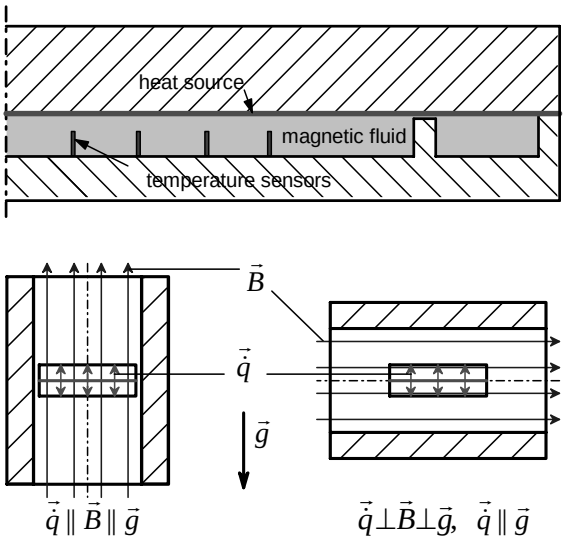

Figure 1: sketch with a cross-sectional view of the planar measurement device (upper side) for thermal conductivity measurements embedded in a helical coil for parallel alignment of magnetic field an heat flux (left side) an for perpendicular alignment (right side)

We carried out thermal conductivity measurements using a device based on a plane heat source method. This device can be positioned parallel and perpendicular to an external magnetic field (Fig 1).
For our measurements we used several ferrofluids which differ in their particle size distribution (Fig. 2) and one magneto rheological fluid.

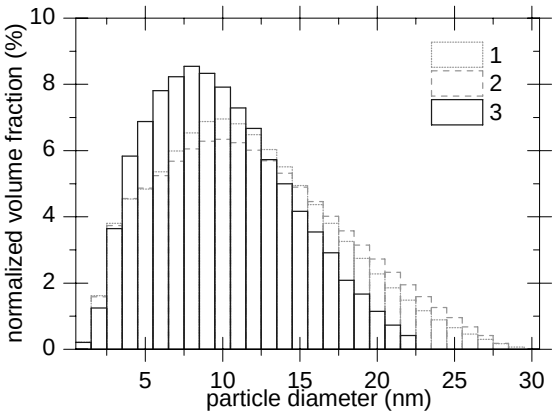

Figure 2: particle size distribution of three of the used samples obtained according to the regularization method [1]

Results

We found that in all examined liquids an impact of a magnetic field on heat flux can be seen. For a parallel alignment of heat flux and magnetic field the thermal conductivity is increased, and decreased for perpendicular alignment (Fig.3). This is in qualitative accordance with [2].
But in contrast to [2] the strongest impact has been observed for samples with a narrow size distribution containing mainly small particles i.e. short chains or even single particles. Vice versa, the impact on samples with a wide size distribution and bigger particles is considerably weaker.

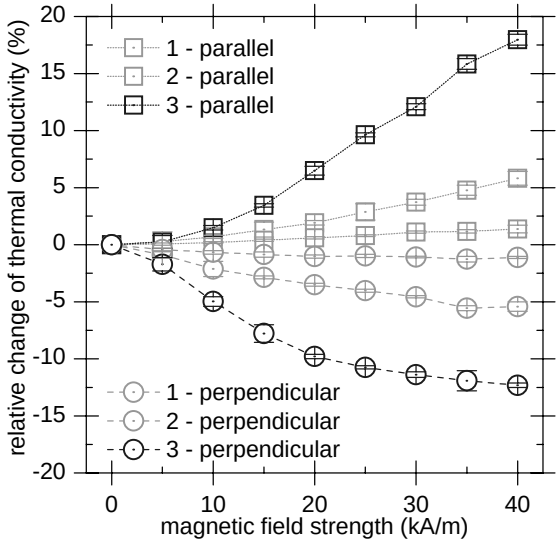

Figure 3: relative change of thermal conductivity as function of an external magnetic field, aligned parallel or perpendicular

Conclusion

This unexpected behavior among the samples can be explained if the diffusion coefficients are considered. According to numerical [3,4] and experimental [5] investigations it can be summarized that ferrofluids with a small interparticle interaction parameter $\lambda^* < 1$ experience an increasing diffusion coefficient parallel to a magnetic field [5], and fluids with $1 < \lambda^* < 5$ experience a decreasing diffusion parameter parallel to a magnetic field [3,4]. We apply these findings on our results and interpret them in the way that potential clustering of bigger particles does not lead to an increased thermal conductivity by heat bridges, but that the impact of a magnetic field on the diffusion coefficient is the more important factor.

The more small particles, which realize an increased diffusion parallel to a magnetic field, are in a ferrofluid the stronger is the increase of the thermal conductivity parallel to the magnetic field. We conclude that the size and the size distribution plays an important role for the magnitude of changes in thermal conductivity due to the impact of an magnetic field on particle motion which varies with its size.

Acknowledgments

Financial support by *Deutsches Zentrum für Luft- und Raumfahrt* under grant number DLR 50 WM 0639 is gratefully acknowledged.

References

[1] T. Weser, K. Stierstadt, Z. Phys. B: Con. Mat. **59** (1985) 253

[2] E. Blums, A. Cebers, M.M. Majorov, Magnetic Fluids, de Gruyter, Berlin, New York 1997

[3] J. Jordanovic, S. Jäger, S.H.L. Klapp, Physical Review Letters **106** (2011) 038301

[4] P. Ilg, M. Kröger, Phys. Rev. E **72** (2005) 031504

[5] J.C. Bacri, A. Cebers, A. Bourdon, G. Demouchy, B.M. Heegard, B. Kashevsky, R. Perzynski, Phys. Rev. E **52** (1995) 52

Shape-induced superstructure in concentrated ferrofluids

S. Disch [1], E. Wetterskog[3], R. P. Hermann[2], A. Wiedenmann[1], G. Salazar-Alvarez[3], L. Bergström[3], Th. Brückel[2]

[1]*Institut Laue-Langevin (ILL), Grenoble, France*
[2] *JCNS and PGI, JARA-FIT, Forschungszentrum Jülich, Germany*
[3]*Dept. of Materials and Environmental Chemistry, Arrhenius Laboratory, Stockholm University, Sweden*

Magnetic nanoparticles, as compared to the bulk material, exhibit unique physical properties such as an enhanced magnetic anisotropy, important for applications in data storage because it impedes magnetization reversal. The magnetic anisotropy is strongly related to the surface and shape of the nanoparticles. The influence of nanoparticle shape on the degree of surface spin canting in iron oxide nanoparticles has recently been reported [1].

In this contribution we will present the field-induced ordering of concentrated ferrofluids. In particular, the influence of shape anisotropy on interparticle interactions will be highlighted in our polarized SANS study on highly concentrated iron oxide nanoparticle dispersions. Whereas a spatially disordered, short range ordered hard spheres interaction potential is found for spherical nanoparticles, nanocubes of a comparable particle size reveal a more pronounced interparticle interaction and the formation of linear aggregates. Contributions of van-der-Waals and dipolar interparticle interactions to the field-induced ordering will be discussed.

References

[1] S. Disch et al., New J. Phys. **14** (2012) 013025.
Quantitative spatial magnetization distribution in iron oxide nanocubes and nanospheres by polarized small-angle neutron scattering

Magnetic nanoparticles as reconfigurable matter

F. Wittbracht, B. Eickenberg, M. Schäfers, J. Meyer and A. Hütten

Physics of Nanostructures, Department of Physics, Bielefeld University, P.O. 100131, 33501 Bielefeld, Germany

Introduction

The intermediate concentration regime of magnetic nanoparticles embedded in a fluidic matrix opens the opportunity to exploit magnetic nanoparticles as reconfigurable matter. Under the influence of homogeneous, rotating magnetic fields, superparamagnetic beads or nanoparticles can be assembled on demand into one- and two-dimensional superstructures executing diverse tasks inside microfluidic devices or as printable magnetoresistive sensors when embedded in conductive matrices. Our contribution is firstly focusing on the application of superparamagnetic beads for particle separation, mixing and bioseparation. Secondly, we will discuss the performance of printable nanoparticular GMR-sensors realized by embedding Cobalt nanoparticles in conductive matrices.

Continuous-flow particle separation

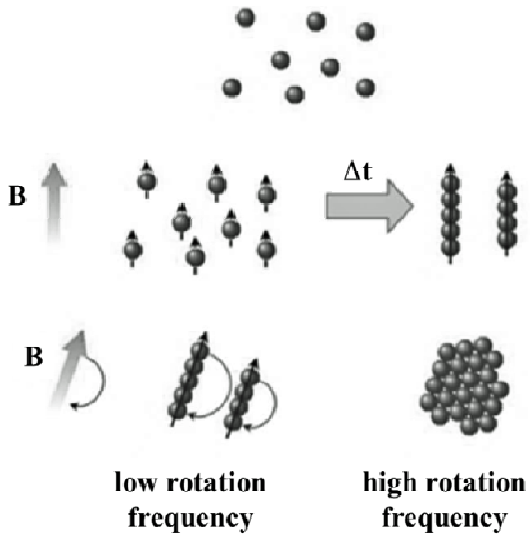

***Fig. 1**: Mechanism of superstructure formation.*

In the absence of an external magnetic field, see fig. 1, superparamagnetic beads are randomly distributed within the matrix. Under the influence of a static homogeneous field their induced inhomogeneous stray fields are causing attractive forces between the particles which results in the formation of one-dimensional – chain like – superstructures [1]. When the magnetic field is rotated, the chains follow this rotation until the frequency exceeds a

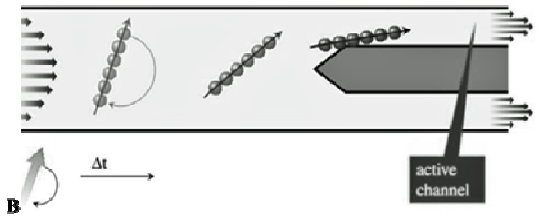

***Fig. 2**: Gate guiding mechanism of the separation device*

critical limit. Above which the viscous drag forces become too strong, the chains can no longer follow the rotation and the formation of two-dimensional, disc-like structures is favored [2]. Rotating bead superstructures are flowing through a microfluidic channel, compare with fig. 2. At a separation junction, where a barrier splits the main channel into two diverging channels, the rotation of the superstructures leads to a transversal movement when the superstructures interact with the barrier. Thus, the bead flow can be limited to one of the two diverging channels [3]. Since the direction of this movement depends on the direction of field rotation, either the upper or the lower channel can be selected. Varying the magnetic field strength, the rotation frequency and the mean channel width of the microfluidic system the separation efficiencies of 1µm beads as a function of the flow velocity are summarized in fig. 3.

Enhanced mixing of two co-flowing liquids

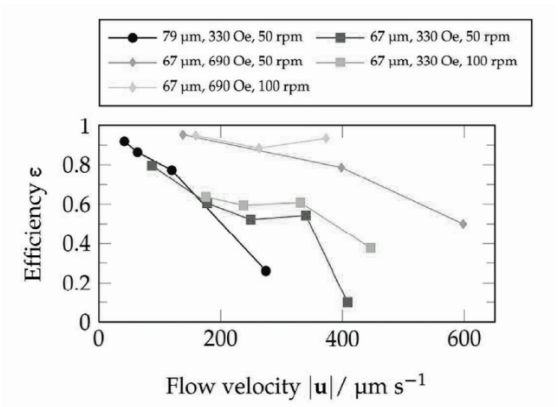

***Fig. 3**: Separation efficiency defined as* $\varepsilon = 2x - 1$ *as a function of flow velocity in microfluidic channels of different mean widths at different external magnetic field strengths and rotation frequencies. X is the fraction of beads passing through a designated channel.*

Under laminar flow conditions in the absence of beads, mixing of the two liquids can only be achieved by diffusion. If beads are dispersed in one of the two liquids, superstructures can be formed under the influence of external magnetic fields. The rotation of these superstructures disturbs the boundary layer between the two flows, creating a convective flux from the upper layer into the lower layer and vice versa, leading to enhanced mixing near the location of the superstructure, similar to fig. 4. Previous experiments showed an increase in diffusivity by 32 % for FAD in water [3].

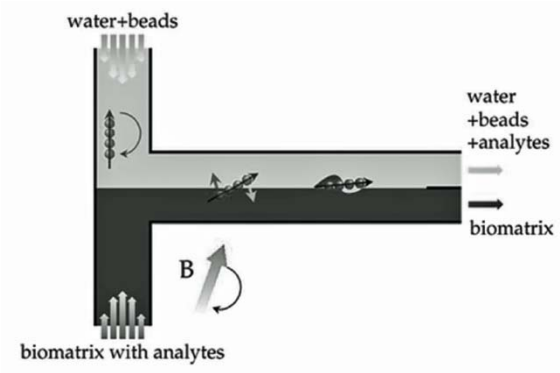

***Fig. 4**: T-intersection in front of separation device for bioseparation*

Bioseparartion

The interaction of rotating magnetic superstructures may be used to separate biomolecules from a biological matrix in a co-flow of two liquid streams, see fig. 4. The beads are introduced in an analyte-free buffer solution which meets a biological matrix at a T-intersection. The bead superstructures contacting the biological matrix and bind the analyte molecules on their functionalized surface. If the T-junction is built in front of a separation device, the two flows are split into separate channels. As a proof-of-principle for this bioseparation concept, biotin-coated polystyrene particles were captured by streptavidin-coated bead superstructure and successfully guided into the activated channel of a separation device.

Nanoparticular GMR sensors

If the liquid matrix is also conductive magnetic nanoparticles embedded can also be arranged in an external magnetic field so as to tailor their next neighbor distance. Spin depended transport via the conductive matrix allows for a nanoparticular GMR-response which exceeds the GMR-effect amplitude of conventional multilayered systems by far as is shown in fig.5.

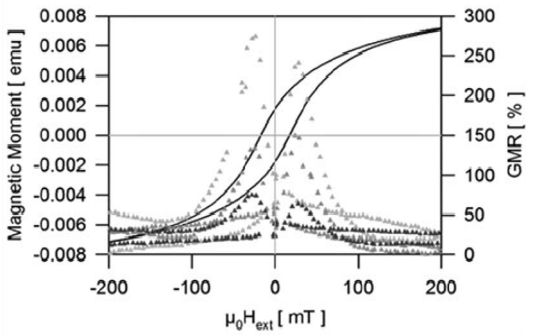

***Fig. 5**: Evolution of GMR-characteristics of magnetic Co nanoparticles embedded in gel matrices when drying out.*

References

[1] A. Weddemann, F. Wittbracht, A. Auge, A. Hütten, Microfluid Nanofluid **10** (2011) 459.

[2] A. Weddemann, F. Wittbracht, B. Eickenberg, A. Hütten, Langmuir **26** (2012) 19225.

[3] F. Wittbracht, A. Weddemann, B. Eickenberg, M. Zahn, A. Hütten, Appl. Phys. Lett., **100**, (2012) 123507.

Relaxation and Anisotropy in magnetic nanocubes

R. Meckenstock[1], A. Terwey[1], C. Schoeppner[1], A. Trunova[1], N. Reckers, M. Farle[1]

[1] *University Duisburg-Essen, experimental physics, Duisburg, Germany*

Ferromagnetic resonance on the nano scale

In the last years the investigation of spin transport effects through spintronic devices and spin dynamics in single nano particles and tailored ensembles has grown. By establishing hybrid structures on the nanoscale consisting of at least one or more magnetic constituents the tailor-ability of magnetic capabilities of the overall specimen will improve dramatically. To investigate these tailor able magnetic capabilities a profound knowledge of the individual constituents can only be archived on the nanoscale.
Therefore one of the most powerful tools for static and dynamic magnetic characterization, the CW ferromagnetic resonance (FMR) has been sensitivity enhanced and combined with tree different detection schemes on the nano-scale. Offering besides the local resolution of FMR in the sub 100 nm regime the possibility to gain element- specific, thermal and structural information simultaneously (see Fig. 1).
In addition, those detection schemes can be turned in active modelling devices offering optical, and thermal and x-ray excitation functionality on the nano scale.

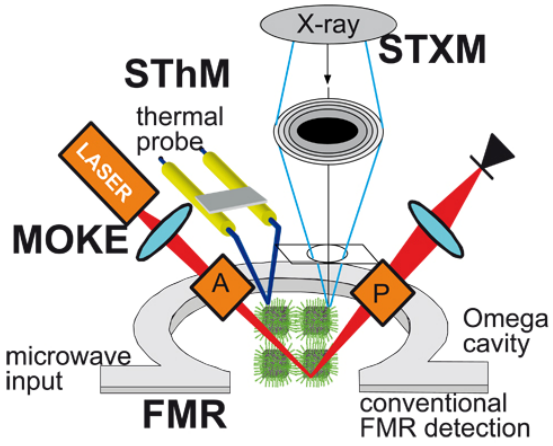

Fig. 1: FMR in an Omega shaped micro cavity; allowing conventional, thermal, optical and X-ray detection and modulation by applying a scanning thermal microscope (SThM), a magneto optical Kerr effect (MOKE) setup and a scanning transition X-ray microscope (STXM)

Tailoring of magnetic state of Fe nano cubes

Here is shown as an example the FMR investigation of a single layer of 15 nm edge length single crystal Fe cubes on a GaAs substrate. The upper part of Fig. 2 shows the statistical average of all possible FMR lines for single crystal Fe cubes lying on a substrate having a (001) surface facing up.
In the lower part of Fig. 2 this simulation is fitted to the measured FMR spectra for the external field in the film plane and perpendicular to it with a single set of magnetic parameters.
The Electron paramagnetic (EPR) line of the ligand system used to grow and separate the Fe cubes can still be seen as a very small but sharp line at about 0.27 T both in in plane and out of plane configuration. In this example the ligand system was removed by oxygen plasma thus only very little amount of ligands is left at the interface of Fe cubes to substrate. These EPR lines of the ligands in contact with Fe allow information of the contact zone. Fourfold symmetry is found in in plane angle dependent EPR experiments on Fe cubes deposited as a monolayer on a substrate without oxygen plasma, which is not found on Fe nano particles having a spherical

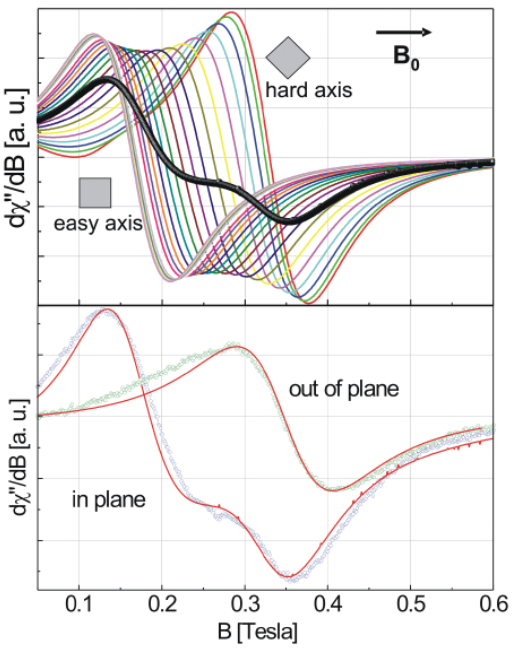

Fig. 2: example of analysing conventional FMR of a single layer of 15nm Fe single crystal nano cubes.

shape. Thus this additional EPR line provides an insight in the interaction of the Fe and the ligand system. Even the magnetic damping in a single nanoparticle can be estimated from the line shape simulations to be very close to that of a single crystal Fe film.

Nevertheless these conventional FMR investigations on this large amount of particles will never be able to provide important insight in the surface anisotropy and its origin especially in combination with changing ligand conditions, or an inside in more complicated structures like core shell particles and their exchange interface interaction. Therefore small agglomerates or single particles investigations will be needed without statistical contributions of the ensembles.

Introduction of omega shaped strip line based micro cavities

Micro cavities used in combination with FMR detected by micro wave absorption has significantly increased the sensitivity by at least 4 orders of magnitude compared to FMR detected by at a conventional cavity reflected microwave power. This means for typical 3d metal FMR the actual detection limit is about 10^5 collective spins [2,3]. This is well within the limit of nano particles or small agglomerates.

Here the reduction of the amount of Fe_xO_y/Fe core shell nano particles from a statistically behaving powder to a mono layer of particles to individual resonances of single particles or small agglomerates in a micro cavity will be shown, featuring the enhancement of information on the magnetic behaviour without changing the parameter set from investigation to investigation.

In addition first results on SThM-FMR and x-ray detected FMR will be shown on other nano structure samples serving as prototype investigations.

Acknowledgments

This work was supported by the SFB 491 and SFB 616

References

[1] C. Antoniak, N. Friedenberger, A. Trunova, R. Meckenstock, F. Kronast, K. Frauth, M. Farle and H. Wende, Nanoparticles From The Gasphase, NanoScience and Technology Part 3, chapter 11, 273-302 (2012)

[2] A. Banholzer, R. Narkowicz, C. Hassel, R. Meckenstock, S. Stienen, O. Posth, D. Suter, M. Farle and J. Lindner, Nanotechnology 22, 295713 (2011)

[3] R. Narkowcz, D. Suter, and R. Stonies, J. Magn. Reson. 175, 275 (2005). [5] R. Narkowcz, D. Suter, and R. Stonies, J. Magn. Reson. 175, 275 (2005).

Optical detection of the rotational dynamics of anisotropic magnetic Nickel nanorods

S. Schrittwieser[1], F. Ludwig[2], J. Dieckhoff[2], A.Tschoepe[3], A. Guenther[3], A. Huetten[4], H. Brueckl[1], J. Schotter[1]

[1] *Molecular Diagnostics, AIT Austrian Institute of Technology, Vienna, Austria*
[2] *Institute of Electrical Measurement and Fundamental Electrical Engineering, TU Braunschweig, Braunschweig, Germany*
[3] *Experimentalphysik, Universitaet des Saarlandes, Saarbruecken, Germany*
[4] *Department of Physics, Bielefeld University, Bielefeld, Germany*

We introduce a novel biosensor concept, which employs hybrid nanoparticles consisting of magnetic nanorods encapsulated by noble metal shells. These nanoparticles have the potential to directly signal the presence of analyte molecules in the sample solution via an increase of the hydrodynamic volume with analyte binding. While the nanoparticles' magnetic cores enable rotation in an external magnetic field, their shells are used to monitor their rotational dynamics through the excitation and observation of longitudinal plasmon resonances (Fig. 1) [1]. We present model calculations on the aspired properties of suitable core-shell nanorods and experimental results proofing the principle of this measurement method for plain Ni-nanorods excited by a rotating magnetic field. Furthermore, we will show how rotational dynamics change upon protein binding using bovine serum albumin (BSA).

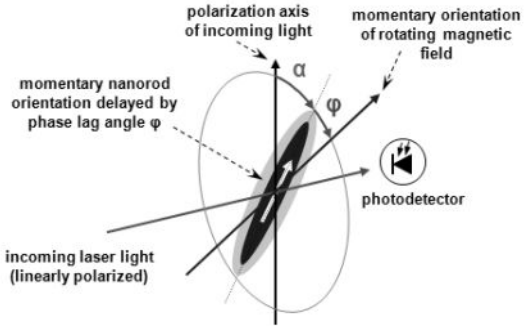

Fig. 1: Concept sketch of nanorod rotation and detection

Method

Our application requires complex multi-component nanoparticles that combine both magnetically and optically anisotropic properties (e.g. an elongated core-shell structure with magnetic core and noble metal shell functionalized by specific antibodies against the target molecule) [2]. While we currently strive to realize our aspired hybrid core-shell nanorods, plain Ni-nanorods dissolved in aqueous solution serve as model system to verify the detection principle (Fig. 2).

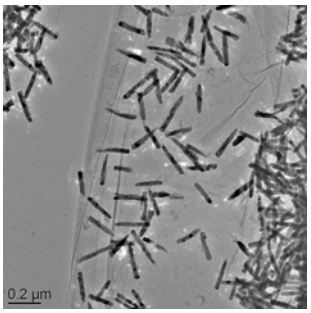

Fig. 2: TEM image of plain Ni-nanorods (173 nm mean length, 28 nm mean diameter)

Nickel nanorods are synthesized by pulsed electrodeposition into alumina templates in an aqueous solution of Ni salts. Particles are stabilized during dissolution of the template with Polyvinylpyrrolidone (PVP) which binds to the surface of the nanorods and serves as a surfactant to obtain single particle dispersions via electrostatic interactions. [3]

We use rotating magnetic fields for alignment control of the nanoparticles in suspension, while their orientation dependent extinction is measured optically (laser diode & photodetector). The phase shift and amplitude of the extinction relative to the rotating field is measured in dependence of field frequency and magnitude by a Lock-In amplifier.

Mathematical modeling

While magnetization processes within solids are well described by the Landau-Lifschitz-Gilbert equation, thermal effects play a major role in ferrofluids. The inclusion of thermal agitation in Gilbert's equation results in the Fokker-Planck equation [4].

Yoshida et al. performed numerical simulations on the Fokker-Planck equation in case of a magnetic fluid in a rotating magnetic field to obtain an empirical expression for a quantitative description of particle dynamics [5]. We use these equations to theoretically model the expected phase lag under realistic variation of particle geometry parameters.

Experimental results

Experimental results demonstrate the evolution of the phase lag of plain Ni-nanorods relative to the rotating magnetic field under varying conditions.

Phase measurement results for plain Ni-nanorods are shown in Fig 4. A theoretical fit to measured data is obtained with reasonable values of the mean and standard deviation of the magnetic moment, the length and the diameter of the Ni-nanorods.

After addition of BSA to the nanorod solution, an increase of the phase lag due to an increased hydrodynamic volume can be detected experimentally (Fig. 5). Theoretical fits are again employed for the case of nanorods with an increased volume due to protein binding and agree well with the experimental data.

The presence of bound BSA is also confirmed by zeta potential measurements as after addition of BSA, the zeta potential changes from positive to negative values.

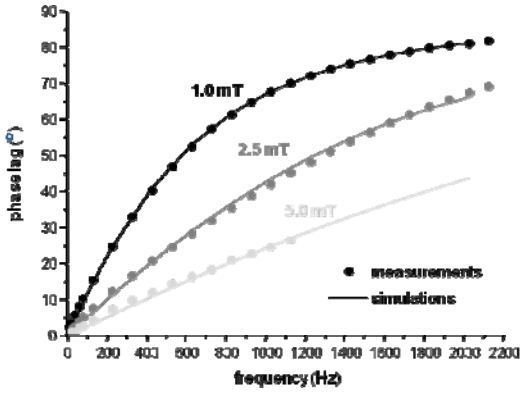

Fig. 4: Phase measurements of plain Ni-nanorods at three different field amplitudes and comparison to theoretical data.

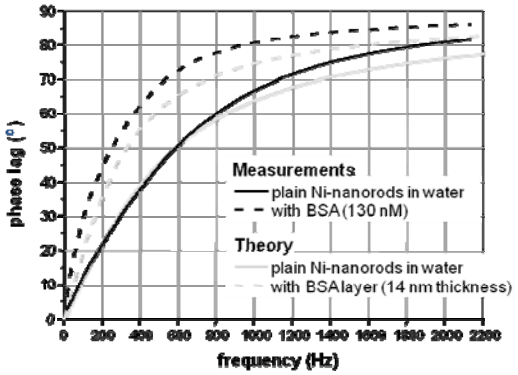

Fig. 5: Phase measurements of plain Ni-nanorods and after addition of BSA. The field amplitude is 1 mT

Acknowledgments

The research leading to these results has received funding from the European Community's 7th Framework Programme under grant agreement n° NMP4-LA.

References

[1] Schotter et al., Austrian patent number 503845, PCT application number WO/2008/124853.

[2] Schrittwieser et al., ACS Nano 6 (2012), 791-801.

[3] Guenther et al., J. Phys.: Condens. Matter 23 (2011), 325103.

[4] Yu et al., Advances in Chemical Physics 87 (1994) 595.

[5] Yoshida et al., J. Appl. Phys. 111 (2012), 053901.

Analysis of the Enhanced Deformation of a Magnetic Fluid Contour

J. Popp[1], K. Zimmermann[1], V.A. Naletova[2], D. Pelevina[2], V. Böhm[1], I. Zeidis[1],

[1]*Ilmenau University of Technology, Dept. of Technical Mechanics, Max-Planck-Ring 12, 98693 Ilmenau, Germany*
[2]*Lomonosov Moskow State University, Institute of Mechanics, Moscow University, Michurinskii Pr. 1, 119899, Moscow, Russia*

For the research of non-pedal locomotion systems and mobile robots basing on ferrofluids and ferroelastomers the enhancement of driving forces is desired. By inserting field concentrating high permeable cores the deformation ability of a magnetic fluid increases and shows continuous and discontinuous reactions. The behavior of the fluid contour is experimentally investigated with reference to the calculations of research partners. The comparison of the results shows a good agreement and provides the tools for manipulation tasks.

Introduction

Unconventional locomotion systems also cover non-wheeled and non-legged (non-pedal) means of transportation. The involved principles mainly base on periodic surface deformation. This can be realized by compliant materials, such as magnetizable fluids and elastomers. Since these materials can be controlled by external magnetic fields, ferrofluid or -elastomer based locomotion systems are potentially used for mobile, energy autonomous robots.

The System and its Behavior

Since the ferrofluid generated forces and the corresponding deformation are generally low for locomotion purposes, the counter-approach applies the selective enhancement of the surface deformation.
Considered is a plane layer of magnetizable fluid, where a high magnetizable cylinder is inserted. An external homogeneous magnetic field is applied in different angles to the fluid, see figure 1.

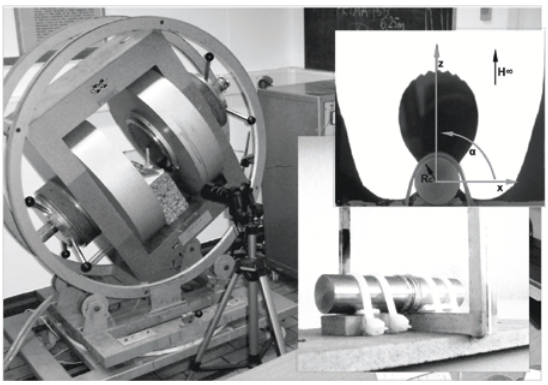

Figure 1: Experimental setup, pivot magnet with positioned fluid container and camera, right side, top: coordinate system, right side, bottom: fluid container with inserted concentrator.

The behavior was theoretically investigated in [1, 2], describing a system containing a cylindrical or a spherical concentrator, the gravity and surface tension forces were taken into account in [2].
While the magnetic field strength is increased, the deformation of the fluid surface is monitored. The ferrofluid contour performs continuous and discontinuous changes to separate into single fluid volumes, to build up new volumes and to rejoin dissociated volumes at the arrival of the magnetic field thresholds.
The contour behavior was examined experimentally incorporating the ferrofluid EMG 902 (Ferrotec GmbH, Germany) and a cylin-

Figure 2: Process of contour deformation in the increasing magnetic field (60° inclination), photo series.

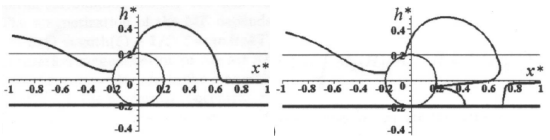

Figure 3: Calculation of the contour deformation in the increasing magnetic field, [1].

drical field concentrator, see figure 1. The study confirmed the predicted surface shapes, see figures 2 and 3. The calculated and experimentally obtained magnetic field values for a discontinuous change of the fluid contour bear a low disagreement. Furthermore, the comparison of the behavior of the fluid contour, when exposed to an increasing and decreasing magnetic field, showed hysteresis. The size of the hysteresis difference becomes more pronounced by higher inclination angles of the magnetic field, see figure 4.

Summary

The obtained data are the basis for the manipulation and control of magnetic fluids. Methods developed from that may use the discontinuous rapid transitions for advanced velocities and the reduction of reaction times. Sceneries, which would benefit from that, range from magnetic fluid actuators controlling other (immiscible) fluid flows, which can be valves, breakers, seals et cetera, to magnetic fluid filled envelops performing enhanced periodic motion for self propulsion or locomotion assistance for other bodies.

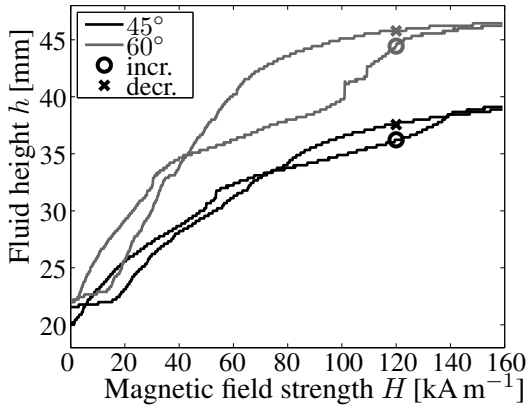

Figure 4: Hysteresis behavior of rising and descending fluid contour.

Acknowledgments

This work is financially supported by Deutsche Forschungsgemeinschaft (DFG), project 15 Zi 540-14/1, the Russian Foundation for Basic Research, project 10-01-91333, and the postgraduation scholarship of the free state of Thuringia, Germany. Furthermore we received generous assistance by Prof. Dr. S. Odenbach and Dr. D. Borin, Faculty of Mechanical Engineering, TU Dresden, Germany, offering equipment and advice.

References

[1] K. Zimmermann, I. Zeidis, V.A. Naletova, V.A. Turkov, D.A. Pelevina, V. Böhm, J. Popp: Surface of a magnetic fluid containing magnetizable bodies in an applied uniform magnetic field. J. MHD. 44 (2), (2008) p175.

[2] V.A. Naletova, D.A. Pelevina, V.A. Turkov: Statics of a Magnetic Fluid Containing Magnetic Field Concentrators. Fluid Dynamics. 44 (6), (2009) 797–803.

[3] V.A. Naletova, D.A. Pelevina, V.A. Turkov, A.V. Rozin, K. Zimmermann, J. Popp, I. Zeidis: Behavior of a free surface of a magnetic fluid containing a magnetizable cylinder. J MAGN MAGN MATER. 324 (2012) 1253–1257.

Magneto-optical nanorheometry of hydrogels with nickel nanorods as colloidal probes

C. Schopphoven, E. Wagner, A. Schneider, A. Tschöpe, R. Birringer

Technische Physik, Universität des Saarlandes, 66041 Saarbrücken, Germany

Nickel nanorods with a length of 125 nm and a diameter of 23 nm were synthesized in an AAO-template based process. Nanorods of this size are uniaxial ferromagnetic single domain particles. These properties allow to exert a torque on the rods by an external magnetic field. In a homogeneous magnetic field H the magnetic moment rotates out of the anisotropy axis against the magnetic shape anisotropy energy. In addition, the particle itself rotates by an angle ω, which is determined by the mechanical compliance of the surrounding elastic matrix. From the torque-balance $T_{mag} = T_{mech}$, the relationship

$$\omega = \frac{m_p 3 \ln(n)}{V_p 4 n^2 G} \cdot \mu_0 H \sin\phi, \qquad (1)$$

can be derived, where m_p is the magnetic moment of a single particle, V_p the mean volume, n the aspect ratio, ϕ the angle between the magnetic moment and the external field and G the elastic shear modulus. The values V_p and n can be obtained through electron microscopy measurements and m_p can be determined by optical transmission measurements as described in [1]. Thus, plotting ω against $\mu_0 H \sin(\phi)$ and subsequent linear regression enables us to estimate the local shear modulus of the elastic matrix.
To obtain ω as a function of the applied magnetic field, we exploit the optical anisotropy of the nickel nanorods, which causes a significantly orientation-dependent extinction of linearly polarized light. The angle ϕ can be calculated for each ω, using the shape anisotropy constant $K_A = 35.8\ \mathrm{kJ/m^3}$, as determined from magnetization measurements

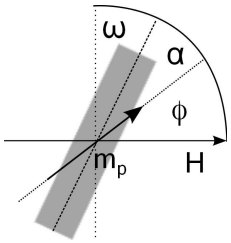

Figure 1: Schematic illustration for the definition of rotation angles

as described in [2]. Hence, the magnetic nanorods are used as nanorheological probes to measure the local shear modulus of elastic matrices by magneto-optical measurements.

Synthesis

The nanorods are synthesized by electrodeposition of nickel into porous alumina templates and subsequently released by dissolving the alumina, while polyvinyl-pyrrolidone (PVP) is added as a surfactant to prevent immediate agglomeration. After a thorough washing process, a stable colloidal dispersion of Ni-nanorods is obtained.
The rods are then dispersed into gelatin sols at 60° C. During gelation, a homogeneous magnetic field is applied to align the rods in field direction. As the temperature decreases, the rods are fixed in this orientation by the evolving gel network and a magnetically textured ferrogel is obtained.

Method

To estimate the shear modulus of the gelatin matrix, a magnetic field is applied perpendicularly to the long rod axis. The resulting rotation angle ω is obtained from the

transmitted intensity of polarized laser light. If the polarization direction is perpendicular to the long rod axis, a maximum intensity I_{max} is transmitted, while a parallel orientation results in a minimum intensity I_{min}. Using both limiting intensities as reference values, any measured transmitted intensity $I(H)$ can be attributed to a specific rotation angle:

$$\omega = \arccos \sqrt{\frac{I(H) - I_{min}}{I_{max} - I_{min}}}. \qquad (2)$$

The angle $\phi = 90° - (\omega + \alpha)$ can be calculated for any $\omega(H)$, by solving the transcendental equation

$$\cos(\omega + \phi) \sin(\omega + \phi) = \frac{M_S}{2K_A} \mu_0 H \sin(\phi), \qquad (3)$$

where M_S is the saturation magnetization of nickel. With both $\omega(H)$ and $\phi(\omega)$ known, the shear modulus can now be calculated, using eq. 1.

Results

The presented method is applied to study the shear modulus of gelatin-based hydrogels. For three different hydrogel samples with gelatin concentrations c of 1.73, 2 and 2.45 wt.% the measurements revealed the logarithmic increase of G with gelation time as well as a linear dependence of G on c^2, as expected [3]. The absolute values however are much larger than macroscopic rheometric measurements suggest. This overestimation may be attributed to an increased polymer network density around the nanoparticles, caused by high chemical affinity of gelatin to the PVP surface layer. This explanation is supported by measurements of the rotational diffusion coefficient, which reveal a significant decrease of D_R upon addition of ≈ 0.1 wt.% gelatin indicating strong adsorption.
Nevertheless the presented method is applicable for semi-quantitative measurements after calibration with a sample of known shear

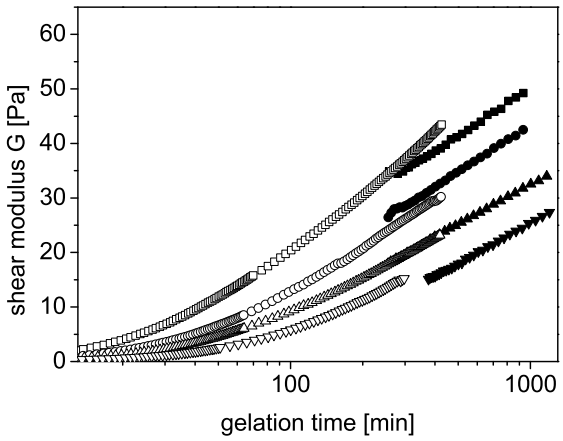

Figure 2: Shear modulus of 2 wt.%-hydrogels measured by conventional rheometry (open) and magneto-optical transmission after calibration (full) at four different temperatures: 17 °C(□), 18 °C(○), 19 °C(△), 20 °C(▽)

modulus. As an example, the shear modulus of 2 wt.%-hydrogels was obtained by magneto-optical (G_{mo}) as well as macroscopic rheometer measurements (G_r) at temperatures between $17°\mathrm{C}$ and $20°\mathrm{C}$. The calibration factor $f = G_r/G_{mo}$ was obtained from the measurements at $19°\mathrm{C}$ and then applied to the whole data set. The calibrated shear moduli shown in Fig.2 exhibit a temperature dependence in good agreement with the macroscopic rheometer measurements.

Acknowledgments

We would like to thank Prof. Dr. C. Wagner for access to the rheometer equipment.

References

[1] T. Klein et al., AIP, 106, 114301 (2009)

[2] P. Bender et al., JMMM, 323, 2055 (2011)

[3] V. Normand et al., Macromolecules, 33, 1063 (2000)

A comparison between micro- and macro- structure of magnetoactive composites

T. Gundermann, S. Günther, D. Borin, S. Odenbach

Technische Universität Dresden, Chair of Magnetofluiddynamics, 01062 Dresden, Germany

Magneto active composites are a kind of smart materials which consists of soft magnetic particles dispersed in an elastomeric matrix. The mechanical properties of this composite material can be changed active and reversible by applying a magnetic field. An essential reason for the property changes is an internal magnetodipolar striction, i.e. a change of the local positions of the particles.
A possibility to determine these particles and there local position in a magneto active composite is given by micro-computed tomography (µ-CT) [1, 2]. The main interest of the current study has been an observation of the magnetic field depended shift of individual particles from their initial positions inside an elastomeric matrix.
For this purpose a µ-CT system has been combined with a sample holder coupled with two permanent magnets (Fig.1), enabling the investigation of the microstructure under influence of an external homogeneous field.

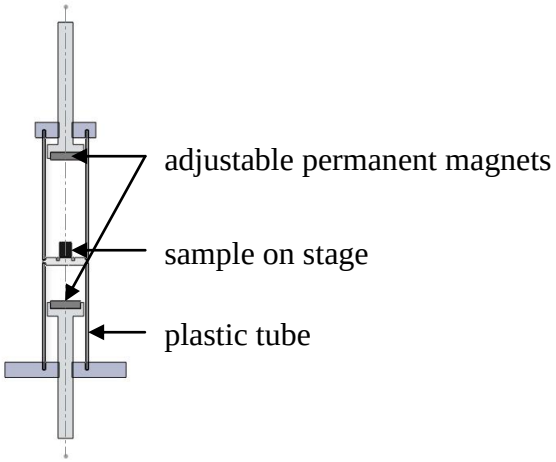

Figure 1: New setup for µ-CT investigations of MRE´s under influence of a magnetic field.

In the experimental investigations samples based on carbonyl iron particles have been used. The particles have been dispersed in a polymeric matrix and the polymer has been created in the presence of a magnetic field driving structure formation of the particles.
After the characterization of the sample in its initial state, i.e. without external stimuli, it has been subjected to the magnetic field and its internal structure has been once more studied by µ-CT. As a result a comparison of the macroscopic change of the sample structure and the particle displacement could be undertaken.

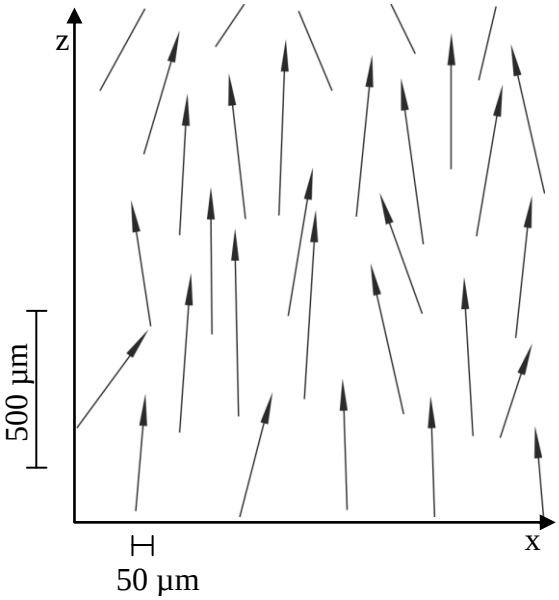

Figure 2: Displacement of the centre of the particles under the influence of a magnetic field. Shown is a cut of the z-x-plane, z is parallel to the applied magnetic field.

The results show a particle movement (Fig. 2) parallel to the applied magnetic field,

which is larger than the particle movement in the direction perpendicular to the magnetic field. In addition, it has been found that the particle shift is larger, than the macroscopical deformation of the sample. This finding leads to the conclusion that the particles in this kind of MR-elastomer can move relative to the matrix with small influence on the matrix deformation only.

Acknowledgments

This project is founded by the European Union and the Free State of Saxony

References

[1] D. Günther, D. Yu Borin, S. Günther, and S. Odenbach, Smart Mater. Struct. **21** 015005 (2012)

[2] T. Borbath, S. Günther, D. Yu Borin, Th. Gundermann and S. Odenbach, Smart Mater. Struct. **21** 105018 (2012)

Magneto-mechanical Coupling in Ferrohydrogels

L. Roeder, M. Reckenthäler, L. Belkoura, A. M. Schmidt*

*Department Chemie, Institut für Physikalische Chemie, Universität zu Köln, Luxemburger Str. 116, D-50939 Köln, *E-Mail: schmidt.annette@uni-koeln.de*

Hybrid nanomaterials accessible by the combination of inorganic and organic compounds implement different functions and characteristics within a single material. The integration of magnetic nanoparticles into swollen polymer networks, resulting in so-called ferrogels, offers the possibility to combine magnetic and gel-like properties.[1] In these materials the shape or mechanical performance of the matrix can be manipulated by external magnetic fields in several ways. The material architecture and composition, the type of interaction between the incorporated magnetic particles and the matrix (i. e. *slip* or *no slip*), as well as the mode of the applied field affect the observation if either magnetostriction, induction of dipolar interactions, or magnetic heating are predominating the materials behaviour.[2,3]

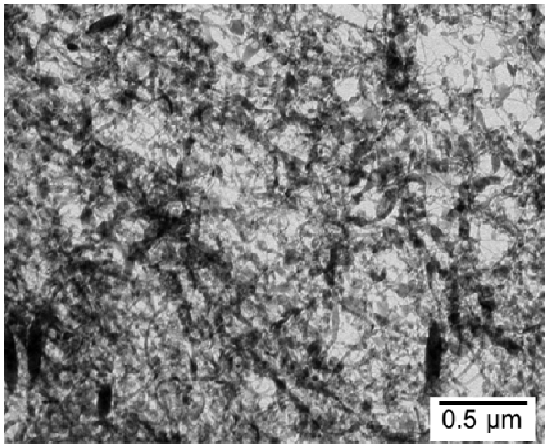

Figure 1: TEM image of a ferrogel crosslinked with α-Fe_2O_3 ellipsoids.

A direct cross-correlation between magnetic and mechanical characteristics is possible by using magnetically blocked or ferromagnetic particles, as their magnetic reorientation is accompanied by mechanical particle rotation.[4] This allows the investigation of the particle dynamics and the counter forces of the polymer matrix concerning viscous and elastic effects by analyzing the magnetic properties in relation to hysteresis effects and the initial susceptibility of the integrated particles.[5,6]

Here we present the synthesis and magnetic properties of α-Fe_2O_3 ellipsoidal nanoprobes in polyacrylamide (PAAm) matrices. For this purpose the ellipsoids are surface-functionalized with methacrylic groups to serve as multifunctional crosslinkers in the network. Afterwards these functionalized particles are covalently linked to the polymer segments during the gel synthesis. This way a novel type of gel architecture is created (Fig. 1).
The stability and the swelling properties of the ferrogels depend strongly on the synthetic conditions, in particular on the monomer (acrylamide, AAm) concentration and the particle content during synthesis (Fig. 2).

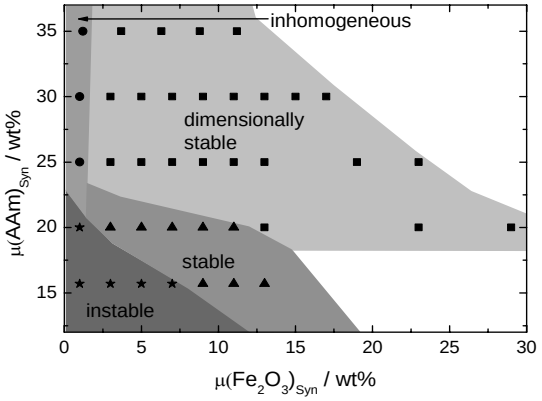

Figure 2: Stability diagram of the synthesized ferrogels.

The swollen and dried ferrohydrogels are investigated in relation to their magnetic

characteristics, and information on the mechanical interaction between the particles and the matrix is obtained from quasi static magnetometry. As the particles are ferromagnetic and covalently linked to the polymer segments the mechanical response is directly transferred to the polymer network and information on the elastic restoring force is obtained (Scheme 1).[7,8]

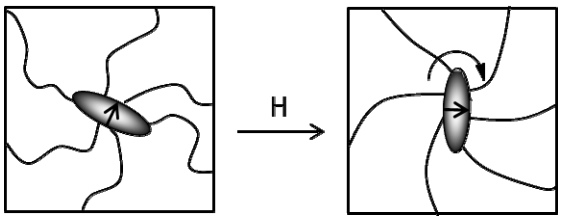

Scheme 1: Illustration of the impact of matrix interaction on the remagnetization behavior of ferromagnetic α-Fe_2O_3 ellipsoids in an applied magnetic field.

Our results provide an insight in the network architecture and the local magneto-mechanical behavior of these novel materials, indicating the potential of magnetic nanoprobes for the structural investigation and manipulation of soft matter by using static magnetic fields.

Acknowledgments

We acknowledge the DFG for financial support in the framework of SPP1259, "Intelligent Hydrogels" and the Emmy Noether program.

References

[1] N. Frickel, R. Messing, A. M. Schmidt, *J. Mater. Chem.* (21), 8466-8474, **2011**.
[2] M. Zrinyi, *Trends Polym. Sci.* (5), 280, **1997**.
[3] R. Messing, A. M. Schmidt, *Progr. Colloid Polymer Sci.* (134), 134, **2008**.
[4] J. A. Galicia, F. Cousin, E. Dubois, O. Sandre, V. Cabuil, R. Perzynski, *Soft Matter* (5), 2614, **2009**.
[5] Y. L. Raikher, V. V. Rusakov, *Brazil. J. Phys*. (31), 366, **2001**.
[6] Y. L. Raikher, V. V. Rusakov, W. T. Coffey, Yu. P. Kalmykov, *Phys. Rev. E* (63), 031402, **2001**.
[7] R. Messing, N. Frickel, L. Belkoura, R. Strey, H. Rahn, S. Odenbach, A. M. Schmidt, *Macromol.* (44), 2990-2999, **2011**.
[8] N. Frickel, R. Messing, T. Gelbrich, A. M. Schmidt, *Langmuir* (26), 2839-2846, **2010**.

Birefringence as a Tool to Characaterize the Matrix of Thermor-eversibel Ferrogels

A. Weikl[1], M. Krekhova[2], H. Schmalz[2], Reinhard Richter[1]

[1] *Experimentalphysik V, Universität Bayreuth, 95440 Bayreuth, Germany*
[2] *Makromolekulare Chemie II, Universität Bayreuth, 95440 Bayreuth, Germany*

Introduction

Smart chemically crosslinked poly-gels with magnetic particles have been synthesized [1,2], which can be controlled by exernal magnetic fields. In contrast to these permanent gels, physical ferrogels are characterized by a reversible gelation, e.g. induced by pH or temperatuer changes. So far we have studied thermo-reversible organoferrogels [3,4] and hydroferrogels [5] using an ABA-type triblock copolymer as gelator. For the case of hydroferrogels we use a Pluronic™ P123 gelator in combination with water-based ferrofluids. The latter gels are "inverse-gels", i.e. liquid at low temperatures, whereas gelation occures at elevated temperatures.
Dependent on the temperature range these gels exhibit a cubic or a hexagonal phase, which show different rheological behaviour [5]. Moreover the phases should have different optical propeties, in particular the hexagonal phase is expected to show birefringence.
In our contribution we present an experimental setup which is capable to examine the temperature dependent birefringence of themoreversible neat gels (NG) and ferrogels (FG) based on Pluronic™ P123 as gelator with high resolution and show first results.

Experimental Setup

A sketch of the experimental setup is given in Figure 1. In the center of the setup, the gel is contained between two glass-plates with a Mylar® film as a spacer. To heat or cool this cell, two ring-shaped Peltier elements with similar shaped heatsinks are used. The temperature is measured via a platinum resistor. To achieve a distinct temperature, a proportional-integral-differential (PID) regulation for the Peltier elements is applied. The latter sit inbetween two crossed linear polarizers, so that a birefringence of the gel can be detected as difference in brightness. After the second polarizer a long distance microscope (Questar 100) with an attached camera is used to take a picture of the probe. For this experiment the average of the birefringence in the picture is investigated. However this setup allows as well to examine local structures in the gel, like those observed in [5].

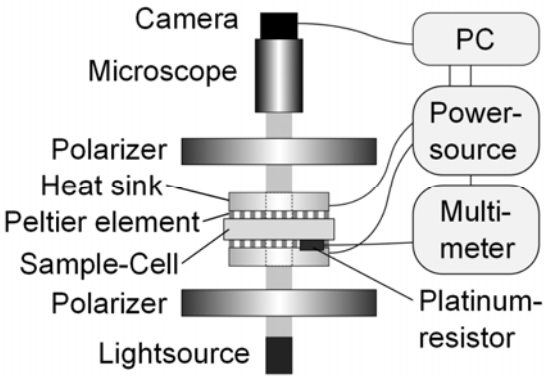

Figure 1: *Sketch of the experimental setup*

Figure 2 displays a photo of the central part of the setup consisting of the Peltier elements and water cooled heat sinks.

Figure 2: *Photo of the sample cell(in the center), the two Peltier elements, and the water cooled heat sinks (outside).*

Results

We prepare a cell with a Mylar® film spacer of 25 µm thickness and fill it with NG with a concentration of 35%, which is liquid at 10°C. By elevation of temperature we bring the sample in the cubic phase. Here we shear the two glass plates against each other in order to break the isotropy of the plane. The matrix of the gel is expected to aligne in the direction of the shear. We heat the sample from 20°C up to 65°C and thereafter cool it down to 20°C with a constant rate of 1°C per minute, recording a picture every 0.1°C.
Figure 3 presents the experimental results. For increasing temperature (black) we observe an increase of the transmitted intensity up to a maximum at 59°C followed by a sudden decay. For decreasing temperature (gray) this maximum is not observed. A possible explanation is that the isotropy of the gel is restored in the liquid phase.

Figure 3: *Evolution of the intensity for increasing (black) and decreasing (gray) Temperature.*

The gradual increase of the transmission in the range from 40°C up to 56°C is correlated with the hexagonal phase, whereas the sudden decay reflects the transsition to the phase of a turbid fluid. This is in accordance with former results [5, 6].

Conclusion and Outlook

To conclude, the temperature dependent birefringence is an important tool to explore the different regimes of a thermoreversible gel. So far we have applied it succesfully to neat gels.
It remains to be investigated how the inclusion of magnetic nanoparticles into the gel matrix affects the transitions between the differnt regimes. This shall be examined for different values and orientations of an externally applied magnetic field.

Acknowledgments

We are grateful for discussions with Ingo Rehberg.

References

[1] M. Zrinyi, Trends in polymer science (Regular ed.) **5**, 280 (1997).

[2] M. Zrinyi, Colloid. Polym. Sci. **278**, 98 (2000)

[3] G. Lattermann and M. Krekhova, Macromol. Rapid. Commun **27**, 1373 (2006), see ibid 1906 for the erratum

[4] M. Krekhova and G. Lattermann, J. Matter. Chem., **18**, 2842 (2008)

[5] M. Krekhova, T. Lang, R. Richter, and H. Schmalz, Langmuir, **26** 19181 (2010)

[6] C. Chaibundit, N. Ricardo, F. Costa, S. Yeates and C. Booth, Langmuir, **23**, 9229 (2007)

Computer simulations on the deformation of ferrogels

R. Weeber[1], S. Kantorovich[1,2,3], C. Holm[1]

[1] *Institute for Computational Physics, University of Stuttgart, Pfaffenwladring 27, 70569 Stuttgart, Germany, www.icp.uni-stuttgart.de*
[2] *Ural Federal University, Lenin Av. 51, 620083, Ekaterinburg, Russia, www.usu.ru*
[3] *Sapienza, University of Rome, Piazza A. Moro 5, 00185, Italy.*

Ferrogels, i.e., hydrogels that additionally contain magnetic single-domain particles, are interesting materials, because their properties arise from an interplay of magnetic and elastic forces. As they can be controlled by tayloring the polymer network forming the gel and by using external magnetic fields to change the interaction of magnetic particles, magnetic gels are considered for applications, e.g., as artificial muscles and drug delivery systems. While many variants of ferrogels can be synthesized today, the detailed microstructure and microdynamics is often unknown.

The most obvious means of deforming a ferrogel is a field gradient. When one boundary of the sample is fixed, the movement of magnetic nano particles into a region with higher field will lead to an elongation or contraction. However, a magnetic gel can also deform in a homogeneous field. There are two distinct mechanisms by which this is possible: a deformation can result from the change of the interaction between magnetic particles, as they are aligned by the external field, or it can be caused by the transmission of the torque acting on magnetic particles onto the polymer matrix, which thereby is deformed.

Computer simulations, in the field of magnetic gels, are of interest, because with them, one can study a model under precisely controlled circumstances and because they can be used to isolate different mechanisms which would occur concurrently in a real system.

We begin our contribution by summarizing the 2d computer model for the deformation by a change in the interaction between magnetic nano-particles. Then, we focus on the 2d and 3d models for deformation by torque transmission. In these systems, the polymer network is cross-linked by magnetic nano particles. I.e., the ends of the polymer chains are chemically attached to the surface of the magnetic particles. When the magnetic particles rotate due to an external field, they pull the

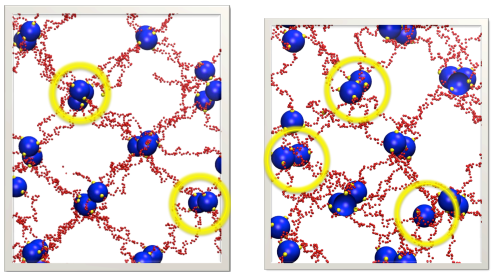

Figure 1: A small part of the 3d gel model without external magnetic field (left), and in a strong field (right). It can be seen that, when a field is applied, the polymer chains are wrapped around the magnetic node particles.

polymer chains and thus deform the gel. A snapshot of such a system is shown in figure 1, both without an applied field and with a strong field applied. In a two-dimensional system, there is only one relevant axis of rotation, namely the axis perpendicular to the plane. This means that the deformation of the gel will always be isotropic, because the stress exerted on the polymer chains is independent of the chain's orientation. In the three-dimensional case, on the other hand, there are three rotation axes. While the magnetic particles can freely rotate around the axis parallel to the field, a rotation around the other two axes would reduce the Zeeman energy and is therefore unlikely in a strong external field. Hence, the orientational fluctuations are different, depending on what axis is regarded. This leads to an anisotropic deformation of the gel.

References

R. Weeber, S. Kantorovich, C. Holm: Deformation mechanisms in 2D magnetic gels studied by computer simulations, Soft Matter Advance Article, 2012

Acknowledgments

RW and CH thank the DFG for funding through the SRC Simtech. The computations have been done at HLRS. Besides that, SK is supported by ERC grant "Patchy Colloids".

Permanent soft elastic magnets with controllable mechanical properties

D.Yu. Borin[1], Th. Richter[1], A.V. Bakhtiiarov[2], G.V. Stepanov[2], S. Odenbach[1]

[1] *Technische Universität Dresden, Chair of Magnetofluiddynamics, 01062, Dresden, Germany*
[2] *Institute of Chemistry and Technology of Organoelement Compounds, Moscow, Russia*

Elastic magnets are commonly made of a rubber matrix with embedded particles made of a magnetically hard material. The particles are incorporated into the matrix before it is vulcanized and they are magnetized either during vulcanization or afterwards. Being once cured and magnetized these elastic materials have fixed mechanical and magnetic properties which are not actively controllable, regardless to the temperature influence. It is only possible to demagnetize them under certain external conditions.

On the other hand there is a kind of multiphase smart composites consisting of an elastic matrix filled with soft magnetic particles. These composites are known as magnetorheological elastomers (MREs) [1]. The most known controllable property of this composite is the so-called magnetorheological effect, which is – in contrast to magnetorheological fluids – an increase of the elasticity in an external magnetic field. As it has been shown before, if the matrix of the MRE is sufficiently soft, i.e. if the elasticity modulus for vanishing magnetic field does not exceed 200 kPa, an enhanced MR effect (up to several 1000%) as well as magnetically driven shape memory and giant deformational effects are observed [2].

As material for the magnetic powder usually carbonyl iron, magnetite or iron oxide are used. Being once cured, MREs have certain viscoelastic properties which are controllable with an applied magnetic field. However, these properties can only be tuned by means of this external stimulus.

We propose the use of a mixture of magnetically hard and soft particles, which will enable the adjustment of the elasticity of MREs after they are cured as well as it will enable a wide active control of their mechanical properties.

In the present work, we consider the influence of the concentration ratio of the magnetically hard and soft particles, the remanence magnetization of the samples and the influence of an applied field on the tensile modulus of an MR elastomer. In the experiments a quasi-static elongation and compression tests as well as dynamic cyclic loading of the MREs with various composition under influence of an external magnetic field have been performed. Furthermore the shear modulus of the samples is determined using oscillating rheometry in order to obtain rheological characteristics of these composite.

Acknowledgments

This project is funded by the European Union and the Free State of Saxony.

G.S. and B.A. are grateful for the financial support to the Federal Agency for Science and Education of Russian Federation.

References

[1] Jolly M R, Carlson J D and Munoz B C 1996 J.Intell. Mater. Sys. Struct. 7.

[2] Stepanov G V, Abramchuk S S, Grishin D A, Nikitin L V, Kramarenko E Yu and Khokhlov A R 2007 Polymer 48.

Magnetite microgels and fatty acid coated nanoparticles for Drug Delivery

R. Tietze[1], S. Lyer[1], S. Dürr[1], J. Mann[1], E. Schreiber[1], R. Turcu[2], A. Schmidt[3], C. Alexiou[1]

[1)]Department of Oto-Rhino-Laryngology, Head and Neck Surgery, Section for Experimental Oncology and Nanomedicine (SEON), Else Kröner-Fresenius-Stiftung-Professorship, University Hospital Erlangen, Germany
[2)]National Institute for Research and Development of Isotopic and Molecular Technologies, Cluj-Napoca, Romania.
[3)] Department Chemie, Universität zu Köln, (Germany).

Introduction:

Nano-sized magnetic drug carriers offer a splendid prospect for directed drug application. The increased drug concentration in cancer tissue reached for this kind of application enables therapeutic effects on tumors that cannot be achieved using conventional chemotherapeutic treatment. Characterizing the drug targeting system and its behavior *in-vitro* is necessary for understanding the biological outcome. In this pilot experiments mitoxantrone (MTO) carrying nanoparticles and nanogels with particles and drug encapsulated were investigated.

Methods:

Iron oxide nanoparticles obtained after alkaline precipitation followed by self-assembling functionalization and nanogels using emulsification-diffusion prior to evaporation were analyzed. Besides basic parameter the binding behavior was investigated using XPS and other spectroscopic techniques. Moreover measurements of the supernatant after treating the samples in different media using HPLC were absolved to give information on total drug load capacity and release behavior. For displaying the morphology of the nano sized objects TEM imaging was done.

Results:

XPS reveals the binding of MTO, which leads to some changes in its structure that cannot be detected for the pure unbound substance. Among others, therapeutic efficacy depends on drug load capacity and drug availability. Whereas fatty acid coated nanoparticles could carry MTO in a veritable amount of 130 µg/ml, the nanogels´ capacity is still lower (40 µg/ml). The morphology of microgels appear more homogenous than fatty acid coated nanoparticles whereby particle clusters of different sizes are visible.

Conclusion:

Fatty acid coated nanoparticles carry a high amount of MTO but strongly vary in size and superstructure morphology. The investigated nanogels still have an insufficient loading capacity for mitoxantrone. Morphology and size distribution seems more homogenous and this could be advantageous for routine synthesis and *in-vivo* trials if the carrying capacity for effective drugs could be further increased.

Acknowledgements:

DFG (AL 552/3-3), Else Kröner-Fresenius-Stiftung, Bad Homburg v.d.H.

Nanorheology of polymer solutions using magnetically blocked $CoFe_2O_4$ nanoparticles

E. Roeben, S. Teusch, M. Dörfer, M. Effertz, A. M. Schmidt[1,*]

[1] *Institut für Physikalische Chemie, Universität zu Köln, Luxemburger Straße 116, D-50939 Köln*

Static and dynamic rheology is an established analytical method to investigate the flow and deformation properties of materials like polymers, which play an important role in industrial processing. For some years there is also an increasing interest to determine the rheological properties on the size scale of micro- or nanometers. Since only a small sample volume is necessary it is possible to investigate the viscoelastic properties of soft matter which cannot be produced in bulk quantities like living cells or biological polymers.[1] For this purpose translation or rotation of colloidal tracer particles embedded in the material, are investigated. In active microrheology the probe is actively driven within the material, either in oscillatory or steady mode. Driving forces are provided for example by laser tweezers, gravity or magnetic forces.[2] Magnetic gradients to affect magnetic microparticles has aroused significant interest in this context. In the present work we investigate the dynamic response of magnetic nanoparticles to oscillating magnetic fields in order to analyze the rheological properties of complex fluids and polymer matrices.

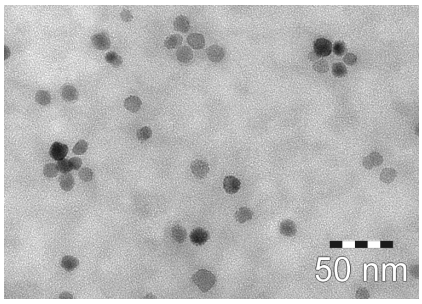

Fig 1: TEM image of the nanoparticles

For this purpose we use magnetically blocked $CoFe_2O_4$ particles (Fig 1) with well-defined hydrodynamic properties as nanoprobes in order to investigate the nanorheological properties of polymer solutions with escalating non-Newtonian properties.

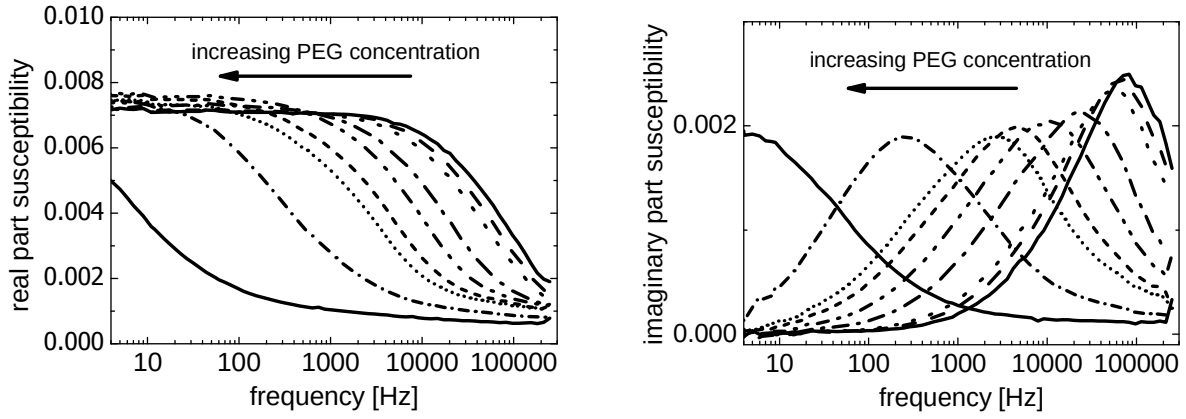

Figure 2: AC susceptibility (left: real part, χ'; right: χ'', imaginary part) of aqueous poly(ethylene glycol) solutions (Mv = 8000 g mol^{-1}) with different polymer concentration.

The particle-matrix interactions are investigated by AC susceptometry (Fig 2), providing an elegant tool to extract rheological properties such as the local viscosity from the complex magnetic susceptibility. By comparing the findings for the different complex fluids with results obtained by conventional rheology, the similarities and differences between the local and the bulk viscosity are demonstrated.

Acknowledgments

We thank Dr. L. Belkoura for TEM imaging of the $CoFe_2O_4$ nanoparticles. We gratefully acknowledge the Deutsche Forschungsgesellschaft (DFG) for financial support within in the framework of SPP 1259 “Intelligent Hydogels”.

References

[1] C. Wilhelm, J. Browaeys, A. Ponton, J.-C. Bacri, *Physical Review E* 67, 011504, **2003**

[2] N. Frickel, R. Messing, A. M. Schmidt, *J. Mater. Chem.* 21, 8466-8474, **201**

The anisotropy of the magnetoviscous effect in ferrofluids

J. Linke[1], M. Gerth-Noritzsch[1], S. Odenbach[1]

[1] *Institute of Fluid Mechanics, Chari of Magnetofluiddynamics, 01062 Dresden, Germany*

Introduction and Background

The flow behaviour and the viscosity of ferrofluids may be tuned by an externally applied magnetic field which opens a range of interesting technical applications. The change of the viscosity is caused by two effects. In ferrofluids with individual non-interacting particles, the free rotation of the particles is slowed down by their magnetic torque counteracting the mechanical torque in the flow. This causes a raise in the viscosity, the so called rotational viscosity. In ferrofluids with strongly interacting particles on the other hand, the formation of chain-like microstructures may occur. The microstructures then obstruct the flow and raise the viscosity. This effect is known as the magnetoviscous effect (MVE) [1]. Both effects are anisotropic - however, the majority of experimental investigations of the MVE have been carried out with only one distinct orientation of the magnetic field.

Experimental setup

To avoid Rosensweig instabilities, two self-contained pressure flow viscometers, one with a capillary and one with a slit geometry, are used to measure the magnetoviscous properties in the ferrofluidic flow. In these systems the viscosity is proportional to the pressure loss along the capillary or die, and the wall shear rate is tunable by means of the flow rate. The magnetic field is generated by a 4-coil Fanselau system [2] which allows a homogeneous field intensity of up to 45 kA/m for a measuring distance of 32 cm in three directions in space. Figure 1 illustrates the Fanselau system and the three field configurations - parallel (a) and perpendicular (b) to the direction of the flow as well as parallel (c) to the vorticity of the flow.

Ferrofluid sample

The ferrofluid for this project was supplied by Strem Chemicals GmbH. It comprises strongly interacting, magnetically hard cobalt particles with a mean particle diameter of 12 nm and a volume concentration of 0.2 vol%. The particles are coated with approx. 3 nm of N-oleoylsarcosine in a kerosene carrier, giving an effective interaction parameter of $\lambda^* = 7.4$.

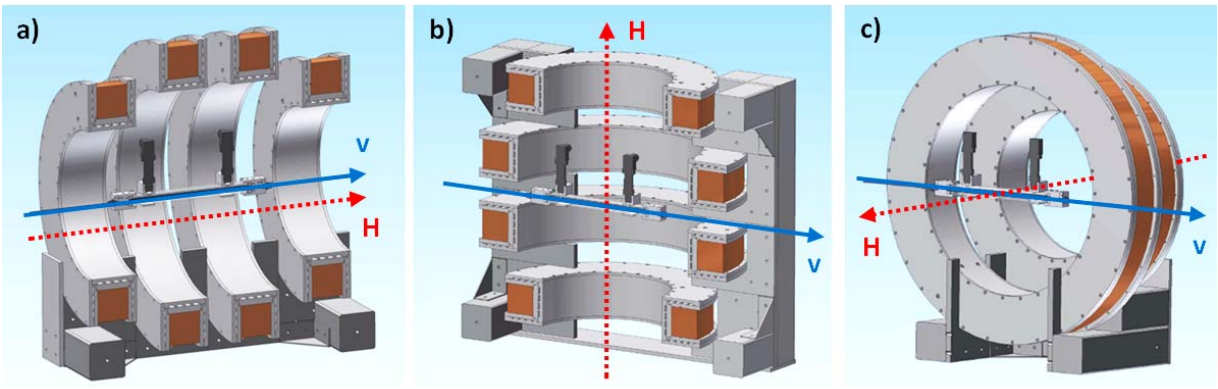

Fig. 1: Cross-sectional view of the experimental set-up with three different configurations of the magnetic field H (dashed line) and the flow direction v (solid line).

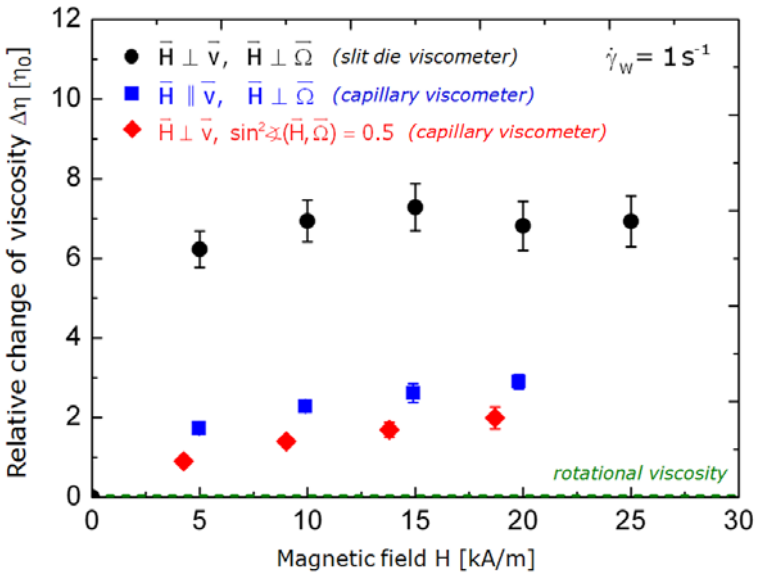

Fig. 2: Maximal theoretical rotational viscosity (dashed line) and measured anisotropic change in viscosity (symbols) of a cobalt ferrofluid for different magnetic field configurations at a wall shear rate of $1s^{-1}$ [3].

Results

The change of the viscosity in the applied magnetic field was found to be more than a magnitude higher than the maximum theoretical rotational viscosity. This supports the theory of the MVE originating from the formation of microstructures due to dipole-dipole interactions. Figure 2 shows the anisotropy of the MVE for three different magnetic field configurations. The largest MVE has been observed for the field direction perpendicular to the flow and perpendicular to the vorticity. In this configuration the microstructures are oriented upright in the slit die leading to a larger hindrance of the flow compared to orientations along the flow. Figure 2 also shows the saturation of the MVE with an increasing field intensity when a balance between the interparticle forces, building up the microstructures, and the shear force, disintegrating the microstructures, is reached. For a constant field the anisotropy of the MVE declines with an increasing shear rate.

Outlook

Further investigations will focus on the systematic variation of the interparticle interactions and the comparison of the results with microstructural computer simulations and the chain-model of Zubarev and Iskakova [4]. Beyond that a modification of the Fanselau system should allow access to the fourth viscosity coefficient to give a complete characterisation of the MVE in magnetic fluids.

Acknowledgments

We gratefully acknowledge the financial support of this project by the Deutsche Forschungsgemeinschaft (DFG grant OD 18-18/01).

References

[1] S. Odenbach (2002) Magnetoviscous Effects in Ferrofluids, Springer.

[2] G. Fanselau (1929), Z. Phys. 54, 260.

[3] M. Gerth-Noritzsch, D. Y. Borin, S. Odenbach (2011), J. Phys.: Condens. Matt. 23, 346002.

[4] A. Yu. Zubarev, L. Yu. Iskakova (2000), Phys. Rev. E, 61(5):5415–5421.

Fast relaxation in structure forming ferrofluids

Aparna Sreekumari[1], Patrick Ilg[1]
[1] *Polymer Physics, Department of Materials, ETH Zürich*

In this work, we study strongly interacting ferrofluids by computer simulations using model parameters that mimic Cobalt-based ferrofluids used in experiments. We have investigated both, internal structures and dynamical properties of these systems for varying dipolar interaction strength. We find indications for a qualitative different structure and behavior above a critical interaction strength which is close to the estimated value for the experimental system.

Introduction:

From the classical work of de Gennes and Pincus [1], it is known that dipolar colloids having strong interactions are inclined to form chained structures. In experimental as well as numerical studies under zero field conditions [2,3,4], microstructure formation has indeed been found in these ferrofluids materials, which will strongly influence the rheological properties. In addition, some numerical studies [5, 6, 7] have also shown evidence for network formation in ferrofluids having strong dipole coupling. This has been predicted in a theoretical study by Tlusty and Safran [8].

Model :

We have used a model which has been studied previously [5, 9], where magnetically hard point dipoles are having i) a short range repulsive interaction which mimics the steric repulsion that stabilizes the ferrofluids system and ii) a long range dipole-dipole interaction. We have performed Langevin dynamics simulations in a system of 1000 particles using translational and rotational Langevin equations of motion.

Results and discussion:

We summarise our results as follows:

We have used our simulations in order to extract model parameters that reproduce the magnetisation curve of Cobalt-based ferrofluids which is shown in a recent study by Gerth-Noritzsch *et al* [10]

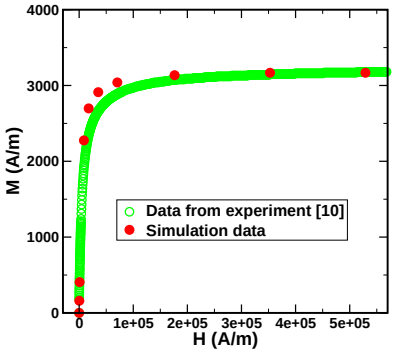

Figure 1: Magnetisation versus magnetic field strength curve: Initial susceptibility (χ_{in}) from (i) experiment = 0.398 (ii) simulation = 0.369. Initial susceptibility value from the simulation is in agreement with experiments [10] within error bars.

We have also studied the structural and dynamical properties of dipolar systems and compare the properties of systems having different dipolar strength. Static structure factor ($S(q)$) of strongly coupled system shows a peak in low wavevectors, which is the indication of large scale structures of complex shape. The

cluster size distribution, which deviates from the predicted exponential behaviour, develops tails - reminiscent of percolating system but without clear power-law regime. From the self-part of the incoherent scattering function ($F_s(k,t)$), we find that the system relaxes quickly at wave-vectors corresponding to first peak of $S(k)$.The exponent from Kohlrausch-Williams-Watts (KWW) fit to $F_s(k,t)$ is greater than 1, which indicates the fast relaxation of local structures. But at small wave-vectors, we find that $F_s(k,t)$ is not decaying to zero within the time span of our simulation, this can be an indication of dynamically arrested states having large relaxation times [11, 12].

Acknowledgments

We acknowledge Swiss National Science Foundation (SNF) together with German Research Foundation (DFG) for funding this project 20PA21E-129506: "Experiment and Computer simulation of the anisotropy of magnetoviscous effect".

References

[1] P. G. de Gennes and P. A. Pincus, Pair correlations in a ferromagnetic colloid, Phys. Kondens. Mater 11, 189-198 (1970).

[2] L. S. Tripp, V. S. Pusztay, E. A. Ribbe and A. Wei, Self-assembly of Cobalt nanoparticle rings, J. Am. Chem. Soc 124, 7914-7915 (2002).

[3] P. J. Camp and G. N. Patey, Structure and scattering in colloidal ferrofluids, Phys. Rev. E 62, 4 (2000).

[4] L. Rovigatti, J. Russo and F. Sciortino, No evidence of gas-liquid co-existance in dipolar hard spheres, Phys. Rev. Lett 107, 237801 (2011).

[5] Z. Wang, C. Holm and H. W. Müller, Molecular dynamics study on the equilibrium magnetization properties and structure of ferrofluids, Phys. Rev. E 66, 021405 (2002).

[6] R. Blaak, M. A. Miller and J.-P. Hansen, Reversible gelation and dynamical arrest of dipolar colloids, Europhys. Lett., 78, 26002 (2007).

[7] P. Ilg and E. Del Gado, Non-linear response of colloidal gels to external fields, Soft matter, 7, 163 (2011).

[8] T. Tlusty and S. A. Safran, Defect-induced phase separation in dipolar fluids, Science, 209, 1328-1331 (2000).

[9] P. Ilg, M. Kröger and S. Hess, Anisotropy of magnetoviscous effect in ferrofluids, Phys. Rev. E 71, 051201 (2005).

[10] M. Gerth-Noritzsch, D. Yu Borin and S. Odenbach, Anisotropy of the magneto viscous effect in ferrofluids containing nanoparticles exhibiting magnetic dipole interaction, J. Phys. Condens. Matter, 23, 346002 (2011).

[11] E. Del Gado and W. Kob, Length scale dependent relaxation in colloidal gels, Phys. Rev, Lett., 98, 028303 (2007).

[12] S. Saw, N. L. Ellegaard, W. Kob and S. Sastry, Phys. Rev. Lett., 103, 248305 (2009).

How to study theoretically the influence of magnetic particle shape anisotropy on the macroproperties of magnetic fluids.

A. Dobroserdova[1], E. Minina[1,2], T. Prokopyeva[1], E. Novak[1], E. Pyanzina[1], S. Kantorovich[1,3]

[1] *Ural Federal University, Lenin av. 51, 620000, Ekaterinburg, Russia.*
[2] *Institute for Computational Physics, University of Stuttgart, Pfaffenwaldring 27, 70569, Stuttgart, Germany*
[3] *Sapienza, University of Rome, Piazza A. Moro 5, 00185, Rome, Italy.*

Introduction

Anisotropic particles form the cutting edge of dipolar soft matter research as they correspond completely to the idea of fine tuning and designing new materials with controllable properties. This anisotropy can be of two types. The fist one is related to the geometrical shape anisotropy of the particle. Here various recent experiments are known, investigating magnetic ellipsoids [1], cylinders (rods) [2], or cubes [3] for example. Another type of anisotropy can be achieved in a spherically symmetric colloidal particle by introducing internal anisotropy. Examples of these particles are particles with magnetic caps [4], silica particles with embedded magnetic cubes [5], or magnetic Janus particles [6]. In the present contribution we develop various analytical methods to investigate both types of anisotropy and describe their influence on the macroscopical properties of fluids with anisotropic particles.

Shape Anisotropy

Ground State Studies. As the first step, the analysis of the possible ground state structures (the most energetically favored configurations at 0 K) for two and three dimensions is carried out. For the system of magnetic ellipsoids in 2D with magnetic moments along short semi-axes ground state structure is similarly to the system of the magnetic spheres (ideal ring and chain) [6]. However the critical number of particles (the number of particles for a ring to become the ground state; for dipolar spheres this critical number is 4) depends dramatically on the semi-axes ratio. The analysis of the interaction of two magnetic rods in 2D as a function of semi-axes ratio is performed. For the semi-axes ratio less than a critical value (diameter to height ratio, $z^*=2^{-1/3}$) we found that the antiparallel orientation of magnetic moments was energetically more advantageous, otherwise the head-to-tail orientation won. In the 3D case the ground state of a system of elongated rods was investigated. We found two possible ground state structures (carpets and bracelets) both of them with antiparallel orientation of magnetic moments. The carpet becomes energetically favorable configuration for odd number of particles, and the bracelet is the ground state for even number of particles.

Finite temperatures. We propose a method of calculating analytically the pair correlation function for the combination of Gay-Berne [7] and magnetic dipole-dipole potential based on the group integral technique [8]. Using this approach we can explicitly separate contributions coming from various types of interactions: magnetic and steric. We analyse the influence of particle anisotropy on the structure factor of these systems, and investigate pressure. We also study magnetization of anisotropic particles. To verify our theoretical predictions we perform MD computer simulations for dipolar Gay-Berne particles in Espresso [9] and extensively compare obtained results. We also make a comparative analysis of the properties of anisotropic dipolar particle systems and those of ordinary spherically symmetrical dipolar hard and soft spheres, and in this way we are trying to point out the control parameters related to

the shape anisotropy for obtaining dipolar systems with desired properties.

Internal anysotropy

Ground State Studies. Recently we put forward a model of a particle, the dipole moment of which is shifted radially from the particle centre towards its surface (sd-particle) [10]. It turned out that the ground state structures in this case strongly depend on the value of the dipolar shift. This model is generalized to the finite number of shifted dipoles to reproduce both magnetic caps and magnetic Janus particles. It turns out that the distribution of shifted dipoles and their number can lead to the change in the effective interparticle potential from attraction to repulsion. The results are also very sensitive to the shift of the dipole and the dimensionality of the system.

Finite temperatures. Previously an extensive computer simulations study of cluster formation and magnetic properties [11] of systems of sd-particles was performed. To accompany this study and to understand better the behaviour of the latter systems we use a perturbation theory to analyse pair correlation functions, structure factors, pressure and magnetization.

Outlook

If the dipole-dipole interaction is strong, various aggregates might be formed both in the systems of shape-anisotropic and internally anisotropic particles. We are currently actively working on the DFT approach to elucidate the cluster size distribution, cluster topology and their influencse on the diffusion, magnetization and structure factors.

Acknowledgments

This work is supported by the President of Russian Federation (Grant No. MK-2221.2011.2), also is partly supported by the Ministry of Education and Science of Russian Federation (Project No. 2.609.2011) and Ural Federal University development program with the financial support of young scientists. SK is also supported by ERC Grant “Patchy Colloids”.

References

[1] Sacanna S. et al, “Fluorescent monodisperse silica ellipsoids for optical rotational diffusion studies”, Langmuir 22, 1822-1827 (2006)

[2] Günter A. et al, “Rotational diffusion of magnetic nickel nanorods in colloidal dispersions”, Journal of Physics: Condensed Matter 23, 325103 (14pp) (2011)

[3] Rossi L., Sacanna S., Irvine W. T. M., Chaikin P. M., Pine D. J., Philipse A.P., “Cubic crystals from cubic colloids”, Soft Matter 7, 4139-4142 (2011)

[4] Baraban L., Makarov D., Albrecht M., Rivier N., Leiderer P., Erbe A., “Frustration-induced magic number clusters of colloidal magnetic particles” Phys. Rev. E: Stat., Nonlinear, Soft Matter Phys., 77, 031407-031412 (2008)

[5] Sacanna S., Rossi L., Pine D.J., “Magnetic Click Colloidal Assembly”, J. Am. Chem. Soc., 134, 6112–6115 (2012)

[6] Nan Z., Mingyuan G., “Magnetic Janus Particles Prepared by a Flame Synthetic Approach: Synthesis, Characterizations and Properties”, Advanced Materials, 21, 184–187, (2009)

[7] Gay J. G. and Berne B. J., “Modification of the overlap potential to mimic a linear site-site potential”, Journal of Chemical Physics 74, 3316-3319 (1981)

[8] Elfimova E. and Ivanov A., “Pair correlations in magnetic nanodispersed fluids”, Journal of Experimental and Theoretical Physics 111, 146-156 (2010)

[9] http://espressomd.org/

[10] Weeber R., Kantorovich S., Cerda J., Holm C., “Ferrofluids with shifted dipoles: ground state structures”, Soft Matter, 7, 5217-5227, (2011)

[11] Klingkit M., Weeber R., Kantorovich S., Holm C., manuscript in preparation.

A rheological characterization of biocompatible ferrofluids.

J.Nowak[1] and S. Odenbach[1]

[1] *Chair of Magnetofluiddynamics, Technische Universität Dresden, Dresden 01062, Germany*

During the last years the application of biocompatible ferrofluids has seen an increasing interest. The suspended magnetic nanoparticles are used as contrast agent in the magnetic resonance imaging [1]. Current research focuses on the use of the fluids for magnetic drug targeting as well as for magnetic heating treatment. It is even suggested by [2] to use a ferrofluid based anaesthetic to prevent an unwanted upward spread of the drug in spinal anaesthesia.

To ensure a non-toxic behaviour the magnetic core is made of iron oxide, e.g. magnetite or maghemite, and the surrounding shell of a biocompatible material, e.g. dextran. Those stabilized nanoparticles are suspended in water.

A well-known effect of ferrofluids is the magnetoviscous effect (MVE), i.e. an increase of viscosity in the presence of a magnetic field. Although it has been investigated for ferrofluids used in the engineering context in some detail [3], this effect was neglected in the characterization of biocompatible ferrofluids up to now.

In the current experimental study the MVE is investigated for two fluids: FluidMAG_DX, distributed by the ChemiCell GmbH (Berlin, Germany) as well as the Fluid FF054L developed by the Alexiou Group (Erlangen, Germany). Characteristic parameters are shown in Table 1. Both ferrofluids are based on magnetite/maghemite multicore particles.

The experiments were carried out with a commercial Anton-Paar Physica MCR 301 rheometer with a cone-plate geometry featuring a diameter of 50 mm and a cone opening angle of 1°. For measurements under the influence of a magnetic field a specially designed shear rate-controlled rheometer [4] with improved hard and software featuring a plate-plate geometry and an attached couette-region with an adjusted distance of approximately 0,1 mm as well as an specially designed stress-controlled rheometer [5] adopting the same geometry as the shear rate-controlled rheometer were used. For all rheological measurements a constant measuring temperature of 20 °C was used.

The magnetic characterizations with respect to the volume fraction of magnetic material as well as the saturation magnetization (Table 1) of the fluids were carried out using a vibrating sample magnetometer (Lake Shore 7407).

Both fluids exhibited Newtonian behaviour in the absence of a magnetic field for comparatively high shear rates (Figure 1) with a comparatively low viscosity slightly above the viscosity of distilled water.

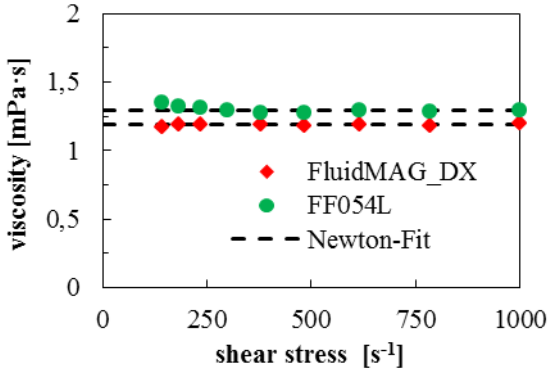

Figure 1: Zero-field viscosity of the ferrofluids.

Fluid	Surfactant	mean hydrodynamic diameter [nm]	Volume fraction of magnetic material [%]	Saturation magnetization [kA/m]
FluidMAG_DX	Dextran	100	0,28	1,27
FF054L	Lauric acid	-	0,12	0,55

Table 1: Characteristic parameters of the ferrofluids under investigation.

Measurements under the influence of a magnetic field revealed a strong MVE, exceeding a few hundred percent for low shear rates as depicted in Figure 2. To make the magnetic field influence independent of the zero-field viscosity $\eta_{(H=0)}$ the effect is denoted as R and is calculated by [3]:

$$R = \frac{\eta_{(H)} - \eta_{(H=0)}}{\eta_{(H=0)}} \qquad (1)$$

with the viscosity under the influence of a magnetic field η_H.

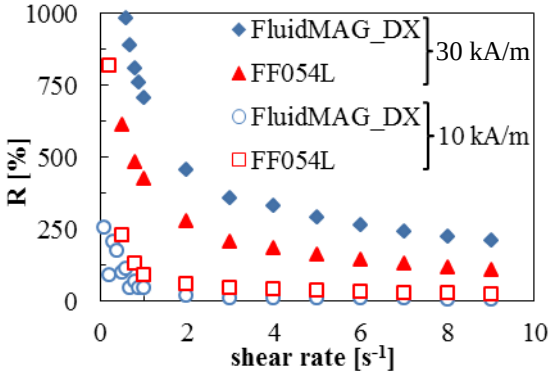

Figure 2: The MVE of the two ferrofluids under investigation for magnetic field strengths of 10 kA/m and 30 kA/m

In the presence of a magnetic field with strength of at least 10 kA/m the fluids showed a behaviour best described by the Herschel-Bulkley model:

$$\tau = \tau_{HB} + k \cdot \dot{\gamma}^n , \qquad (2)$$

with the stress τ, the yield stress τ_{HB}, the consistency parameter k and the Power-Law index n.

The theoretically predicted yield stress was proved using the stress-controlled rheometer for the FluidMAG_DX fluid, but with significant deviation from the values obtained by the mathematical fits. This might be caused by the high sensitivity of the mathematical fit against shear rates below 1 s^{-1} as well as due to the fact that the measurements of the yield stress took place close to the devices' resolution. For the same reason the yield stress could not be proved for the FF054L ferrofluid.

The measured strong changes in the behaviour of the fluids might be associated with the formation of structures of the magnetic multicore nanoparticles, being driven by a high interaction parameter of the investigated fluids. These findings have to be taken into account in several medical applications of biocompatible ferrofluids, e.g. drug targeting or MRI, as they have the potential tochange the flow behaviour of the deployed ferrofluids significantly.

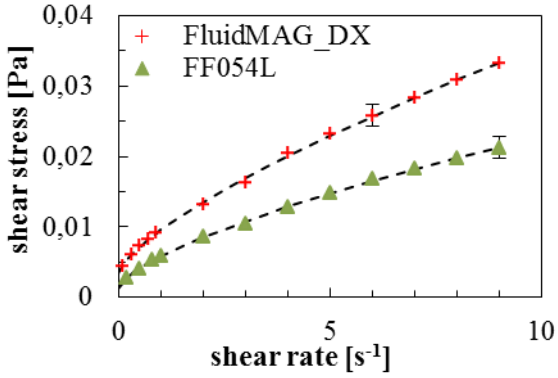

Figure 3: Flow curves of the two ferrofluids at a magnetic field strength of 30 kA/m. Dashed lines represent the Herschel-Bulkley fits.

Acknowledgments

We thank the Alexiou Group (Erlangen, Germany) for providing the FF054L ferrofluid sample.

References

[1] M. D. Shultz, S. Calbin, P. P. Fatouros, S. A. Morrison and E. E. Carpenter; (2007) Enhanced ferrite nanoparticlesas MRI contrast agents; J. Mag. Mater 311:464-468

[2] R. H. Thiele, D.A. Colquuhoun, G. T. Gillies and M. Tiouriine; (2012) Manipulation of Hyperbaric Lidocaine using a weak Magnetic Field: A Pilot Study: Anesth. Anlag. 114:1365-1367

[3] S. Odenbach; (2002) The Magnetoviscous Effect in Ferrofluids; Berlin: Springer

[4] S. Odenbach, T. Rylewicz and M. Heyer; (1999) a Rheometer dedicated fort he investigation of viscoelastic effects in commercial magnetic fluids; J.Magn.Mater 201:155-158

[5] H. Shanazian and S. Odenbach; (2008) New driving unit for the direct measurement of yield stress with a stress controlled rheometer; App. Rheol. 18:54974-54981

Magnetic Multicore Nanoparticles as Tracers for Magnetic Particle Imaging

Silvio Dutz[1], Dietmar Eberbeck[2], Robert Müller[1], Matthias Zeisberger[1]

[1]*Institute of Photonic Technologies, Albert-Einstein-Straße 9, Jena, 07745, Germany*
Email: silvio.dutz@ipht-jena.de
[2]*Physikalisch-Technische Bundesanstalt, Abbestraße 2-12, Berlin, 10587, Germany*

The performance of magnetic particle imaging (MPI) strongly depends on the magnetic properties of the magnetic nanoparticles (MNP) acting as imaging agents such as magnetic moment and its mobility determined by the magnetic anisotropy and the hydrodynamic size of the MNP. Ideal particles show a very steep slope of the magnetisation during magnetic reversal combined with a high saturation magnetisation and a low coercivity. Usually, an increase in magnetic moment entails also in enhancement in magnetic anisotropy energy, i.e. the coercive force. Thus, beside the enhancement of the magnetic volume of the tracers one has to reduce the anisotropy constant.

In previous investigations it was shown that magnetic multicore particles (MCNP) are promising candidates for suitable MPI tracers [1,2]. Present MCNP consist of single domain cores in the size range from 10 to 15 nm which form larger clusters with diameters of 40 nm up to a few hundred nm. Aim of this study was the investigation of the suitability of MCNP for MPI in more detail. For this, MCNP of different cluster sizes were prepared as described before [3]. To obtain a set of samples which differ in their cluster sizes the MCNP were classified into fractions of different mean sizes by means of a centrifuge. The obtained fractions (20 per sample) were characterised structurally by dynamic light scattering (DLS), X-ray diffraction (XRD), and transmission electron microscopy (TEM) as well as magnetically by vibrating sample magnetometry (VSM), magnetorelaxometry (MRX), and magnetic particle spectroscopy (MPS). By the fractionation particles with hydrodynamic diameters (DLS, z-average) ranging from 100 nm to 800 nm were obtained.

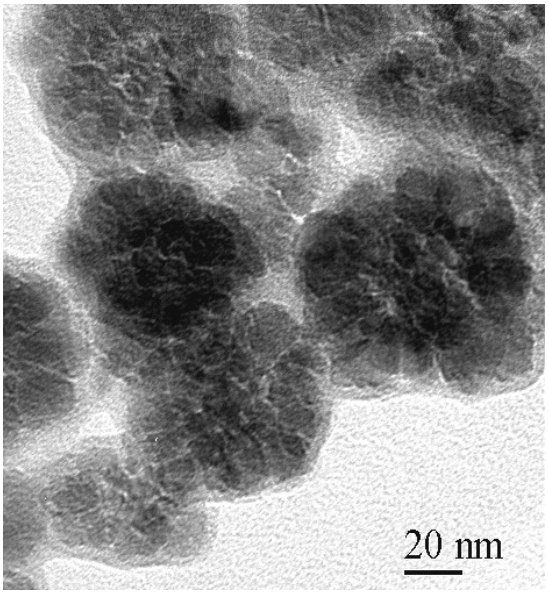

Figure 1: Typical TEM image of the investigated magnetic multicore nanoparticles.

VSM measurements confirmed a correlation of the hydrodynamic cluster size with the magnetic anisotropy energy of the particles in these fractions - e.g., with increasing particle size the coercivity of the particles varied from 0.15 kA/m to 2.1 kA/m. The MPS investigations showed a clear dependence of the quality of MPS signal on the hydrodynamic diameter of the particles and thus the cluster size. So the amplitude ratio of the higher (15...40) harmonics to the 3rd har-

monic span over one order of magnitude, where the smaller MCNP showed the highest values, i.e. they are the most appropriate fractions for MPI.
In this contribution we describe the preparation and fractionation of the MCNP. We show the results of the samples characterisation and give an interpretation of the correlation between the different determined parameters and the quality of the MPS signal. Finally, we discuss the design of promising future MCNP for MPI based on our findings in this study.

References

[1] S. Dutz et al. Larger single domain iron oxide nanoparticles for magnetic particle imaging. Magnetic Nanoparticles - Proceedings of the First International Workshop on Magnetic Particle Imaging: 37-43. World Scientific (2010).

[2] D. Eberbeck et al. Evidence of aggregates of magnetic nanoparticles in suspensions which determine the magnetisation behaviour. Magnetic Nanoparticles - Proceedings of the First International Workshop on Magnetic Particle Imaging: 66-72. World Scientific (2010).

[3] S. Dutz et al. Ferrofluids of magnetic multicore nanoparticles for biomedical applications. J. Magn. Magn. Mater. 321/10: 1501-1504 (2009).

Ferrofluids with Ultrasmall Magnetite Particles for Magnetic Resonance Imaging (MRI)

N. Buske

Magneticfluids, Köpenicker Landstr. 203, 12437 Berlin

Motivation

Ferrofluids for Magnetic Resonance Imaging (MRI) should be composed of in-vivo compatible magnetic-core/shell particles, like maghemite and/or magnetite cores and modified polysaccharide shells. Nowadays the hydrodynamic core/shell-particle size should be downsized below 50 nm, typically in the range of 20-30 nm. The advantages of these **U**ltrasmall **S**uper **P**aramagnetic **I**ron **O**xideparticles (USPIO) are long half life in blood circulation and higher stability against agglomeration in carriers e.g., typical buffers.

Goal

The aim of the study is to develop a simple preparation method to produce USPIO-ferrofluids in lab. scale for preclinical and clinical applications. The desired final product contains ultrasmall magnetite particles covered with dextran or carboxymethylated dextran (CMD), which are homogenously dispersed in buffers.

Methods

The conditions for USPIO- core/shell synthesis were adopted from a method described previously [1]. The following purification and concentration steps to obtain the final product were optimized. The hydrodynamic average size (Z(ave)), the volume size (Zv), the polydispersity index (PI) were measured by means of a Zetasizer 3000 (Malvern, UK). Additionally, the Fe-concentration and the polysaccharide amount were determined using spectroquant (MERCK with reagent Fe-1) and anthrone method, respectively.
Magnetization curves of the USPIO-Ferrofluids were determined by a Vibration Sample Magnetometer (VSM, Lake Shore, USA).

Results

Z(ave) and Zv-values in the range of 15-25 nm with narrow PI-values of 0.1-0.2 were measured. These values were indicating in order of the calculated dimensions in Fig. 1. The hydrodynamic sizes correspond to the dimensions of single core/shell-particles. Multi-core compositions and agglomerated particles were not found. More details to maintain the USPIO-size during the preparation steps will be presented in the poster.

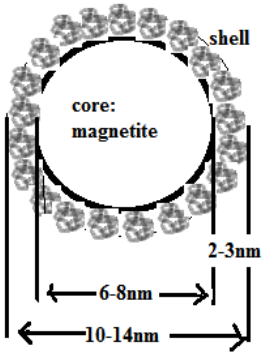

Fig. 1: Scheme of a single USPIO-particle. The core size is deviated from VSM-results using Chantrell equation, the shell thickness corresponds to the measured hydrodynamic Z(ave)-values of solved dextran and CMD.

The presented preparation route for USPIO-ferrofluids can be achieved for further modification of core and/or shell compositions to obtain improved MRI-signals or for use in other fields of clinical applications.

Acknowledgments

The author thanks the Capsulution AG for supporting this study and S. Dutz (IPHT, Jena) for the VSM measurements. The study was financially supported by the BMBF: NIMINI-MRI Nr. 01EZ0815.

References

[1] E.V. Groman et al.: US patent 6599498

The effect of different iron oxide nanoparticle coatings on cellular accumulation and cytotoxicity in tumour cells

K. Lange[1], M. Kettering[1], A. Eitner[2], C. Bergemann[3], W. A. Kaiser[1], I. Hilger[1]

[1] *Dept. of Experimental Radiology, Institute of Diagnostic and Interventional Radiology I, Jena University Hospital – FSU Jena, Erlanger Allee 101, D-07747 Jena, Germany*
[2] *Institute of Anatomy II, University Hospital – FSU Jena, Teichgraben 7, D-07743 Jena, Germany*
[3] *chemicell GmbH Eresburgstrasse 22-23, D-12103 Berlin, Germany*

Purpose

Magnetic nanoparticles (MNPs) are promising tools for highly selective tumour diagnosis and therapies [1, 2]. For therapeutic purposes, e.g. local magnetic heating, the effectiveness depends on i) a high specific heating power [3] and ii) a high level of intracellular MNP accumulation to sufficiently destroy tumour cells [4]. Therefore, it is essential to know how to control the intracellular accumulation of MNPs. The aim of the present study is to show the effect of MNP coatings (mainly polysaccharids) with different functional groups on cellular loading and cytotoxicity per se.

Materials and Methods

20 MNP samples with comparable iron oxide cores (magnetite/maghemite, 10.6 ± 0.4 nm) were reviewed. For experiments, 0.27 mg/cm^2 MNPs were given to a confluent BT-474 culture, a human adenocarcinoma cell line, for 24 h (37 °C, 5 % CO_2, 95 % relative humidity). After removing unbound magnetic material, cell viability was analysed enzymatically with a methyl tetrazolium salt (MTS) assay and microscopically using different stainings (Calcein AM, propidium iodide and nucleus staining with Hoechst dye). Cellular loading level was examined by laser scanning microscopy.

Results

The behaviour of different MNP coatings was heterogeneous: we found MNPs accumulating strongly in cells but leading to low or moderate cytotoxic effect (e.g. polyacrylamid coating) and MNPs taken up poorly but leading to high cytotoxic effect (e.g. PEI coated MNP) per se. Effects on cellular accumulation and cytotoxicity did not correlate with coating material and functional groups.

Conclusion

The results show the necessity to explore the cellular loading and the cytotoxic side effects of every new MNP formulation. Also, protein-MNP interaction also could influence cellular loading which will require further investigations.
Polyacrylamide coated magnetic nanoparticle show good suitability, in principle, for tumour therapy due their strong accumulation in the tumour cells and non-toxicitiy per se.

Acknowledgments

The technical assistance of Y. Ozegowski and S. Burgold is gratefully acknowledged. Special thanks to R. Ludwig and Dr. G. Rimkus for their help. These investigations were supported by the German Research Foundation (DFG).

References

[1] I. Hilger, R. Hergt, W.A. Kaiser, IEE Proc Nanobiotechnol. 2005; 152: 33-39.
[2] A. Ito, M. Shinkai, H. Honda et al., J Biosci Bioeng. 2005; 100: 1-11.
[3] R. Hergt, S. Dutz, R. Müller et al., J. Phys.: Condens. Matter. 2006; 18: S2919-S2934.
[4] M. Kettering, J. Winter, M. Zeisberger et al., Nanotechnology. 2007; 18: 175101

Nanoparticles for Cancer Treatment - from Cell Culture to Tissue-Matrix

S. Lyer[1], S. Dürr[1], R. Tietze[1], H. Rahn[2], K. Gitter[2], F. Wiekhorst[3], M. Liebl[3], B. Frey[4], U. Gaipl[4], L. Trahms[3], S. Odenbach[2], C. Alexiou[1]

[1] *Department of Oto-Rhino-Laryngology, Head and Neck Surgery, Section for Experimental Oncology and Nanomedicine (SEON), Else Kröner-Fresenius-Stiftung-Professorship, University Hospital Erlangen, Germany*
[2] *Chair of Magnetofluiddynamics, Technische Universitaet Dresden, Dresden, Germany*
[3] *Physikalisch-Technische Bundesanstalt, Berlin, Germany*
[4] *Department of Radiation Oncology, University Hospital Erlangen, Germany*

Introduction

Cancer treatment was one of the most important challenges in medicine for the last decades and it will be the same for the coming decades, either. Since patient numbers are rising and new treatment modalities, like for example antibodies, are very expensive and often not as effective as this kind of targeted treatment promised to be, the application of nanoparticles is one of the options for a upcoming better cancer therapy.

Magnetic Drug Targeting (MDT) is using superparamagnetic iron-oxide nanoparticles coupled to chemotherapeutics for a targeted therapy of solid tumors. Herby the particles and the drug are accumulated in the target region by an external magnetic field [1,2,3,4]. Although promising *in vivo* data are already available, basic research on different fields like cell culture, fluid dynamics and the interaction of the nanoparticles with the vascular- and tissue-matrix has to be done, for a successful implementation of MDT in the clinical routine.

Methods

For all experiments iron-oxide nanoparticles (NP) of a mean diameter of 100nm to 150nm were used.

Cell Culture: The cell-lines VX-2 (rabbit), SCC-15 (human) and PC-3 (human) were examined. NP, the chemotherapeutic agent Mitoxantrone (MTO), and the compound (NP+MTO) were tested. Real-time cell analysis (RTCA), WST-1 assay and annexin A5-FITC/propidium iodide staining were used. Moreover, the effect of the magnetic field was analyzed using field strength of 0.4T in each well. Bovine artery model: Freshly isolated bovine femoral arteries were mounted in a circuit. An albumin supplemented (0.625%) Krebs-Ringer buffer (pH7.4) was used as vehicle fluid. Arteries were placed in 16mm distance to the tip of the pole shoe. The arteries were removed from the circuit either directly or 15 minutes after magnetic field application and divided in 11 sections and embedded in paraffin for magnetorelaxometry measurements. The relaxation signal of the nanoparticles was measured using a single-channel superconducting quantum interference device (SQUID) gradiometer at a detection limit of 1ng iron.

Tube model: A flexible silicon tube with an inner diameter of 2mm was fixed in a holder with millimeter scale and connected to a circulation with a peristaltic pump. A buffer-flow of 6ml/min or 3ml/min was set and the nanoparticles were injected via a T-connection. The tubes were placed under the tip of the poleshoe and magnetic field gradients of approx. 40T/m and 60T/m were applied. The flow-through was collected and the iron-content was measured by colorimetry.

Results

Cell culture experiments with all three cell-lines showed a dose dependent effect of all substances tested. Nanoparticles not loaded with Mitoxantrone (MTO), were not toxic at concentrations below 100µg/ml. The pure chemotherapeutic MTO and the compound NP-MTO exhibited a toxic effect, which was dose and time dependent. The experiments showed also, that the binding of MTO to the nanoparticles did not influence the toxic effect of MTO. Finally it could be observed, that a magnetic field of 0.4T did increase the hurtful effect of high compound-concentrations on the cells.
The results of the ex vivo bovine artery model revealed, that an increasing magnetic field leads to increasing accumulation of iron oxide nanoparticles under the tip of a poleshoe in the arteries. This could be shown concordantly by histology and magnetorelaxometry.
First results of the silicon-tube-model showed, that – depending of the salts in the buffer – the accumulation of nanoparticles under the poleshoe is increasing with the complexity of the buffer. By that means it was possible to identify salt combinations, which are not suitable for diluting the particles prior to the application.

Conclusion

Cancer treatment with nanoparticles using external magnetic fields, offers promising opportunities for patients as well as clinicians. But before this technique can be translated into the clinics, basic research has to be done, to understand the complex parameters, which are influencing the effect of the particles on the tumors.
Therefore, we are presenting here results of experiments that cover a broad spectrum of research areas and techniques.
One the one hand we could show in cell culture, that it is possible to produce compound of iron-oxide nanoparticles with a chemotherapeutic agent (MTO) and that the binding of the drug to the particles does not alter the toxic effect on the cancer cells.
Additionally the use of a magnetic field with 0.4T leads to an accumulation of the particles at the bottom of the well-plates and is enhancing the effectivity of the compound, using high concentrations but not with lower doses. Therefore, we believe, that the application of NP-drug-compounds should be performed as near as possible to the tissue, which is aimed to be treated with MDT.
Using the bovine artery model, we could show, that it is possible to accumulate superparamagnetic iron-oxide nanoparticles under the tip of the poleshoe of an electro magnet and that the amount of particles being detained is dependent on the strength of the applied magnetic field gradient. But this model is complex and laborious and therefore a tube-model seems to be more feasible for routine experiments. The first results are promising and will set the basis for studies concerning the positioning of the magnetic field in an optimal manner, combining different imaging techniques and the knowledge about the behaviour of the nanoparticles in the bloodstream and under the influence of an external magnetic field.

Acknowledgments

DFG (AL552/3-3), Else Kröner-Fresenius-Stiftung, Bad Homburg v.d.H.

References

[1] R. Tietze et al.: Quantification of drug-loaded magnetic naoparticles in rabbit liver and tumor after in vivo administration. J Magn Mag Mater 321:1465-1468, 2009
[2] S. Lyer, et al.: Visualisation of tumour regression after local chemotherapy with magnetic nanoparticles - a pilot study. Anticancer Res 30: 1553-1557, 2010
[3] R. Tietze et al.: Visualization of superparamagnetic nanoparticles in vascular tissue using XµCT and histology. Histochem Cell Biol 135:153-158, 2011
[4] R. Tietze et al.: Nanoparticles for cancer therapy using magnetic forces. Nanomedicine 7: 447-457, 2012
.

Characterization of magnetic viral vectors by magnet resonance imaging

I. Almstätter[1], O. Mykhaylyk[2], J. Altomonte[3], M. Settles[1], Ch. Plank[2], R. Braren[1]

[1] *Institute of Radiology, Molecular Imaging,* [2] *Institute of Experimental Oncology and Therapy Research and* [3] *II. Med. Clinic, Gastroenterology, Klinikum rechts der Isar, Technische Universität München, Germany*

Non-invasive imaging methods such as magnet resonance imaging (MRI) are important diagnostic tools with a broad spectrum of clinical applications. Magnetic nanoparticles (MNPs) can be used as superparamagnetic MRI contrast agents reducing the transverse relaxation time T_2^*. However, magnetic properties of MNPs are highly dependent on MNP interaction. Aim of this work was to quantify the effect of MNP assembly, i.e. complex formation with virus into magnetic viral vectors (MNP-V), or by internalization of MNPs or MNP-Vs into cells, on the magnetophoretic mobility and r_2 and r_2^* relaxivity. Tissue-mimicking agarose phantoms with homogeneously distributed MNPs, MNP-Vs, and cells with internalized MNPs or MNP-Vs were prepared. To evaluate the effect of cell internalization, selected cell lines were labeled with free MNPs or infected with MNP-Vs and the iron content of the labeled cells was quantified chemically. The magnetic moment of the MNPs, MNP-Vs and cells loaded with MNPs or

MNP-Vs were evaluated from magnetophoretic mobility data, showing a higher magnetic moment of MNP-Vs compared to dispersed MNPs. The selected core-shell type MNPs were characterized by excellent r_2 and r_2^* relaxivity values for the free and cell associated/internalized particles. Assembly of MNPs with viral particles resulted in a reduced r_2^* relaxivity of these MNP-Vs compared to free MNPs. The internalization of MNP-Vs into cells increased the r_2^* relaxivity compared to free MNP-Vs, but the values were still lower than those of free MNPs. The modulation of the relaxivities of internalized MNPs is presumably resulting from the intracellular compartmentalization of the associated/internalized particles. In future *in vivo* studies, in particular on viral cancer therapy, such tissue-mimicking phantoms with labeled cells could be used as standard of reference for the non-invasive quantification of exogenic iron from magnetic nano-assemblies in animal tissue by MRI.

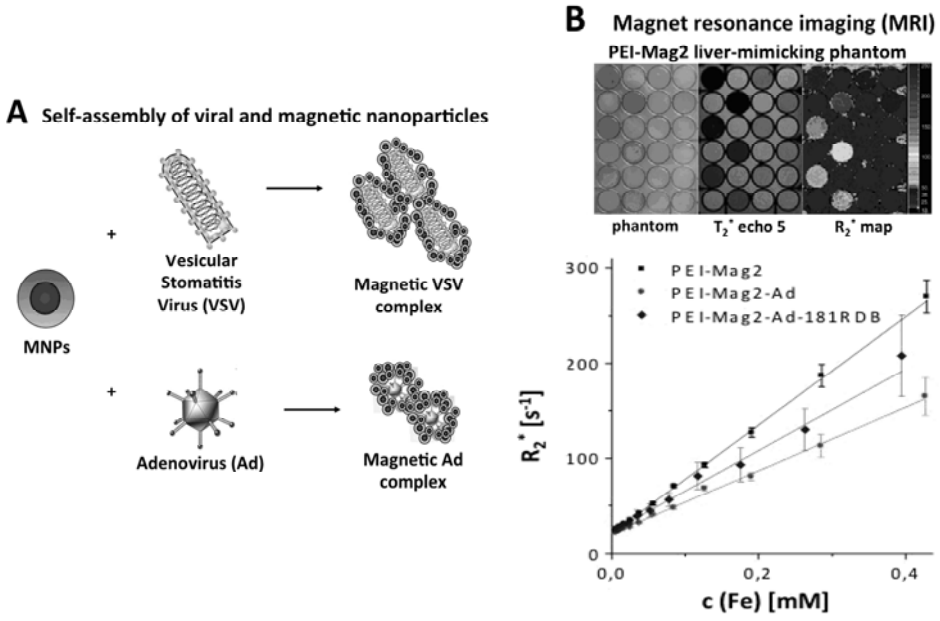

(A) Schematic of the self-assembling of the viral and magnetic particles into magnetic viral vectors. **(B)** Exemplary MNP calibration phantom and the resulting r_2^* relaxivity plots. The pictures of the PEI-Mag2 phantom show from left to right a photography of the liver tissue-mimicking phantom with decreasing iron-load (brown), the T_2^* weighted image (echo time 18.1 ms) and the corresponding color-coded R_2^* map.

Characteristics of PEI-shells affect short-term and long-term survival of endothelial cell cultures

F. Bähring[1], F. Schlenk[2], C. Jörke[1], C. Bergemann[3], D. Fischer[2], A. Hochhaus[1], J. H. Clement[1]

[1] *Klinik für Innere Medizin II, Abteilung Hämatologie und Internistische Onkologie, Universitätsklinikum Jena, Erlanger Allee 101, D-07747 Jena, Deutschland; franziska.baehring@med.uni-jena.de*
[2] *Institut für Pharmazie, Abt. Pharmazeutische Technologie, Friedrich-Schiller-Universität Jena, Deutschland*
[3] *chemicell GmbH, Eresburgstrasse 22-23, 12103 Berlin, Deutschland*

Introduction

Nanomaterials are important tools for biomedical applications. The interaction of nanoscaled materials, e.g. magnetic nanoparticles with biological fluids needs a biocompatible shell. Furthermore the composition of that shell should allow coupling of compounds, their reversible protection and controllable release at the desired place of biological action. A widely distributed class of shell-building substances are the polycationic polyethylenimines (PEI) [1,2]. The aim of this study is to analyse the time-dependant effect of various PEI variants as component of core/shell nanoparticles and as free substance on the vitality of endothelial cells.

Methods

Positively charged nanoparticles with different types of PEI shells were provided by chemicell GmbH. The hydrodynamic diameter ranged from 100 to 500 nm and the molecular weight of polyethylenimine from 1,200 to 750,000 Da. FluidMAG-D was used as control. For viability assays the human brain microvascular endothelial cell line (HBMEC) was seeded in black-walled 96-well culture plates overnight with a density of $1.5*10^4$ cells per well. After a three hour incubation with various concentrations of nanoparticles or the corresponding shell-building substances the effects on the viability was tested with the PrestoBlue™ Cell Viability Assay (Invitrogen, Darmstadt, Germany). The pure substances were used in a 1/10 concentration because we calculate 10% w/w of the core/shell nanoparticles. For studying the effects of the core/shell nanoparticles and the shell components on the HBMEC cells over a longer time period the xCELLigence System (RTCA DP) (Roche Applied Science, Mannheim, Germany) was used. Cells were seeded with a density of $2*10^4$ cells per well. After 24 hours the cells were incubated with the core/shell nanoparticles or the substances for up to 72 hours. The incubation media remained on the cell cultures for the entire incubation time.

Results

Various PEI-coated nanoparticles were studied for their influence on the viability of HBMEC cells (Table 1).

Table 1: Characteristics of core/shell nanoparticles

Nanoparticles	Matrix	Size [nm]
fluidMAG-PEI/1 (Lot: 1102/11)	Polyethylenimine, MW 1200 Da	~ 200
fluidMAG-PEI/2 (Lot: 1202/11)	Polyethylenimine, MW 2000 Da	~ 200
fluidMAG-PEI/25 (Lot: 1302/11)	Polyethylenimine, MW 25000 Da	~ 200
fluidMAG-PEI/100 (Lot: 1402/11)	Polyethylenimine, MW 100000 Da	~ 300
fluidMAG-PEI/500L (Lot: 1902/11)	Polyethylenimine, MW 500000 Da, linear	~ 500
fluidMAG-PEI/750 (Lot: 1502/11)	Polyethylenimine, MW 750000 Da	~ 200
fluidMAG-PEI/750/O (Lot: 1702/11)	Polyethylenimine, MW 750000 Da, without counter-ion	~ 250
fluidMAG-PEI/750G (Lot: 1802/11)	Polyethylenimine, MW 750000 Da, monolayer	~ 250
fluidMAG-PEI/750GL (Lot: 1602/11)	Polyethylenimine, MW 750000 Da, cross-linked	~ 400
fluidMAG-PEI/EP (Lot: 1002/11)	Epoxy-Polyethylenimine	~ 250
fluidMAG-PEA (Lot: 2002/11)	Poly-(dimethylamin-co-epichlorhydrin-co-ethylendiamin)	~ 200
fluidMAG-D (Lot: 1512/10)	Starch	~ 150

We could show that fluidMAG-PEI/100 and fluidMAG-PEI/750/O affect the viability of HBMEC cells in a concentration-dependant manner (Figure 1).

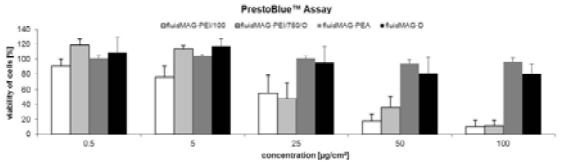

Figure 1: Viability of HBMEC after incubation with selected core/shell nanoparticles

Next we asked if the cytotoxic effects are attributed to the shell. In order to evaluate the different PEI-derivatives we calculated the concentration as 10% of the initial core/shell nanoparticle concentration. Surprisingly, not only PEI/100 and PEI/750/O, but also PEA exhibit cytotoxic effects on HBMEC in a concentration-dependant manner (Table 2).

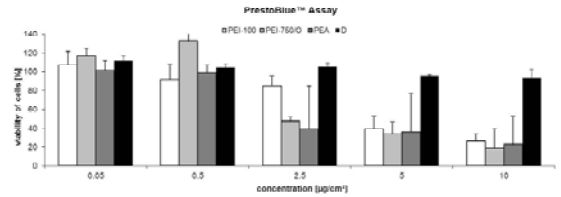

Figure 2: Viability of HBMEC after incubation with different shells

In order to verify these results, we performed real-time cell analysis over a time-period of 72 hours. We could confirm that fluidMAG-PEA does not affect the vitality of HBMEC even with the highest concentration of 100 µg/cm^2 compared to fluidMAG-D. The application of PEA showed a concentration-dependant effect. 2.5 µg/cm^2 PEA led to a rapid reduction of attached cells immediately after application of the substance. This was followed by a recovery period of about 3 hours passing into a growth phase ending in a final steady state phase caused by confluency of the cell layer. In contrast, at 5 µg/cm^2 cells showed also a recovery, but no further increase in number. A concentration of 10 µg/cm^2 does not even allow recovery of the cells and ends in their total loss. Similar results were obtained with PEI/750/O. Starch as control substance did not affect the cell culture at any concentration applied.

Conclusion

Substances which are used for coating nanoparticles exhibit different biological effects as free substances or bound to the iron oxide core of the magnetic nanoparticle. Monitoring of the cellular responses over a longer time period allows differentiation of acute and long-lasting consequences. This is of future importance to better understand interaction of nanostructured materials with cells.

Acknowledgement

This work was supported by the Bundesministerium für Bildung und Forschung (BMBF), 03X0104D

References

[1] O. Boussif et al., A versatile vector for gene and oligonucleotide transfer into cells in culture an vivo: polyethylenimine, Proc Natl Acad Sci USA 92(16): 7297-7301, 1995

[2] M. Neu et al., Recent advances in rational gene transfer vector design based on poly(ethylene imine) and its derivatives, J Gene Med 7(8): 992-1009, 2005

Quantification of Magnetic Nanoparticle Uptake in Cells by Temperature Dependent Magnetorelaxometry

C. Knopke[1], F. Wiekhorst[1], I. Gemeinhardt[2], M. Ebert[2], J. Schnorr[2], M. Taupitz[2], L. Trahms[1]

[1] *Physikalisch-Technische Bundesanstalt, Abbestrasse 2-12, Berlin, Germany*
Tel: 0049 (0)30 34817723
[2]*Charité, University Medicine Berlin, Charitéplatz 1, Berlin, Germany*

Magnetorelaxometry (MRX) is proven to be a powerful tool for the quantitative detection of magnetic nanoparticles (MNP) utilized in novel medical therapy modalities like magnetic drugtargeting or magnetic hyperthermia[1]. So far we adopted MRX measurements at room temperature for in-vitro quantification of MNP in blood and tissue samples. Since the MRX relaxation time crucially depends on MNP size, particles with less than about 17 nm in diameter decay too fast at room temperature[2] and are not detectable within the recording time window of present MRX devices. To circumvent this limitation we performed temperature dependent MRX measurements to
demonstrate the applicability of MRX for quantifying the uptake of small MNP in tumor cells.

Two tumor cell lines (HeLa and Jurkat) were incubated with small sized iron oxide MNP, Feraheme (ferumoxytol, AMAG pharmaceuticals, d ~ 5 nm) and CD021110 (carboxy dextran coated preclinical MNP, Charité, d ~ 4 nm) at varying concentrations for about 30 h, after which samples of about 10^6 cells were harvested. Additionally, reference samples of known iron amount were prepared (dilution series). A conventional SQUID magnetometer (MPMS-XL, Quantum Design) was utilized for temperature dependent relaxation measurements between 5 K and 300 K. First a magnetizing field of 2 mT is applied for 8 min to magnetize the MNP in the sample followed by the recording of the
relaxation signals for about 40 min. By normalization of the reference relaxation amplitudes to the amplitudes of the cell samples (see figure) a straightforward quantification was carried out. For cross validation the cell samples and references were analyzed by M(H) measurements using the same device and by non-linear ac-susceptometry using an MPS spectrometer (Bruker BioSpin).

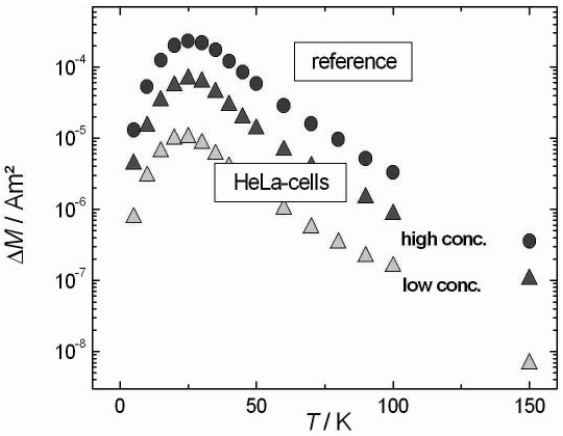

The cell samples incubated with CD021110 displayed a relaxation at decreased temperatures with a maximum relaxation amplitude at about 25 K. For both cell types we quantified an iron uptake in the microgram range scaling with the concentration of MNP during the incubation. In contrast, for Feraheme, no uptake was
detected for either of both cell types. These results were confirmed by the M(H) and MPS measurements. From the temperature dependent MRX measurements of the reference samples a detection limit of about
100 ng iron (absolute) was estimated.

The extension of MRX measurements to lower temperatures allows the in-vitro quantification of MNP of smaller sizes,

which at room temperature cannot be detected due to the short relaxation times. Furthermore, changes in the particle size distribution during the uptake of the MNP by a biological system can be resolved as a shift in the temperature dependence of the relaxation amplitude. A size specific cellular uptake of MNP can be quantified.

Acknowledgments

This work was financially supported by the DFG research program KFO 213 Magnetische Nanopartikel für die Zelluläre und Molekulare MR-Bildgebung TR408/5-2 and SocraTec R&D GmbH.

References

[1] Pankhurst, Q A, J Connolly, S K Jones, und J Dobson. „Applications of magnetic nanoparticles in biomedicine“. Journal of Physics D: Applied Physics 36, Nr. 13 (Juli 7, 2003): R167–R181.

[2] Wiekhorst, Frank, Uwe Steinhoff, Dietmar Eberbeck, und Lutz Trahms. „Magnetorelaxometry assisting biomedical applications of magnetic nanoparticles“. Pharmaceutical Research 29, Nr. 5 (Mai 2012): 1189–1202.

Investigations on quantification of magnetic nanoparticles after perfusion of a placenta

R. Müller[1], L. Seyfarth[2], M. Gläser[1,3], U. Enke[2], E. Schleussner[2], A. Hofmann[4], W. Fritzsche[1]

[1] *Institute of Photonic Technology (IPHT), Jena, Germany*
[2] *Department of Obstretrics and Gynecology, Jena University Hospital, Germany*
[3] *University of Applied Sciences, Jena, Germany*
[4] *HTS Systeme GmbH, Wallenfels, Germany*

Nanoparticles (NP) are potential tools for medical applications. Nevertheless, the current lack of knowledge about their potential toxicity connected with a possible spatial distribution in the human body requires new methods to determine the latter one. Placentae can play a central role as human tissue models as they do not constitute an ethical problem. Furthermore, magnetic NPs are used as MRI contrast agent but their behaviour at the placenta barrier is not known. To date, no standardised methods are available for quantification of NP in human tissue.

Aim of our work are long term measurements of NP in a floating suspension in tube shaped sample volume in order to conclude their (time dependent) whereabouts after perfusion of a placenta for up to 6 hours. We used a modified MagnetReader [1, 2] what detects magnetic moments of a few µAm^2 (VSM in the order of 100 µAm^2) via analysis of the higher harmonics caused by a frequency mix of ac-magnetic fields with a field amplitude of 4.5 mT. Since the signal depends as well on the magnetisation curve of NPs the method is only semiquantitative. The results are compared with absolute values of higher concentrated suspensions in steady state measured by VSM.

The influence of the flow rate of the suspension (i.e. integration time) and changes in the particle concentration was investigated. Important is the material of the measuring cuvette. In dependence on the coating material particles could adsorb at the surface of the cuvette (in presence of a magnetic field) what suggests on the one hand an enhanced signal measured by the MagnetReader (7) but on the other hand lower particle concentrations in the reservoir (1) measured by VSM on small taken samples. The setup of the experiment is shown in Fig. 1. Only after excluding these effects a statement about a binding of particles in the placenta tissue is possible.

Up to now only experiments on the maternal side of the placenta were carried out with particles. Successful measurements were done with an initial particle concentration of about 8 µg/ml.

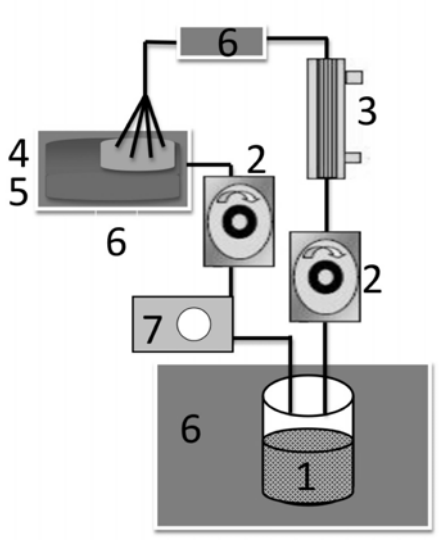

Fig. 1: Setup of the perfusion experiment
1 magnetic particles suspended in perfusion media (stirrer is not shown)
2 pump
3 oxygenator
4 placenta, maternal side with connected cotyledon
5 placenta - fetal side
6 heating bath 37°C
7 MagnetReader (computer not shown)

Figs. 2 and 3 show examples of the particle concentration vs perfusion time measured on polyethyleimine coated particles by VSM and starch coated particles by Magnetreader, respectively.
A certain deposition of NP in the placenta tissue could be confirmed qualitatively by micro-CT investigations (H. Rahn, TU Dresden) and magnetorelaxometry (M. Büttner, FSU Jena).

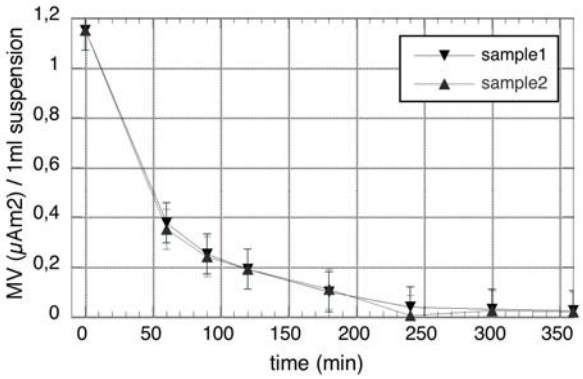

Fig. 2: VSM measurements of the particle concentration (FluidMag-PEI) of samples taken from the perfusion-fluid reservoir

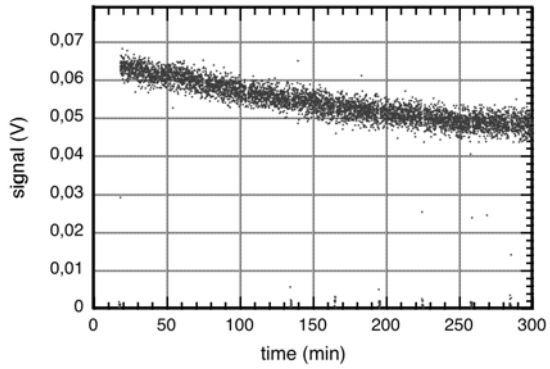

Fig. 3: Offset corrected longterm measurements of particle suspension (Fluid-Mag-D) in the perfusion system with placenta tissue with Delrin cuvette.

A further improvement of the system (smaller offset signal by reduced particle adsorption at the cuvette) is under progress. A double sided perfusion experiment with measurements on the maternal as well as fetal side of the placenta is coming soon.

Acknowledgments

The particles were provided by chemicell GmbH in Berlin.
The work was supported by the BMBF grant 03X0104E, project “NanoMed”.

References

[1] H.-J. Krause “Biomagnetsensor für die point-of-care-Diagnostik”, Final report Project 16IN0244, Forschungszentrum Jülich, 2007
[2] P. Miethe et al, Patent WO 2004/077044 A1

Success of magnetic assisted epithelial cell sorting depends on the nanoparticle shell and the therapeutic regiment

K. Voigt[1], J. Wotschadlo[1, 2], P. Konowski[1], M. Schwalbe[1], K. Pachmann[1], T. Liebert[2], T. Heinze[2], A. Hochhaus[1], J. H. Clement[1]

[1] *Klinik für Innere Medizin II, Abteilung Hämatologie und Internistische Onkologie, Universitätsklinikum Jena, Erlanger Allee 101, D-07747 Jena, Deutschland;* katharina.voigt1@med.uni-jena.de
[2] *Kompetenzzentrum für Polysaccharidforschung, Friedrich Schiller Universität Jena, Humboldtstrasse 10, 07743 Jena, Deutschland*

Introduction

In cancer the main cause of death is the formation of distant metastases. Once the primary epithelial tumor is established, cells may begin to dissociate and spread to other parts of the body. These circulating epithelial tumor cells (CETCs) are able to form metastases. The elimination of CETCs from circulation is a major challenge. In hematology and oncology magnetic nanoparticles are regularly used for labeling and detection of cells. We used a variety of carboxymethylated (CM) polysaccharides including dextran (CMD), cellulose (CMC), pullulan (CMP) to study the influence of the polymer backbone on the cellular uptake.

Methods

To test the different carboxymethylated polysaccharides we incubated peripheral blood leukocyte fractions for 4 min with the coated magnetic nanoparticles. Peripheral blood leukocytes were prepared by erythrocyte lysis (Qiagen, Hilden, Germany) from whole blood samples of breast cancer patients. The labeled cells were separated by using a SuperMACS Separator (Miltenyi-Biotech, Bergisch-Gladbach, Germany) and were quantified as positive (retained fraction) and negative fraction (effluent fraction). The cells of both fractions were analyzed by flow cytometry (FACSCalibur, Becton-Dickinson, Heidelberg, Germany) and by Laser-Scanning-Cytometry (LSC, Compucyte Corporation, Cambridge, MA, USA).

Results

A considerable difference in the uptake rate of particles coated with carboxymethylated polysaccharides was determined. CETCs showed an intense interaction with all tested CM-coated particles, whereas leukocytes exhibited a diverse tendency to interact. For the selective enrichment of CETCs from peripheral blood, CMD-coated nanoparticles showed the lowest interaction with peripheral blood leukocytes. Additionally, the conversion of purchasable salt dextran (COO- Na+) into an acidic structure (COOH) has a better effect on separation efficiency. All in all we analyzed 135 breast cancer patients (300 samples overall) with CMD-coated particles. A median of 80±27% was collected from the entire CETCs in the positive fraction. We observed a difference in the enrichment efficiency of CETCs with regard to the individual therapy status of the patient. Pre-operative patients (n=10) or patients in follow-up care (n=50) show a better selective enrichment of CETCs in the positive fraction (pre-operative 93±33%; follow-up care 92±16%) than patients undergoing chemotherapy (n=23; approx. 33±31%).

Conclusion

We are able to enrich CETCs from peripheral blood leukocyte fractions quantitatively using CMD-coated magnetic nanoparticles. The treatment-dependant degree of enrichment needs further investigations. Nevertheless this noninvasive method may be a tool to effectively eliminate CETCs from the periphery.

Enzymatically activated nanoparticle cluster formation as a model for the transition from Brownian to Néel relaxation

F. Wiekhorst[1], L. Figge[2], U. Steinhoff[1],
E. Schellenberger[2], L. Trahms[1]

[1] *Physikalisch-Technische Bundesanstalt, Abbestrasse 2-12, 10587 Berlin*
[2] *Charité, University Medicine Berlin, Charitéplatz 1, 10117 Berlin*

Introduction

The controlled application of magnetic nanoparticles (MNP) in medicine requires detailed knowledge of their dynamic behavior strongly depending on the local hydrodynamic environment. While the magnetic core of the MNP exhibits a Néel relaxation behavior, the rotational motility of the entire MNP leads to a Brownian relaxation. The effective relaxation is a superposition of both mechanisms. Here, we present a model system that allows to continously increase the effective hydrodynamic diameters and in consequence the Brownian relaxation time of MNP at a slow rate. Using this model system we investigated the impact on the parameters relaxation time and amplitude as they are determined by our standard magneto-relaxometry (MRX) setup [1]. An MRX measurement generally consists of two phases: In the magnetizing phase a moderate magnetizing field partially aligns the MNP moments along the field direction. In the measurement phase starting shortly after the switching-off of the magnetizing field, the magnetic field changes originating in the decay of the samples net magnetic moment are detected by a magnetic field sensor. The MRX relaxation curve is mainly characterized by relaxation amplitude and relaxation time. While the relaxation amplitude has been used to localize and quantify distributions of MNP administered to organs, the relaxation time is exploited to reflect the hydrodynamic state of MNP. Together with the short measurement duration typically in the range of seconds, MRX is well suited to study kinetic processes of MNP changing their hydrodynamic state in this temporal range.

Our model system is based on an enzymatically activated MNP cluster formation process. Negatively charged MNP are coated with a polycationic peptide-PEG-conjugate, which contains a cleavage site for the enzyme matrixmetalloproteinase-9 (MMP-9) [2]. As a result of specific cleavage by MMP-9 the MNP lose their sterically stabilizing PEG-shell and mixed charged MNP surfaces enable the cluster formation of the MNP.

Materials and Methods

We used iron oxide MNP (median core size=12 nm, *c*(Fe)=32 mmol/l, carboxymethyl dextrane coating, hydrodynamic diameter=31 nm). Prior to the enzyme activation 13 µl of the MNP were incubated with 9 µl conjugate consisting mainly of a central cationic amino acid chain on both ends connected to polyethylenglycol (PEG) chains serving for a sterically stabilization of the MNP conjugate. The central cationic amino acid chain binds via surface charges to the negatively charged dextrane shell of the MNP. The link between the central amino acid chain and PEG chains can later be specifically cleaved by adding the enzyme matrix-metalloproteinase-9 (MMP-9). The samples were dissolved in 128 µl enzyme buffer. Finally, 3.5 µl of MMP-9 enzyme was added (sample A) immediately before starting the first MRX measurement. As a control another sample prepared in the same way but without adding

enzyme (sample B) was used together with a sample (sample C) containing solely 45 µl MNP suspension.

For the measurements we utilized the PTB single channel MRX device. The samples were magnetized at 1.6 mT for 1 s and the relaxation was measured at a sampling rate of 100 kHz in the interval from 450 µs to 0.36 s after switching-off of the field. The data were preprocessed including a logarithmically filtered downsampling, a background correction using a measurement without sample and an offset subtraction. For each relaxation curve B(t) then amplitude $\Delta B = B(t=680\ \mu s) - B(t=0.32\ s)$ and relaxation time as the time interval after t=680 µs in which $B(t)$ has dropped by the factor $e \approx 2.7183$ were determined.

Results

The relaxation time $t_{1/e}$ as a function of the time after adding the enzyme (sample A) is shown in Fig. 1 together with that of the controls (B and C). A strong increase in the relaxation time is observed starting at about 5 minutes reaching a maximum of $t_{1/e}$=37 ms at about 15 minutes, followed by a slight decrease to $t_{1/e}$=25 ms. After 100 minutes no further changes in the relaxation time were detected and a total precipitation of the MNP was observed visually. In contrast, the control B showed only a slight increase in the relaxation time from $t_{1/e}$=3 ms at the beginning to about $t_{1/e}$=6 ms after 1000 min, while the pure MNP stayed stable at $t_{1/e}$=0.8 ms. Both controls showed no visual indication of precipitation. The relaxation amplitude of the enzyme sample A (black line in Fig.1) exhibits a maximum at the steepest increase of $t_{1/e}$ at about 10 min and drops down afterwards reaching after 100 min a stable value of about a quarter of the starting amplitude.

We simulated the cluster formation in a numerical model, where we calculated the effective relaxation times for a lognormal moment distribution of the MNP with increasing hydrodynamic diameters due to the cluster formation.

The basic features observed in the MRX measurements could be reproduced. It turned out, that the observed changes in relaxation time and amplitude depend on the parameters of the original moment distribution, the cluster formation process, and the MRX detection interval.

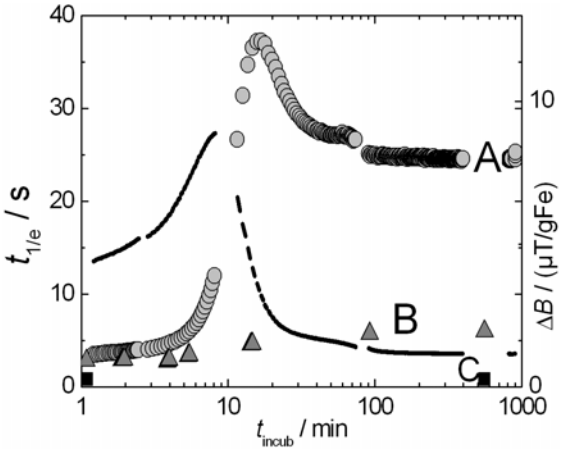

Fig. 1: Relaxation times $t_{1/e}$ (circles: enzyme sample A, triangles: control B, squares: pure MNP C, scale at left margin) and relaxation amplitude (black line: enzyme sample A only, scale at right margin).

Conclusion

The presented enzyme activated MNP cluster formation is an excellent model system to study the cluster formation of MNP by MRX and to improve the measurement and signal analysis procedures of MRX for the detection of binding kinetics. It is not only suitable to study MNP cluster formation but also to investigate MNP interactions with their biological environment.

Acknowledgments

This work was financially supported by the DFG research program KFO 213 *Magnetische Nanopartikel für die Zelluläre und Molekulare MR-Bildgebung* TR408/5-2 and *Funktionalisierung superparamagnetischer Nanopartikel* SCH1416/2-2.

References

[1] F. Wiekhorst, U. Steinhoff, D. Eberbeck, L. Trahms (2012) Pharm Res **29**:1189-1202

[2] E. Schellenberger, F. Rudloff, C. Warmuth, M. Taupitz, B. Hamm, J. Schnorr (2008) Bioconjug Chem **19**:2440-2445

Study of heat distribution during magnetic heating treatment

F. Henrich[1], H. Rahn[1] and S. Odenbach[1]

[1] *Chair of Magnetofluiddynamics, Technische Universität Dresden, Dresden 01062, Germany*

Magnetic nanoparticles are used for the minimal invasive cancer treatment magnetic heating treatment (MHT). This minimal invasive treatment has been studied on animal models, such as tumour bearing mice [1-2]. Further on, some research has been performed on humans [3].

For the success of MHT the magnetic nanoparticles should be distributed in the tumour with a well defined homogeneous concentration.

The real particle distribution is unknown, so the temperature distribution is unknown consequently. For the experimental investigation of the heat distribution a phantom has been developed. With the help of this phantom the temperature distribution within the particle enriched area of a tumour but also in the surrounding tissue can be detected. The aim is a minimal-invasive measurement of the temperature at the outer regions leading to the core temperature generated within a tumour. A possibility to approach this aim is a comparison of the experimental values with simulation based on the experimental data. Thus, a heat transfer from tissue regions enriched with magnetic nanoparticles to the surrounding tissue can be determined.

The developed phantom has to fulfil following requirements:

- the body material has to show similar properties as human tissue with respect to thermal conductivity
- homogeneous structure
- thermal stability up to 100°C
- magnetic nanoparticles must be immobilised in the material
- long-term stable

An elastomere polyurethan gel (PUR) [5] has been chosen as it is used for body parts phantoms in forensics, wound ballistics and medicine [6]. Magnetic nanoparticles are suspendable within the elastomere. It can be casted to any shape and after curing it is long-term stable, so the included nanoparticles are immobilised permanently.

The phantom consists of two concentric cylinders made of PUR. The inner cylinder contains magnetic nanoparticles with a concentration of 13 mg/ml. This nanoparticle concentration has been adapted to the nanoparticles concentration used for magnetic drug targeting.

The outer cylinder is produced of pure PUR. The temperature measurement is performed with four thermocouples (Type T, copper and copper-constantan). Figure 1a shows a technical drawing of the phantom.

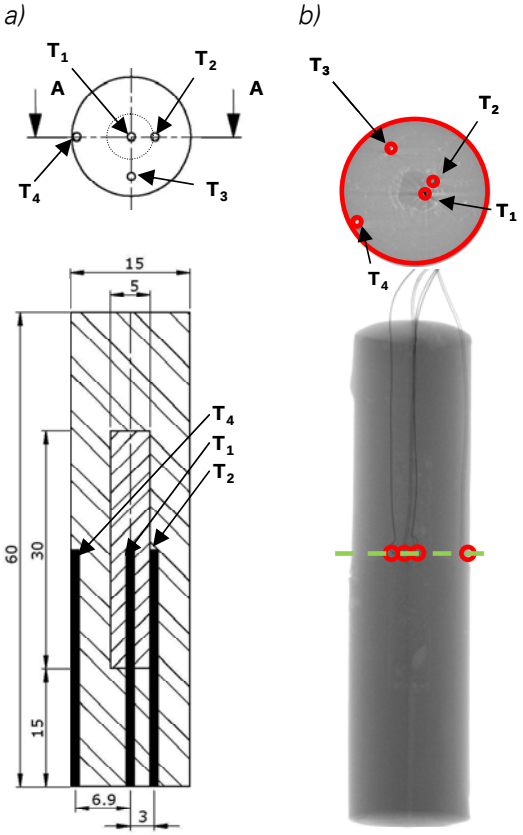

Figure 1: a) technical drawing of the phantom with included thermocouples; b) tomographic image of the phantom.

X-ray microcomputed tomography has been used to check the real positions of the

inner cylinder as well as of the thermocouples.

For the magnetic heating experiments the phantom has been exposed to an alternating magnetic field. The range of the magnetic field strengths varies between 19.5 kAm^{-1} to 57.4 kAm^{-1}. The initial temperature was 37 °C realised by a phantom surrounding water bath. The measurements were performed at the "Magnetohydrodynamics" laboratory of the Helmholtz Zentrum Dresden Rossendorf (HZDR).

The measurements are shown in Figure 2. A temperature rise for all thermocouples was detected. The maximum temperature, measured in the centre of the inner cylinder (thermocouple T1), was 41.5 °C for the highest magnetic field strength; at the thermocouple T4 a temperature of 37.3 °C.

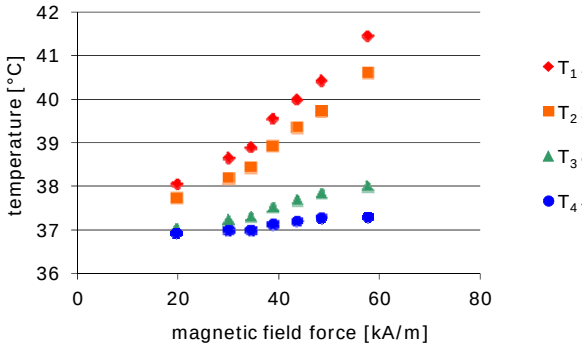

Figure 2: Temperatures measured with thermocouples at different magnetic field strengths.

A simulation model was based on the experimental magnetic heating data and tomographic data concerning positions of the cylinders and thermocouples. The simulation was performed with finite elements analysis software COMSOL Multiphysics®.

In Figure 3 the experimental and the simulated results are compared with each other for two different magnetic field strengths. The temperature profiles show a similar trend. The deviations between the measured and simulated values are in the range of 10 %.

As a conclusion we can say, that the established phantom fulfils the requirements. The maximal reached temperature was 41.5 °C at the highest magnetic field strength. But 2.5 mm away from the centre point the detected temperature was 38 °C only. Thus, a homogeneous nanoparticle distribution is desirable.

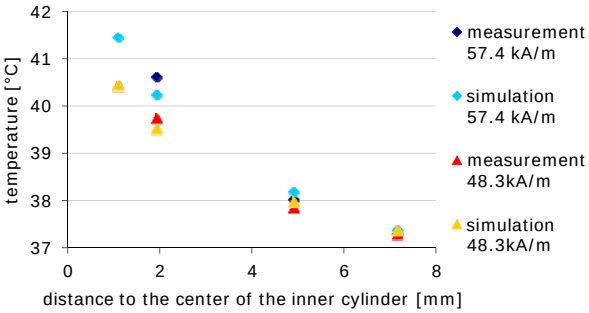

Figure 3: Comparison of the experimental and simulation data.

Acknowledgments

These studies are supported by the Deutsche Forschungsgemeinschaft (DFG-OD 18/16-1. We also thank ELANTAS Beck GmbH fort the providing us the elastomere. Many thanks we would like to say Stefan Erlebach from the Magnetohydrodynamics laboratory of the Helmholtz Zentrum Dresden Rossendorf (HZDR) for the help during the measurements.

References

[1] I Hilger et al.; Electromagnetic Heating of Breast Tumors in Interventional Radiology: In Vitro and in Vivo Studies in Human Cadavers and Mice; Radiology 218 (2001) 570 – 575

[2] I Hilger, A Rapp, K O Greulich and W A Kaiser; Assessment of DNA Damage in Target Tumor Cells after Thermoablation in Mice; Radiology 237 (2005) 500 – 506

[3] A Jordan, et al.; Presentation of a new magnetic field therapy system for the treatment of human solid tumors with magnetic fluid hyperthermia; Journal of Magnetism and Magnetic Materials 225 (2001) 118 – 126

[5] http://www.elantas.de; ELANTAS Beck GmbH, Hamburg, Deutschland

[6] K Sellier und B P Kneubuehl; Wundballistik und ihre ballistischen Grundlagen; Springer Verlag; Berlin 2001.

Investigations on a branched tube model in magnetic drug targeting – systematic measurements and simulation

K.Gitter, S. Odenbach

TU Dresden, Institute of Fluid Mechanics, Chair of Magnetofluiddynamics, 01062 Dresden, Germany

Magnetic drug targeting

Magnetic drug targeting has been established as a promising technique for tumour treatment. Due to its high targeting efficiency unwanted side effects are considerably reduced, since drug-loaded nanoparticles are concentrated within a target region due to the influence of a magnetic field.

Experiments – targeting maps

In order to contribute to the understanding of basic phenomena experiments on a half-Y-branched glass tube model as a model-system for a blood vessel supplying a tumour were performed. As a result of measurements, novel drug targeting maps, combining e.g. the magnetic volume force, the position of the magnet and the net amount of targeted nanoparticles were presented.
In a first targeting-map [1], which summarizes results for 63 magnet positions, the concentration of the injected ferrofluid is 2.95vol%. Up to 97% of the nanoparticles were successfully targeted into the chosen branch; however, the region where yield was considerable is rather small. A high concentration of injected ferrofluid brings the danger of accretion in the tube. It is shown that an increase in magnetic volume force does not necessarily lead to a higher amount of targeted nanoparticles.
In a second targeting-map [2] the concentration of injected ferrofluid is reduced to 0.14vol%. At a first glance the result with low concentration is promising, since the danger of accretion is avoided. Nevertheless, one has to consider, that, unless the magnetic volume force in the branch-point was provided in the necessary strength, an application would not be successful.

Simulation

The current focus is a finite-element simulation based on the considered setup and artery-model. Following [4], the fluid flow is described by the Navier-Stokes equations, the magnetic field is derived from Maxwell's equations and mass flux is given by the advection-diffusion equation.
The magnetic volume force acting on a volume of magnetic fluid combines the magnet and the ferrofluid data and is proportional to the field dependent magnetisation and the gradient of the field strength. The diffusion equation additionally allows the implementation of a concentration-dependent magnetic volume force.

Focus of simulation

Our experimental investigations mentioned above and [3] have shown that the miscibility of even the water-based ferrofluid and water is low. Since in medical applications the ferrofluid will be injected close to an appropriate junction one cannot assume a homogeneous mixture approaching the branch-region.
Therefore, the main focus of the presented simulation is a model where at the point of injection the ferrofluid and the carrier-fluid are initially separated and further mixture occurs due to the velocity field, diffusion, volume forces and magnetophoresis.

Details and setup

The artery-model, see Fig. 1, is a half-Y-branched glass tube which consists of a straight circular tube with a precision-fitted branch in 45°, which is thought to supply the target area. The inner diameter is 1.6 mm, which is constant in all sections of the model.

The magnetic field is generated by an axially magnetized cylindrical permanent magnet, which has a diameter of 10mm, a height of 5mm and a magnetic flux density of B_0=310mT at the centre of the surface.
The following simulation models a high concentration of injected ferrofluid of 2.95vol%, which refers to [1].
At the inflow as boundary condition a parabolic velocity profile is modelled for the flow and a concentration profile is applied for diffusion.
At the outflows so called “do nothing conditions” are applied for flow and diffusion.
The chosen boundary conditions implement a flow regime that is solely driven by the boundary conditions at the inflow.
In this simplified simulation the fluid is assumed to have Newtonian behaviour.

Selected results

The results of the 3D-simulation are presented as a top view onto a horizontal cutting-plane through the middle of the artery-model. Furthermore, three profiles (a-c), which have a distance of 3mm to the branch-point, display details in a cross-section of the tubes.

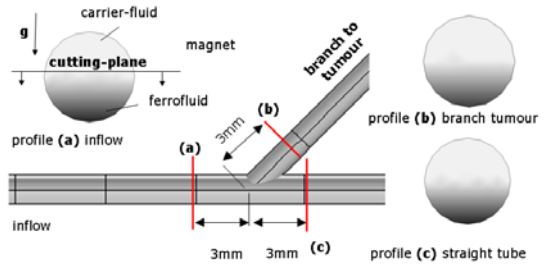

Fig. 1: Artery model with branch to tumor in 45°. Presentation of 3D-results as a top view onto a horizontal cutting-plane through the centre of the model and in addition three profiles (a-c) with a distance of 3mm to the branch-point. The initial state of the concentration is shown in the profiles

The profiles (a-c) of Fig. 1 show with c/c_0 the initial state of the concentration distribution.
As a result Fig. 2 shows the steady-state of the velocity u/u_0 and Fig. 3 the flux $N=c \bullet u$. An accretion covering the wall occurs in the region between a point 5mm upstream the branch and the branch-point.

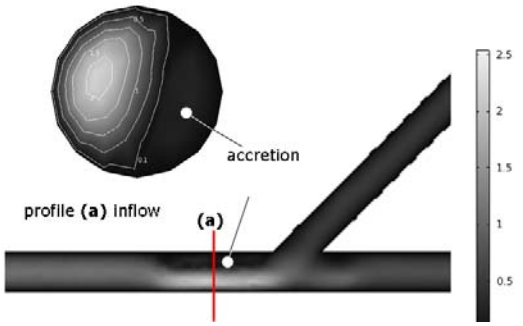

Fig. 2: Steady-state of the velocity u/u_0. Due to the influence of the magnetic field an accretion occurs in the inflow before the branch-point leading to an increase of velocity in the free area

Profile (a) in Fig. 2 shows the velocity u/u_0 through the accretion. In a broad range facing the magnet the velocity is low. On the contrary in the free section the maximum velocity is up to 2.5 times higher than u_0
.

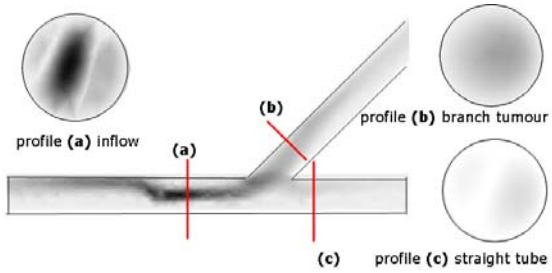

Fig. 3: Steady-state of the Flux $N=c \bullet u$. In spite of the accretion a high percentage of ferrofluid is targeted into the branch, as seen by comparing profiles (b) and (c).

The profiles (b) and (c) of the flux N in Fig. 3 indicate the high percetage of ferrofluid targeted into the branch of 88% which is in good agreement with experimental results of 92%.

Acknowledgments

The financial support by the Deutsche Forschungsgemeinschaft, grant OD18/13, is gratefully acknowledged..

References

[1] K. Gitter, S. Odenbach, JMMM, 323 (23), 2011.
[2] K. Gitter, S. Odenbach, JMMM, 323 (10), 2011.
[3] R. Ganguly, B. Zellmer, I.K. Puri, Phys. Fluids, (17) 2005.
[4] K. Gitter, S. Odenbach, IEEE Trans. Mag., submitted 2012.

Towards Therapeutic Applications of Superparamagnetic Nanoparticles

O. Lunov, T. Syrovets, and Th. Simmet

Institute of Pharmacology of Natural Products & Clinical Pharmacology, Ulm University, Ulm, Germany

Nanotechnology and the medical application of nanoparticles are rapidly growing fields. Characteristic size of nanoparticles allows them to exhibit novel and significantly improved physical, chemical, and biological properties, phenomena, and processes. Therefore, nanoparticles of various sizes, materials and surface modifications have many industrial and medical applications. Hence, our knowledge about interactions of nanoparticles with living cells as well as the physiological and pathophysiological effects of such nanoparticles on cellular functions remains rather limited.

The **aim** of this study was to investigate the uptake mechanism of two diagnostically used superparamagnetic carboxydextran-coated superoxide nanoparticles of 60 nm (SPIO) and 20 nm (USPIO) by human macrophages as well as their cellular effects.

Transmission electron microscopy of particles revealed a mean size of iron oxide core about 5 nm. Within 1 h, both SPIO and USPIO are rapidly taken up by macrophages[1]. Using pharmacological and antisense *in vitro* knockdown approaches, we show that the uptake of SPIO and USPIO does not involve phagocytosis, probably due to the small size of the nanoparticles. Our data indicated that the main uptake mechanism for both SPIO and USPIO is clathrin-mediated scavenger receptor A-dependent endocytosis[2].

A single intravenous injection of SPIO into mice leads to a rapid accumulation of the particles in liver macrophages, called Kupffer cells, and to a long-lasting increase of iron deposition in liver and kidneys as detected by MRI (Fig. 1)[3].

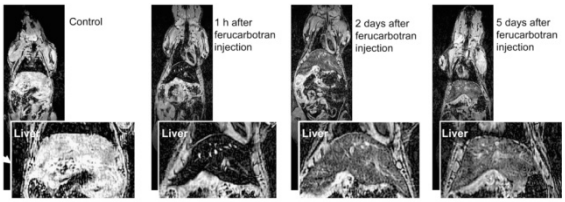

Fig. 1. Kinetics of nanoparticle distribution in mice after a single i.v. injection of SPIO nanoparticles.

Moreover, the intravenous injection of SPIO into mice triggers apoptosis and the subsequent depletion of liver macrophages. Notably, the nanoparticle-induced apoptosis of murine Kupffer cells can be prevented by treatment of the mice with the therapeutic radical scavenger edaravone[3].

Manipulation of magnetic nanoparticles by externally applied magnetic fields offers the unique opportunity to influence cell functions and even the behavior of living organisms. Thus, we have demonstrated a strong increase of the endocytosis rate by an externally applied magnetic field (Fig. 1). With the magnetic force of the same order of magnitude as the actin force (tens of *pN*), the characteristic endocytosis time and rate can be controlled by a magnetic field[4].

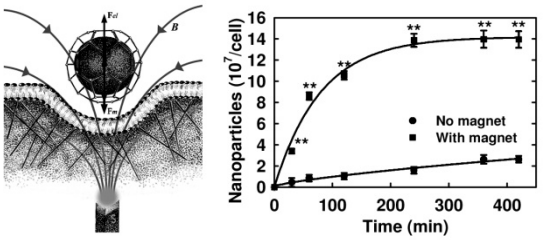

Fig. 2. Scheme of magnetically controlled endocytosis and number of internalized SPIO nanoparticles as a function of time with and without magnet.

Due to magnetic energy losses during the alternative magnetization processes, SPIO can be used as a source of heat in hyperthermia cancer treatment. We have shown that clusters of magnetic nanoparticles being positioned on the cell membrane and subjected to an alternating magnetic field are able to elevate the cell membrane temperature up to 10°C, which is enough to initiate cell apoptosis (Fig. 3). We have created a mathematical model of membrane heating with nanoparticle clusters, calculated the spatiotemporal distributions of temperature, and demonstrated the applicability of the membrane hyperthermia strategy[5].

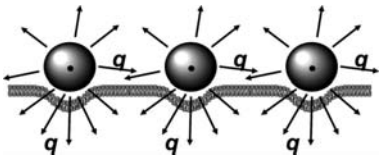

Fig. 3. Clusters of magnetic nanoparticles on a cell membrane (schematically).

In order, to estimate the antitumor efficacy of the nanoparticles *in vivo* and reduce the number of animal experiments, we have developed a pre-animal test system based on tumors xenografted onto chick chorioallantoic membranes (CAM)[6, 7]. Suspensions of various tumor cell lines xenografted onto CAM develop into solid three-dimensional tumors, which actively proliferate, induce angiogenesis, and infiltrate into the CAM tissue. The system is perfectly suitable for the analysis of pharmacokinetics and antitumor activity of tested materials (Fig. 4).

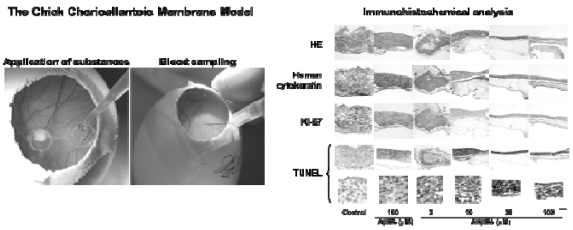

Fig. 4. The chick chorioallantoic membrane model (CAM). Prostate tumor grown on CAM, blood sampling for pharmacokinetic studies, and immunohistochemical analysis.

In conclusion, engineered superparamagnetic nanomaterials hold great opportunities as diagnostic and therapeutic agents. More intensive *in vivo* studies are, however, required to ensure their safe and successful biomedical application.

Acknowledgments

We thank G.U. Nienhaus (Inst. Applied Physics & Center for Functional Nanostructures, KIT, Karlsruhe) for help with cell imaging and V. Rasche (Experimental Cardiovascular Imaging, Ulm University) for MRI imaging of mice.

References

1. Lunov O, Syrovets T, Büchele B, Jiang X, Röcker C, Tron K, Nienhaus GU, Walther P, Mailander V, Landfester K, Simmet Th. The effect of carboxydextran-coated superparamagnetic iron oxide nanoparticles on c-jun N-terminal kinase-mediated apoptosis in human macrophages. *Biomaterials*. 2010;31:5063-5071
2. Lunov O, Zablotskii V, Syrovets T, Röcker C, Tron K, Nienhaus GU, Simmet Th. Modeling receptor-mediated endocytosis of polymer-functionalized iron oxide nanoparticles by human macrophages. *Biomaterials*. 2011;32:547-555
3. Lunov O, Syrovets T, Röcker C, Tron K, Nienhaus GU, Rasche V, Mailander V, Landfester K, Simmet Th. Lysosomal degradation of the carboxydextran shell of coated superparamagnetic iron oxide nanoparticles and the fate of professional phagocytes. *Biomaterials*. 2010;31:9015-9022
4. Zablotskii V, Lunov O, Dejneka A, Jastrabik L, Polyakova T, Syrovets T, Simmet Th. Nanomechanics of magnetically driven cellular endocytosis. *Appl Phys Lett*. 2011;99:183701
5. Lunov O, Zablotskii V, Pastor JM, Pérez-Landazábal JI, Gómez-Polo C, Syrovets T, Simmet Th. Thermal destruction on the nanoscale: Cell membrane hyperthermia with functionalized magnetic nanoparticles. *Am Inst Phys CP* 2010;1311:288-292
6. Syrovets T, Gschwend JE, Büchele B, Laumonnier Y, Zugmaier W, Genze F, Simmet Th. Inhibition of IκB kinase activity by acetyl-boswellic acids promotes apoptosis in androgen-independent PC-3 prostate cancer cells in vitro and in vivo. *J Biol Chem*. 2005;280:6170-6180
7. Estrada AC, Syrovets T, Pitterle K, Lunov O, Büchele B, Schimana-Pfeifer J, Schmidt T, Morad SA, Simmet Th. Tirucallic acids are novel pleckstrin homology domain-dependent Akt inhibitors inducing apoptosis in prostate cancer cells. *Mol Pharmacol*. 2010;77:378-387

Concept of magnetic microbubbles for magnetic field and ultrasound triggered drug and gene delivery

D. Vlaskou, O. Mykhaylyk, C. Plank.

Institute of Experimental Oncology and Therapy Research, Klinikum rechts der Isar, TUM, Munich

In current therapies, pharmacological active drugs reach the target site with poor specificity and dose-limiting toxicity. During last decade magnetic targeting concept is developed to improve the delivery in gene and drug therapy. Nevertheless, one of the factors limiting efficacy of magnetic targeting *in vivo* is low magnetic responsiveness of the carrier. Based on the "Magnetofection" concept [1] and in order to enhance the response to an external magnetic field we combine the magnetic drug-targeting concept with ultrasound-triggered delivery by developing magnetic microbubbles [2, 3]. These are gas-filled spheres in size of 1-5µm that comprise in their shell a multitude of magnetic nanoparticles (MNPs). Microbubbles can serve as targeted drug delivery vehicle able to carry therapeutic agents (genes, drugs) into target cells. They can be accumulated at a site of magnetic field application and can be destructed by high frequency ultrasonic field resulting in active agents release in the area of interest. We have developed numerous formulations of the magnetic microbubbles consisting of the lipid shell with embedded MNPs. We designed the first generation of our microbubbles (magnetic acoustically active lipospheres MAALs) based on a composition developed for the delivery of hydrophobic drugs, which comprised soybean oil and an outer layer of amphipathic lipids [2]. We incorporated additionally a cationic lipid-transfection reagent to bind nucleic acids or an anionic lipid composition to bind cytostatica and loaded the bubbles with MNPs [4]. These formulations have a high binding capacity for nucleic acids (plasmid DNA; antisense oligonucleotide; siRNA) and cytostatica as MTX, Doxorubicin, Paclitaxel and have favourable magnetic properties compared to MNPs. Our second generation of magnetic microbubbles (MMBs) are perfluoropropane spheres stabilized by lipid monolayer shell loaded with highly positively or negatively charged magnetic nanoparticles with an iron oxide core and suitable coatings [3, 4]. Different MMBs formulations that are highly responsive to ultrasound and gives excellent contrast in ultrasound imaging can be highly loaded with lipids, viral particles or optionally with biotinylated liposomes (biotinylated MMBs). *In vitro* the MMBs exhibited highly efficient DNA and siRNA delivery to adherent and suspension cells in static and in flow conditions mimicking the blood stream [2, 3, 5]. *In vivo* we studied the magnetic microbubbles biodistribution in mice and confirmed the possibility to trap them at the target site under application of the gradient magnetic field. The therapeutic efficacy of the MMB formulations was demonstrated in different animal models after systemic and local administration (e.g. dorsal skinfold chamber mouse model; preclinical model of ischemic skin flap survival in rats) [6]. Gene and drug delivery efficiency was strongly improved under application of a gradient magnetic field. In some cases additional ultrasound application resulted in a synergistic effect. Molecular imaging is a field where magnetic microbubbles may also contribute to visualization of the carrier at the molecular level because of their high compressibility resulting in high contrast in ultrasound imaging. MNPs embedded in the bubble shell give an excellent MRI contrast. Thus, MMBs offer a valuable dual US and MRI imaging modality. Magnetic microbubbles may be useful for cancer therapy, vascular thrombolysis and gene therapy.

Acknowledgments

This work was supported by the Nanobiotechnology program (www. nanobio.de) of the German Federal Ministry of Education and Research, Nanobiotechnology grants 13N8186 and 13N8538. Financial support of the German Research Foundation DFG Research Unit FOR917 (Project PL 281/3-1), BMBF project ELA 10/002, and German Excellence Initiative via the “Nanosystems Initiative Munich (NIM)” is gratefully acknowledged.

References

[1] C. Plank, O. Zelphati, O. Mykhaylyk, Magnetically enhanced nucleic acid delivery. Ten years of magnetofection-progress and prospects, Adv Drug Deliv Rev, 63 (2011) 1300-1331.

[2] D. Vlaskou, O. Mykhaylyk, F. Krötz, N. Hellwig, R. Renner, U. Schillinger, B. Gleich, A. Heidsieck, G. Schmitz, K. Hensel, C. Plank, Magnetic and Acoustically Active Lipospheres for Magnetically Targeted Nucleic Acid Delivery, Advanced Functional Materials, 20 (2010) 3881-3894.

[3] D. Vlaskou, P. Pradhan, C. Bergemann, A.L. Klibanov, K. Hensel, G. Schmitz, C. Plank, O. Mykhaylyk, Magnetic Microbubbles: Magnetically Targeted and Ultrasound-Triggered Vectors for Gene Delivery in Vitro, AIP Conference Proceedings, 1311 (2010) 485-494.

[4] D. Vlaskou, O. Mykhaylyk, C. Plank, Magnetic and Acoustically Active Microbubbles loaded with nucleic acids for gene delivery, ´Nanotechnology for Nucleic Acid Delivery` in: D. Oupicky and M. Ogris (Ed.) *Methods in Molecular Biology*, chapter 15, Springer, 2013.

[5] P. Del Pino, A. Munoz-Javier, D. Vlaskou, P. Rivera Gil, C. Plank, W.J. Parak, Gene Silencing Mediated by Magnetic Lipospheres Tagged with Small Interfering RNA, Nano Lett, 10 (2010) 3914-3921.

[6] T. Holzbach, D. Vlaskou, I. Neshkova, M.A. Konerding, K. Wortler, O. Mykhaylyk, B. Gansbacher, H.G. Machens, C. Plank, R.E. Giunta, Non-viral VEGF(165) gene therapy - magnetofection of acoustically active magnetic lipospheres ('magnetobubbles') increases tissue survival in an oversized skin flap model, Journal of Cellular and Molecular Medicine, 14 (2010) 587-599.

Charge dependent influence of polymeric coated superparamagnetic iron oxide nanoparticles on blood and blood brain barrier

F. Schlenk[1]; F. Bähring[2]; C. Bergemann[3]; J.H. Clement[2]; D. Fischer[1]

[1]*Institute of Pharmacy, Department of Pharmaceutical Technology, Friedrich-Schiller-University Jena, Otto-Schott-Straße 41, 07745 Jena, Germany;*
[2]*Clinic for Internal Medicine II, Hematology/Oncology, Jena University Hospital, Erlanger Allee 101, 07747 Jena, Germany;*
[3]*chemicell GmbH, Eresburgstraße 22-23, 12103 Berlin, Germany*

Introduction

Superparamagnetic iron oxide nanoparticles (SPIONs) are used as contrast agents for diagnostic purposes in magnetic resonance tomography (MRT) [1]. Since they are commonly applied intravenously it is inevitable to investigate their hemocompatibility and biocompatibility. Furthermore, due to different application requirements permeation properties of SPIONs towards physiological barriers are of fundamental interest. An important physiological barrier is the blood brain barrier (BBB) represented by a tight endothelial cell layer connected with tight junctions. Polymer coatings on these nanoparticles may influence their uptake into brain tissue [2].

Objective

The objective of this study was to analyze the influence of SPIONs functionalized with different charged polymers on in vitro hemocompatibility, cytotoxicity and integrity of the blood brain barrier in dependency to particle concentration, incubation time and surface charge.

Experimental

Iron oxide particles were coated with neutral (starch), anionic (carboxymethyl dextran) and cationic (chitosan) polymers. Particle size and charge were analyzed by photon correlation spectroscopy and laser Doppler anemometry, respectively.

Hemocompatibility was analyzed using sheep erythrocytes investigating the hemolytic activity and erythrocyte aggregation potential of coated SPIONs in 12 different concentrations ranging from 0.024 to 50 µg/mL. For quantification of hemolysis released hemoglobin was measured spectrophotometrically at 544 nm after 1 h incubation at 37°C followed by centrifugation. Erythrocyte aggregation caused by SPIONs was analyzed by light microscopy and quantified by an absorbance assay at 645 nm.

The cytotoxic potential of the nanoparticles was determined using human brain microvascular endothelial cells (HBMEC) by CellTiter-Glo® luminescence measurements in 5 concentrations ranging from 0.5 µg/cm^2 to 100 µg/cm^2.

For the in vitro blood brain barrier model primary endothelial cells were isolated from cerebral microvessels by combined mechanical and enzymatic treatment from porcine brains. Subsequently, endothelial cells were cultivated on polycarbonate filter inserts (diameter 3.0 µm) and influence of SPIONs on the blood brain barrier in 2 different concentrations (25 µg/cm^2, 100 µg/cm^2) was investigated up to 24 h. [3] Membrane integrity was determined by measuring transendothelial electrical resistance (TEER).

Results

Mean diameters of starch, carboxymethyl dextran and chitosan coated particles were 136 nm, 165 nm and 118 nm, respectively (Figure 1a). As expected, zeta potentials of the SPIONs were dependent on the particle coating material (Figure 1b).

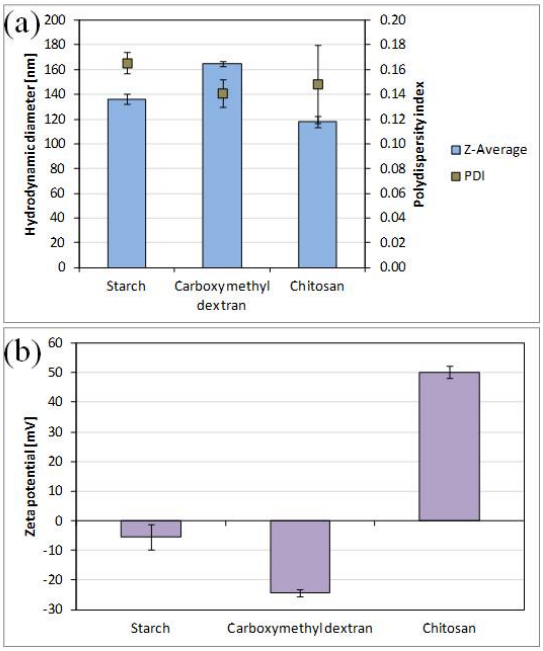

Figure 1: Hydrodynamic diameter, poly-dispersity indices (a) and zeta potentials (b) of investigated SPIONs.

Cationic chitosan coated SPIONs caused concentration dependent erythrocyte aggregation, whereas SPIONs with neutral and anionic charge showed no erythrocyte aggregation (Figure 2). In the analyzed particle concentrations up to 50 µg/mL no lysis of red blood cells could be detected.

No cytotoxicity was observed in CellTiter-Glo® assay for all tested SPIONs in concentrations up to 100 µg/cm^2.

Integrity of primary porcine endothelial cells was not affected by neutral or anionic functionalized SPIONs, however, chitosan coated SPIONs provoked decreasing TEER with increasing concentration.

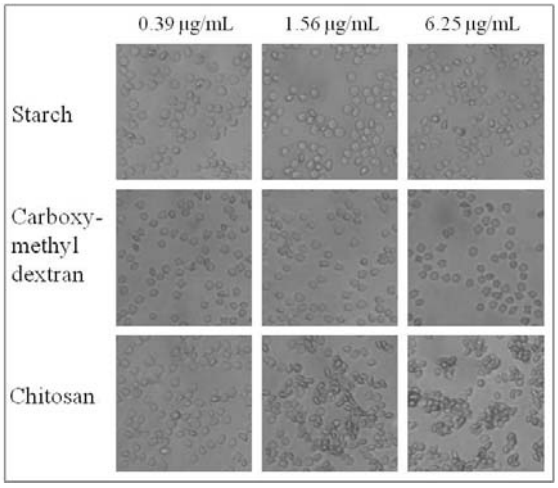

Figure 2: Concentration dependent erythrocyte aggregation of starch, carboxy-methyl dextan and chitosan coated SPIONs.

Conclusion

While neutral and anionic functionalized SPIONs caused no hemotoxicity, cytotoxicity or cerebral endothelial cell interference, cationic chitosan coated SPIONs led to decreased biocompatibility as well as an opening of the blood brain barrier in vitro.

References

1. Chertok, B., et al., Biomaterials, 2008. **29**(4): p. 487-96.
2. Rempe, R., et al., Biochem Biophys Res Commun, 2011. **406**(1): p. 64-9.
3. Winter, S., et al., Nitric Oxide, 2008. **18**(3): p. 229-39.

Acknowledgments

This work has been supported by the Federal Ministry of Education and Research (BMBF), funding code 03X0104D.

The authors would like to thank Angela Herre for technical assistance and Dr. Harald Schubert and Petra Dobermann from the Institute of Laboratory Animal Science and Animal Protection for supply of sheep blood samples.

List of Participants

Christoph Alexiou
Klinik und Poliklinik für Hals-, Nasen- und Ohrenkranke, Waldstr. 1, D-91054 Erlangen
Tel.: 0049-9131 8534769
Fax: 0049-9131 8584828
E-mail: c.alexiou@web.de

Fabiana Arantes
TU Dresden, Institut für Strömungsmechanik, Lehrstuhl Magnetofluiddynamik, D-01062 Dresden
Tel.: 0049-351 46332062
Fax: 0049-351 46333384
E-mail: farantes@if.usp.br

Günther K. Auernhammer
Max-Planck-Institut für Polymerforschung, Postfach 3148, 55021 Mainz
Tel.: 0049-6131 379113
Fax: 0049-6131 379100
E-mail: auhammer@mpip-mainz.mpg.de

Stephan Barcikowski
Universität Duisburg-Essen, Lehrstuhl Technische Chemie I, Universitätsstr. 7, 45141 Essen
Tel.: 0049-201 183-3145
Fax: 0049-201 183-3049
E-mail: stephan.barcikowski@uni-due.de

Franziska Bähring
Universitsklinikum Jena, Erlanger Allee 101, 07747 Jena
Tel.: 0049-3641 9325821
Fax: 0049-3641 9325827
E-mail: franziska.baehring@med.uni-jena.de

Silke Behrens
Institut für Katalyseforschung und -technologie, Karlsruher Institut für Technologie, D-76021 Karlsruhe
Tel.: 0049-721 60826512
Fax: 0049-721 60822244
E-mail: silke.behrens@kit.edu

Philipp Bender
Universität des Saarlandes, FR 7.3 Technische Physik / Prof. Dr. Rainer Birringer, Campus D2 2, Postfach 151150
Tel.: 0049-681 3025189
Fax: 0049-681 3025222
E-mail: nano@p-bender.de

Valter Böhm
Technische Universität Ilmenau, Technische Mechanik, PF 100565, D-98684 Ilmenau
Tel.: 0049-3677 691812
Fax: 0049-3677 691823
E-mail: valter.boehm@tu-ilmenau.de

Dmitry Borin
TU Dresden, Institut für Strömungsmechanik, Lehrstuhl Magnetofluiddynamik, D-01062 Dresden
Tel.: 0049-351 46332307
Fax: 0049-351 46333384
E-mail: dmitry.borin@tu-dresden.de

Helmut R. Brand
Universität Bayreuth, Universitätsstr., 95444 Bayreuth
Tel.: 0049-921 553331
Fax: 0049-921 555820
E-mail: brand@uni-bayreuth.de

Norbert Buske
MagneticFluids, Köpenicker Landstr. 203, D-12437 Berlin
Tel.: 0049-30 53007805
E-mail: n.buske@magneticfluids.de

Joachim Clement
Universitätsklinikum Jena, Erlanger Allee 101, D-07747 Jena
Tel.: 0049-3641 9325820
Fax: 0049-3641 9325822
E-mail: joachim.clement@med.uni-jena.de

Jan Dieckhoff
TU Braunschweig, EMG, Hans-Sommer-Straße 66, D-38106 Braunschweig
Tel.: 0049-531 3913876
Fax: 0049-531 3915768
E-mail: j.dieckhoff@tu-bs.de

Silvio Dutz
IPHT Jena, Albert-Einstein-Straße 9, D-07745 Jena
Tel.: 0049-3641 206317
Fax: 0049-3641 206139
E-mail: silvio.dutz@ipht-jena.de

Dietmar Eberbeck
Physikalisch-Technische Bundesanstalt Berlin, Abbestr. 2-12, D-10587 Berlin
Tel.: 0049-30 34817208
Fax: 0049-30 34817361
E-mail: dietmar.eberbeck@ptb.de

Sarah Essig
Karlruher Institut für Technologie, Hermann-von-Helmholtz-Platz 1, D-76344 Eggenstein
Tel.: 0049-721 60824320
Fax: 0049-721 60822244
E-mail: sarah.essig@kit.edu

Kurt Gitter
TU Dresden, Institut für Strömungsmechanik, Lehrstuhl Magnetofluiddynamik, D-01062 Dresden
Tel.: 0049-351 46334863
Fax: 0049-351 46333384
E-mail: kurt.gitter@tu-dresden.de

Gunnar Glöckl
Universität Greifswald, Felix-Hausdorff-Str. 3, 17487 Greifswald
Tel.: 0049-3834 864809
Fax: 0049-3834 864886
E-mail: gunnar.gloeckl@uni-greifswald.de

Angelika Gorschinski
KIT, Campus Nord, Hermann-von-Helmholtz-Platz 1, D-76344 Eggenstein
Tel.: 0049-721 60824229
Fax: 0049-721 60822244
E-mail: angelika.gorschinski@kit.edu

Thomas Gundermann
Technische Universität Dresden, Lehrstuhl für Magnetofluiddynamik, D-01062 Dresden
Tel.: 0049-351 46334672
Fax: 0049-351 46333384
E-mail: thomas.grundmann@tu-dresden.de

Dirk Heinrich
TU Berlin, Hardenbergstraße 36, D-10623 Berlin
Tel.: 0049-30 31422476
Fax: 0049-30 31427705
E-mail: dhein@physik.tu-berlin.de

Rolf Hempelmann
Universität des Saarlandes, D-66123 Saarbrücken
Tel.: 0049-681 3024750
Fax: 0049-681 3024759
E-mail: r.hempelmann@mx.uni-saarland.de

Christian Holm
Universität Stuttgart, Institute for Computational Physics, Pfaffenwaldring 27, 70569 Stuttgart
Tel.: 0049-685 63701
Fax: 0049-685 68563658
E-mail: christian.holm@icp.uni-stuttgart.de

Andras Hütten
Universität Bielefeld, Universitätsstr. 25, 33615 Bielefeld
Tel.: 0049-521 1065418
Fax: 0049-521 1066046
E-mail: huetten@phys.uni-bielefeld.de

Patrick Ilg
ETH Zürich, Wolfgang-Pauli-Str. 10, CH-8093 Zürich, Switzerland
Tel.: 0041-63 20839
E-mail: pilg@mat.ethz.ch

Jurij Jakobi
Universität Duisburg-Essen, Universitätsstr. 7, 45141 Duisburg
Tel.: 0049-201 1836295
Fax: 0049-201 1833049
E-mail: jurij.jakobi@uni-due.de

Sofia Kantorovich
University of Rome, La Sapienza, P. A. di Moro 5, 00187 Roma, Italy
E-mail: sofia@icp.uni-stuttgart.de

Sabine Klapp
TU Berlin, Institut für Theoretische Physik, Hardenbergstr. 36, 10623 Berlin
Tel.: 0049-30 23763
E-mail: Klapp@physik.tu-berlin.de

Regine von Klitzing
TU Berlin, Institut für Chemie, Stranski-Laboratorium f. physik. und theor. Chemie, Straße des 17. Juni 124, 10623 Berlin
Tel.: 0049-30 31423476
Fax: 0049-30 31426602
E-mail: klitzing@mailbox.tu-berlin.de

Christian Knopke
PTB Berlin, Abbestr. 2 - 12, 10587 Berlin
Tel.: 0049-30 34817090
E-mail: christian.knopke@ptb.de

Martin Krichler
Technische Universität Dresden, Lehrstuhl für Magnetofluiddynamik, D-01062 Dresden
Tel.: 0049-351 46334672
Fax: 0049-351 46333384
E-mail: martin.krichler@tu-dresden.de

Aidin Lak
Technische Universität Braunschweig, EMG, Hans-Sommer-Str. 66, 38106 Braunschweig
Tel.: 0049-531 3913860
Fax: 0049-531 3915768
E-mail: a.lak@tu-bs.de

Adrian Lange
TU Dresden, Institut für Strömungsmechanik, Lehrstuhl Magnetofluiddynamik, D-01062 Dresden
Tel.: 0049-351 46339867
Fax: 0049-351 46333384
E-mail: adrian.lange@tu-dresden.de

Michael Lentze
DFG, Deutsche Forschungsgemeinschaft, 53170 Bonn
Tel.: 0049-228 8852777
Fax: 0049-228 8852449
E-mail: michael.lentze@dfg.de

Maik Liebl
PTB Berlin, Abbestr. 2 - 12, 10587 Berlin
Tel.: 0049-30 34817721
E-mail: maik.liebl@ptb.de

Julia Linke
Technische Universität Dresden, Lehrstuhl für Magnetofluiddynamik, D-01062 Dresden
Tel.: 0049-351 46336445
Fax: 0049-351 46333384
E-mail: julia.linke@tu-dresden.de

Hartmut Löwen
Universität Düsseldorf, Universitätsstr. 1, 40225 Düsseldorf
Tel.: 0049-211 8111377
Fax: 0049-211 8112262
E-mail: hloewen@hhu.de

Robert Ludwig
Universität Erlangen, Uniklinikum, Erlanger Allee 101, 07745 Jena
Tel.: 0049-3641 9325925
E-mail: robert.ludwig@med.uni-jena.de

Frank Ludwig
Technische Universität Braunschweig, EMG, Hans-Sommer-Straße 66, 38106 Braunschweig
Tel.: 0049-531 3913863
Fax: 0049-531 3915768
E-mail: f.ludwig@tu-bs.de

Oleg Lunov
Universität Ulm, Helmholtzstr. 20, 89081 Ulm
Tel.: 0049-731 50065615
Fax: 0049-731 50065602
E-mail: oleg.lunov@uni-ulm.de

Stefan Lyer
Klinik und Poliklinik für Hals-, Nasen- und Ohrenkranke, Waldstr. 1, D-91054 Erlangen
Tel.: 0049-9131 8534769
Fax: 0049-9131 8534828
E-mail: stefan.lyer@uk-erlangen.de

Ralf Meckenstock
Universität Duisburg-Essen, Lotharstr. 1, 47057 Duisburg
Tel.: 0049-203 3792094
Fax: 0049-203 3792098
E-mail: ralf.meckenstock@uni-due.de

Andreas Menzel
Universität Düsseldorf, Universitätsstr. 1, 40225 Düsseldorf
Tel.: 0049-211 8112060
Fax: 0049-211 8112262
E-mail: menzel@thphy.uni-duesseldorf.de

Robert Müller
IPHT, Albert-Einstein-Str. 9, D-07745 Jena
Tel.: 0049-3641 206349
Fax: 0049-3641 206399
E-mail: robert.mueller@ipht-jena.de

Olga Mykhaylyk
TU München, Experimentelle Onkologie, Ismaningstr. 22, 81675 München
Tel.: 0049-89 41406182
Fax: 0049-89 41404475
E-mail: olga.mykhaylyk@lrz.tu-muenchen.de

Valentin Nica
Tel.: 0040 42363837
E-mail: NICAVAL@gmail.com

Stefan Odenbach
TU Dresden, Institut für Strömungsmechanik, Lehrstuhl Magnetofluiddynamik, D-01062 Dresden
Tel.: 0049-351 46332062
Fax: 0049-351 46333384
E-mail: stefan.odenbach@tu-dresden.de

Simon Pelz
Universität Köln, Department Chemie, D-50939 Köln
Tel.: 0049-221 4705473
Fax: 0049-221 4705482
E-mail: spelz@uni-koeln.de

Harald Pleiner
Max-Planck-Institut für Polymerforschung, Postfach 3148, D-55021 Mainz
Tel.: 0049-6131 379246
Fax: 0049-6131 379340
E-mail: pleiner@mpip-mainz.mpg.de

Jana Popp
Technische Universität Ilmenau, Technische Mechanik, PF 100565, D-98684 Ilmenau
Tel.: 0049-3677 691845
Fax: 0049-3677 691823
E-mail: jana.popp@tu-ilmenau.de

Elena Pyanzina
Ural Federal University, Lenin Av. 51, 620083 Ekaterinburg, Russia
E-mail: elena.pyanzina@usu.ru

Helene Rahn
TU Dresden, Institut für Strömungsmechanik, Lehrstuhl Magnetofluiddynamik, D-01062 Dresden
Tel.: 0049-351 463-35159
Fax: 0049-351 463-33384
E-mail: helene.rahn@tu-dresden.de

Reinhard Richter
Experimentalphysik 5, Universität Bayreuth, D-95440 Bayreuth
Tel.: 0049-921 55-3351
Fax: 0049-921 55-3647
E-mail: reinhard.richter@uni-bayreuth.de

Eric Roeben
Universität Köln, Department Chemie, D-50939 Köln
Tel.: 0049-221 4705573
Fax: 0049-221 4705482
E-mail: eroeben@uni-koeln.de

Lisa Roeder
Universität Köln, Insitut für Physikalische Chemie, Luxemburger Str. 116, 50939 Köln
Tel.: 0049-221 4705472
Fax: 0049-221 4705482
E-mail: lisa.roeder@uni-koeln.de

Ekrem Sahin
Institut für Katalyseforschung und -technologie, Karlsruher Institut für Technologie, D-76131 Karlsruhe
Tel.: 0176 99074723
E-mail: ekrem.sahin@kit.edu

Florian Schlenk
Universität Jena, Otto-Schott-Str. 41, 07745 Jena
Tel.: 0049-3641 949944
Fax: 0049-3641 949942
E-mail: florian.schlenk@uni-jena.de

Annette Schmidt
Universität zu Köln, Luxemburger Strasse 116, D-50939 Köln
Tel.: 0049-221 4705410
Fax: 0049-221 4705482
E-mail: annette.schmidt@uni-koeln.de

Christoph Schopphoven
Universität des Saarlandes, Technische Physik, D-66123 Saarbrücken
Tel.: 0049-681 3025189
E-mail: christoph@schopphoven.de

Jörg Schotter
Austrian Institute of Technology, Donau-City-Straße 1, A-1220 Wien, Austria
Tel.: 0043-50 5504308
Fax: 0043-50 5504399
E-mail: joerg.schotter@ait.ac.at

Stefan Schrittwieser
Austrian Institute of Technology, Donau-City-Straße 1, A-1220 Wien, Austria
Tel.: 0043-50 5504309
Fax: 0043-50 5504399
E-mail: stefan.schrittwieser.fl@ait.ac.at

Thomas Simmet
Universität Ulm, Clinical Pharmacol., Helmholtzstr. 20, 89081 Ulm
Tel.: 0049-731 50065600
Fax: 0049-731 50065602
E-mail: thomas.simmet@uni-ulm.de

Lisa Sprenger
Technische Universität Dresden, Lehrstuhl für Magnetofluiddynamik, D-01062 Dresden
Tel.: 0049-351 46332034
Fax: 0049-351 4633384
E-mail: lisa.sprenger@tu-dresden.de

Aparna Sreekumari
ETH Zürich, Altwiesenstrasse 84, CH-8051 Zürich, Switzerland
Tel.: 0041-44 6336862
E-mail: aparna.sreekumari@mat.ethz.ch

Uwe Steinhoff
PTB Berlin, Abbestr. 2 - 12, 10587 Berlin
Tel.: 0049-30 34817419
E-mail: uwe.steinhoff@ptb.de

René Steinmeier
Volkswagen AG, Christian-Pommer-Str. 3, 38112 Braunschweig
Tel.: 0049-5361 9966984
E-mail: Rene.Steinmeier@volkswagen.de

Klaus Stierstadt
Mainzer Str. 16a, 80804 München
E-mail: Klaus.Stierstadt@physik.uni-muenchen.de

Tatiana Syrovets
Universität Ulm, Helmholtzstr. 20, 89081 Ulm
Tel.: 0049-731 50065604
Fax: 0049-731 50065602
E-mail: tatiana.syrovets@uni-ulm.de

Michael Szech
Universität Bayreuth, Experimentalphysik, 95440 Bayreuth
Tel.: 0049-921 553349
Fax: 0049-921 553647
E-mail: michael@szech-online.de

Kathleen Thom
Universität Greifswald, Institute of Pharmacy, Felix-Hausdorff-Str. 3, 017487 Greifswald
Tel.: 0049-3834 864846
Fax: 0049-3834 864886
E-mail: kathleen.thom@uni-greifswald.de

Rainer Tietze
Klinik und Poliklinik für Hals-, Nasen- und Ohrenkranke, Waldstr. 1, D-91054 Erlangen
Tel.: 0049-9131 8534769
Fax: 0049-9131 8534828
E-mail: rainer.tietze@uk-erlangen.de

Lutz Trahms
PTB Berlin, Abbestr. 2 - 12, 10587 Berlin
Tel.: 0049-30 34817213
E-mail: lutz.trahms@ptb.de

Andreas Tschöpe
Universität des Saarlandes, Experimentalphysik, D-66123 Saarbrücken
Tel.: 0049-681 3025187
Fax: 0049-681 3025222
E-mail: antsch@mx.uni-saarland.de

Sylvia Türk
TU Dresden, Institut für Strömungsmechanik, Lehrstuhl Magnetofluiddynamik, D-01062 Dresden
Tel.: 0049-351 46334819
Fax: 0049-351 46333384
E-mail: sylvia.tuerk@tu-dresden.de

Dialechti Vlaskou
TU München, Experimentelle Onkologie, Ismaningstr. 22, 81675 München
Tel.: 0049-89 41404452
Fax: 0049-89 41406182
E-mail: dvlaskou@gmx.net

Katharina Voigt
Uniklinik Jena, Erlanger Allee 101, 07740 Jena
Tel.: 0049-3641 9325854
E-mail: katharina.voigt1@med.uni-jena.de

Anja Waske
IfW Dresden, Helmholtzstr. 20, 01069 Dresden
Tel.: 0049-351 4659846
Fax: 0049-351 4659452
E-mail: a.waske@ifw-dresden.de

Rudolf Weeber
Institute for Computational Physics, Universität Stuttgart, Pfaffenwaldring 27, D-70569 Stuttgart
Tel.: 0049-711 68563613
E-mail: weeber@icp.uni-stuttgart.de

Arne Weikl
Universität Bayreuth, Experimentalphysik, 95440 Bayreuth
E-mail: Arne_Weikl@kabelmail.de

Heiko Wende
Universität Duisburg-Essen, Lotharstr. 1, 47057 Duisburg
Tel.: 0049-203 3792838
Fax: 0049-203 3793601
E-mail: heiko.wende@uni-due.de

Albrecht Wiedenmann
Institut Laue-Langevin, 6 rue Jules Horowitz, B.P. 156, F-38042 Grenoble Cedex 9, France
Tel.: 0033-476 207744
Fax: 0033-476 207120
E-mail: wiedenmann@ill.fr

Frank Wiekhorst
PTB Berlin, Abbestr. 2 - 12, 10587 Berlin
Tel.: 0049-30 34817347
E-mail: frank.wiekhorst@ptb.de

Igor Zeidis
Technische Universität Ilmenau, Technische Mechanik, PF 100565, D-98684 Ilmenau
Tel.: 0049-3677 691845
Fax: 0049-3677 691823
E-mail: igor.zeidis@tu-ilmenau.de

Klaus Zimmermann
Technische Universität Ilmenau, Technische Mechanik, PF 100565, D-98684 Ilmenau
Tel.: 0049-3677 692474
Fax: 0049-3677 691823
E-mail: klaus.zimmermannn@tu-ilmenau.de